UNIVERSITY OF CALIFORNIA
RIVERSIDE

Using Computational Chemistry and Experimental Approaches to Characterize Light-Absorbing Properties, Chemical Reactivity and Toxicity of Organic Aerosols and Atmospheric Traces Gases

A Dissertation submitted in partial satisfaction
of the requirements for the degree of

Doctor of Philosophy

in

Environmental Toxicology

by

Jin Y. Chen

June 2021

Dissertation Committee:
Dr. Ying-Hsuan Lin, Chairperson
Dr. Roya Bahreini
Dr. Prue Talbot

The Dissertation of Jin Y. Chen is approved:

Committee Chairperson

University of California, Riverside

ABSTRACT OF THE DISSERTATION

Using Computational Chemistry and Experimental Approaches to Characterize Light-Absorbing Properties, Chemical Reactivity and Toxicity of Organic Aerosols and Atmospheric Traces Gases

by

Jin Y. Chen

Doctor of Philosophy, Graduate Program in Environmental Toxicology
University of California, Riverside, June 2021
Dr. Ying-Hsuan Lin, Chairperson

Air pollution is a key environmental factor that contributes to the global burden of disease and climate change. Light-absorbing properties and toxicity mechanisms of atmospheric aerosols and trace gases have not been fully studied in part due to complex chemical compositions and a lack of authentic chemical standards. Even though computational chemistry approaches are quick and useful to predict chemical reactivity and optical absorption of atmospheric pollutants, experimental data are required to validate theoretical results. Therefore, a combination of computational and experimental approaches is necessary to characterize light-absorbing properties, chemical reactivity and toxicity atmospheric pollutants in both gas and aerosol phases.

This dissertation investigates the climate effects of brown carbon (a class of light-absorbing organic aerosols), and health impacts of carbonyl compounds by using a

combination of computational chemistry and experimental approaches. First, by using time-dependent density functional theory and experimental UV-Vis measurements, this dissertation identifies effects of functional groups, pH, and solvation environments on the light-absorbing properties of brown carbon aerosols. Second, the density functional theory methods and dithiothreitol reactivity assays were used to characterize electrophilicity of atmospheric carbonyls and their pathways to modify nucleophiles. Subsequently, to extend the findings to a multipollutant system, carbonyl chemical composition in electron cigarette vaping emissions is characterized using an impinger setup. Global and local site reactivities are computed to help predict the toxicity of carbonyls.

Using a combination of computational chemistry and experimental approaches help to assess light-absorbing properties of brown carbon and health effects of carbonyls. Overall, results from this dissertation contributes to an improved molecular understanding of reactivity, toxicity and light-absorbing properties of important atmospheric pollutants that are associated with public health and climate change.

Table of Contents

List of Tables

List of Figures

List of Schemes

Chapter I. Introduction

1.1 Background Significance

Air pollution is a leading environmental risk factor affecting public health and climate. Toxicological and epidemiological studies have linked ambient air pollution to asthma, lung cancer, and cardiovascular diseases.[1-3] World Health Organization assessed that ambient air pollution caused 3 million deaths annually worldwide.[4] As an imperative component of air pollution, ambient particulate matter (PM) was estimated to cause 4.2 million deaths in 2015.[5] In addition, PM has abilities to scatter and absorb solar radiation, which can influence changes in global climate.[6, 7]

PM (or aerosol) describes any liquid or solid particles suspended in the gases. Ambient PM can be emitted from natural and anthropogenic activities. Primary PM emissions include incomplete combustion of fossil fuels, biomass burning, volcanic eruptions, sea salt, dust, and pollen.[8-12] PM can also be formed through secondary pathways by gas-to-particle conversion to yield products such as secondary organic aerosol (SOA).[13-15] Due to various emission sources and complex atmospheric processes, health effects related to PM are predominantly attributed to PM sizes, concentrations, and chemical composition. PM sizes are categorized by aerodynamic diameters, such as PM_1 and $PM_{2.5}$ which have aerodynamic diameters less than and equal to 1 μm and 2.5 μm, respectively. PM with very fine aerodynamic diameter (e.g., < 100 nm) are extremely hazardous to health, since they are small enough to enter the blood circulation and the brain.[16, 17] To compare, the higher PM concentration generally results in higher mortality risk.[18]

PM is a complex, heterogenous mixture with different chemical components that are potential contributors to toxicity and health outcomes. Mainly, PM chemical components consist of black or elemental carbon, organic and inorganic compounds such as sulfate, nitrate, and ammonium. A major proposed toxicity mechanism of PM is the ability of PM constituents to generate reactive oxygen species (ROS) that can induce oxidative stress within biological systems.[19, 20] To quantify ROS generation potential (i.e., oxidative potential) of PM, an acellular chemical method called dithiothreitol (DTT) has been developed and used in the aerosol science community.[21] DTT is a dithiol compound used as a surrogate for biological antioxidants such as glutathione (GSH). Redox-active species such as quinones and transition metals are found to consume DTT significantly.[22-24] However, there are limited studies on DTT consumption by other chemical species such as carbonyl compounds, which may undergo different reaction pathway such as Michael-addition to deplete DTT.[25]

Carbonyl compounds such as aldehydes and ketones are reactive electrophiles that can deplete biological antioxidants or nucleophiles and subsequently cause cell cytotoxicity. Carbonyls can be directly emitted from activities such as cigarette smoking,[26] cooking,[27] or be formed secondarily from oxidation of volatile organic compounds.[28, 29] Simple carbonyls such as formaldehyde (HCHO) and acetaldehyde (CH_3CHO) are abundant in ambient air and cigarette smoke.[26, 30] Another class of carbonyls is α,β-unsaturated carbonyl (e.g., mesityl oxide and *trans*-cinnamaldehyde), which composes an alkene group conjugated to the C=O functional group. This structural feature makes α,β-unsaturated carbonyls known as polarized compounds that can covalently attack biological

thiols through Michael-addition.[31] Currently, there is limited studies on reactivity of carbonyls in PM, especially in terms of DTT consumption. Therefore, it is crucial to assess carbonyl reactivity toward DTT and evaluate potential toxicity pathway such as Michael-addition.

Aside from its significant impacts on public health, ambient PM's radiative forcing is a driver of climate change. Radiative forcings are changes in the Earth's energy budge caused by natural and anthropogenic substances and activities.[7] Radiative forcings greater or less than zero indicates near-surface warming or cooling, respectively.[7] PM scatter and absorb solar radiation, and its radiative forcing over 1750–2011 was estimated as -0.9 W m^{-2} as opposed to +2.3 W m^{-2} for greenhouse gases.[7] PM such as pure sulfates and those originate from volcanic eruptions have a cooling effect on the climate system, while carbonaceous PM (e.g., black carbon and brown carbon) contribute to warming effect.[6, 7, 32] Brown carbon (BrC) is a class of light-absorbing carbonaceous particles with wavelength-dependent light absorption near ultraviolet.[32, 33] It is estimated to account for 19 % of the tropospheric heating.[34] BrC is majorly emitted from biomass burning and known chromophores that are responsible for light absorption include nitroaromatics, conjugated systems, and Maillard reaction products.[33, 35-37] Due to various emission sources and precursors, light-absorbing properties of BrC chromophores have not been fully characterized. This is in part due to incomplete knowledge of their molecular structures and lack of authentic standards.

1.2 Objectives of This Dissertation

This dissertation intents to explore toxicity, reactivity, and light-absorbing properties of important aerosol components such as carbonyls and brown carbon. Three main research objectives are detailed in Chapters II-IV. Chapter II, light-absorbing properties of brown carbon, especially organonitrogen-containing compounds will be assessed using both computational chemistry and experimental UV-Vis measurements. Chapter III aims to characterize electrophilic reactivity and oxidative potential of carbonyl compounds using both computational chemistry and thiol-reactivity approaches. Chapter IV aims to characterize carbonyl composition and health risk from e-cigarette vapor using both computational chemistry and analytical chemistry techniques. Overall, findings from this dissertation will contribute to our current understanding of PM effects on public health and climate change.

References

1. Nastos, P. T.; Paliatsos, A. G.; Anthracopoulos, M. B.; Roma, E. S.; Priftis, K. N., Outdoor particulate matter and childhood asthma admissions in Athens, Greece: a time-series study. *Environ. Health* **2010,** *9* (1), 45.

2. Pope, C.; Burnett, R.; Thun, M.; Calle, E.; Krewski, D.; Ito, K.; Thurston, G., Lung cancer, cardiopulmonary mortality, and long-term exposure to fine particulate air pollution. *JAMA* **2002,** *287* (9), 1132-1141.

3. Pope III, C. A.; Burnett, R. T.; Thurston, G. D.; Thun, M. J.; Calle, E. E.; Krewski, D.; Godleski, J. J., Cardiovascular mortality and long-term exposure to particulate air pollution: epidemiological evidence of general pathophysiological pathways of disease. *Circulation* **2004,** *109* (1), 71-77.

4. Organization, W. H., Ambient air pollution: A global assessment of exposure and burden of disease. **2016**.

5. Cohen, A. J.; Brauer, M.; Burnett, R.; Anderson, H. R.; Frostad, J.; Estep, K.; Balakrishnan, K.; Brunekreef, B.; Dandona, L.; Dandona, R., Estimates and 25-year trends of the global burden of disease attributable to ambient air pollution: an analysis of data from the Global Burden of Diseases Study 2015. *The Lancet* **2017,** *389* (10082), 1907-1918.

6. Ramanathan, V.; Crutzen, P.; Kiehl, J.; Rosenfeld, D., Aerosols, climate, and the hydrological cycle. *science* **2001,** *294* (5549), 2119-2124.

7. Pachauri, R. K.; Allen, M. R.; Barros, V. R.; Broome, J.; Cramer, W.; Christ, R.; Church, J. A.; Clarke, L.; Dahe, Q.; Dasgupta, P., *Climate change 2014: synthesis report. Contribution of Working Groups I, II and III to the fifth assessment report of the Intergovernmental Panel on Climate Change*. IPCC: 2014.

8. Reddy, M. S.; Venkataraman, C., Inventory of aerosol and sulphur dioxide emissions from India: I—Fossil fuel combustion. *Atmospheric Environment* **2002,** *36* (4), 677-697.

9. bin Abas, M. R.; Oros, D. R.; Simoneit, B. R., Biomass burning as the main source of organic aerosol particulate matter in Malaysia during haze episodes. *Chemosphere* **2004,** *55* (8), 1089-1095.

10. Mroz, E. J.; Zoller, W. H., Composition of atmospheric particulate matter from the eruption of Heimaey, Iceland. *Science* **1975**, 461-464.

11. O'Dowd, C. D.; Smith, M. H.; Consterdine, I. E.; Lowe, J. A., Marine aerosol, sea-salt, and the marine sulphur cycle: A short review. *Atmospheric Environment* **1997,** *31* (1), 73-80.

12. Després, V.; Huffman, J. A.; Burrows, S. M.; Hoose, C.; Safatov, A.; Buryak, G.; Fröhlich-Nowoisky, J.; Elbert, W.; Andreae, M.; Pöschl, U., Primary biological aerosol particles in the atmosphere: a review. *Tellus B: Chemical and Physical Meteorology* **2012,** *64* (1), 15598.

13. Pandis, S. N.; Harley, R. A.; Cass, G. R.; Seinfeld, J. H., Secondary organic aerosol formation and transport. *Atmospheric Environment. Part A. General Topics* **1992,** *26* (13), 2269-2282.

14. Ng, N.; Kroll, J.; Chan, A.; Chhabra, P.; Flagan, R.; Seinfeld, J., Secondary organic aerosol formation from m-xylene, toluene, and benzene. *Atmospheric Chemistry and Physics* **2007,** *7* (14), 3909-3922.

15. Kroll, J. H.; Seinfeld, J. H., Chemistry of secondary organic aerosol: Formation and evolution of low-volatility organics in the atmosphere. *Atmospheric Environment* **2008,** *42* (16), 3593-3624.

16. Nemmar, A.; Hoet, P. M.; Vanquickenborne, B.; Dinsdale, D.; Thomeer, M.; Hoylaerts, M.; Vanbilloen, H.; Mortelmans, L.; Nemery, B., Passage of inhaled particles into the blood circulation in humans. *Circulation* **2002,** *105* (4), 411-414.

17. Oberdörster, G.; Sharp, Z.; Atudorei, V.; Elder, A.; Gelein, R.; Kreyling, W.; Cox, C., Translocation of inhaled ultrafine particles to the brain. *Inhalation toxicology* **2004,** *16* (6-7), 437-445.

18. Laden, F.; Schwartz, J.; Speizer, F. E.; Dockery, D. W., Reduction in fine particulate air pollution and mortality: extended follow-up of the Harvard Six Cities study. *American journal of respiratory and critical care medicine* **2006,** *173* (6), 667-672.

19. Li, N.; Sioutas, C.; Cho, A.; Schmitz, D.; Misra, C.; Sempf, J.; Wang, M.; Oberley, T.; Froines, J.; Nel, A., Ultrafine particulate pollutants induce oxidative stress and mitochondrial damage. *Environ. Health Perspect.* **2003,** *111* (4), 455-460.

20. Li, N.; Hao, M.; Phalen, R. F.; Hinds, W. C.; Nel, A. E., Particulate air pollutants and asthma: a paradigm for the role of oxidative stress in PM-induced adverse health effects. *Clinical immunology* **2003,** *109* (3), 250-265.

21. Cho, A.; Sioutas, C.; Miguel, A.; Kumagai, Y.; Schmitz, D.; Singh, M.; Eiguren-Fernandez, A.; Froines, J., Redox activity of airborne particulate matter at different sites in the Los Angeles Basin. *Environ. Res.* **2005,** *99* (1), 40-47.

22. Verma, V.; Shafer, M. M.; Schauer, J. J.; Sioutas, C., Contribution of transition metals in the reactive oxygen species activity of PM emissions from retrofitted heavy-duty vehicles. *Atmos. Environ.* **2010,** *44* (39), 5165-5173.

23. Charrier, J. G.; Anastasio, C., On dithiothreitol (DTT) as a measure of oxidative potential for ambient particles: evidence for the importance of soluble transition metals. *Atmos. Chem. Phys.* **2012,** *12* (19), 9321-9333.

24. Saffari, A.; Daher, N.; Shafer, M. M.; Schauer, J. J.; Sioutas, C., Seasonal and spatial variation in dithiothreitol (DTT) activity of quasi-ultrafine particles in the Los Angeles Basin and its association with chemical species. *Journal of Environmental Science and Health, Part A* **2014,** *49* (4), 441-451.

25. Chen, J. Y.; Jiang, H.; Chen, S. J.; Cullen, C.; Ahmed, C. S.; Lin, Y.-H., Characterization of electrophilicity and oxidative potential of atmospheric carbonyls. *Environmental Science: Processes & Impacts* **2019,** *21* (5), 856-866.

26. Pang, X.; Lewis, A., Carbonyl compounds in gas and particle phases of mainstream cigarette smoke. *Sci. Total Environ.* **2011,** *409* (23), 5000-5009.

27. Schauer, J. J.; Kleeman, M. J.; Cass, G. R.; Simoneit, B. R., Measurement of emissions from air pollution sources. 4. C1− C27 organic compounds from cooking with seed oils. *Environ. Sci. Technol.* **2002,** *36* (4), 567-575.

28. Carter, W. P., A detailed mechanism for the gas-phase atmospheric reactions of organic compounds. *Atmos. Environ. Part A. General Topics* **1990,** *24* (3), 481-518.

29. Atkinson, R., Gas-phase tropospheric chemistry of volatile organic compounds .1. Alkanes and alkenes. *J. Phys. Chem. Ref. Data* **1997,** *26* (2), 215-290.

30. Possanzini, M.; Di Palo, V.; Cecinato, A., Sources and photodecomposition of formaldehyde and acetaldehyde in Rome ambient air. *Atmos. Environ.* **2002,** *36* (19), 3195-3201.

31. Schultz, T.; Yarbrough, J.; Johnson, E., Structure–activity relationships for reactivity of carbonyl-containing compounds with glutathione. *SAR and QSAR in Environmental Research* **2005,** *16* (4), 313-322.

32. Andreae, M. O.; Gelencsér, A., Black carbon or brown carbon? The nature of light-absorbing carbonaceous aerosols. *Atmospheric Chemistry and Physics* **2006,** *6* (10), 3131-3148.

33. Sun, H.; Biedermann, L.; Bond, T. C., Color of brown carbon: A model for ultraviolet and visible light absorption by organic carbon aerosol. *Geophysical Research Letters* **2007,** *34* (17).

34. Feng, Y.; Ramanathan, V.; Kotamarthi, V., Brown carbon: a significant atmospheric absorber of solar radiation? *Atmospheric Chemistry and Physics* **2013,** *13* (17), 8607-8621.

35. Liu, S.; Shilling, J. E.; Song, C.; Hiranuma, N.; Zaveri, R. A.; Russell, L. M., Hydrolysis of organonitrate functional groups in aerosol particles. *Aerosol Science and Technology* **2012,** *46* (12), 1359-1369.

36. Zhang, X.; Lin, Y.-H.; Surratt, J. D.; Weber, R. J., Sources, composition and absorption Ångstrom exponent of light-absorbing organic components in aerosol extracts from the Los Angeles Basin. *Environmental science & technology* **2013,** *47* (8), 3685-3693.

37. Powelson, M. H.; Espelien, B. M.; Hawkins, L. N.; Galloway, M. M.; De Haan, D. O., Brown carbon formation by aqueous-phase carbonyl compound reactions with amines and ammonium sulfate. *Environmental science & technology* **2013,** *48* (2), 985-993.

Chapter II: Time-Dependent Density Functional Theory Investigation of the UV-Vis Spectra of Organonitrogen Chromophores in Brown Carbon

2.1 Introduction

As a critical component of radiative forcing, atmospheric aerosols represent an important driver of global climate change, yet large uncertainties remain unresolved.[1] Light-absorbing carbonaceous matter in atmospheric aerosols, such as black carbon emitted from incomplete combustion, is known to absorb solar radiation and release excess energy as heat that contribute to global warming.[2, 3] Brown carbon (BrC) is a class of light-absorbing organic aerosols with high levels of chemical complexity and variability. The primary sources of BrC include biomass burning,[4, 5] fossil fuel combustion,[6] and biogenic humic substances.[7] BrC can also be produced from volatile organic compound (VOC) precursors through multigenerational processes and multiphase chemistry.[8, 9] With a distinctive brown color, BrC absorbs natural sunlight at near UV (300-400 nm) to visible (400-700 nm) wavelengths.[9, 10]

Results from recent field, laboratory and modeling studies have suggested that BrC chromophores are crucial in determining the overall optical properties of organic aerosols.[11-14] Although comprehensive characterization of BrC chemical compositions is challenging because of their complex nature, a few class of compounds have been identified as BrC chromophores, including nitrogen-containing organics (e.g., nitroaromatics and organonitrates),[13, 15] conjugated systems (e.g., humic-like substance (HULIS)),[16] and Maillard-type reaction products resulting from reactions between

carbonyls and amines/ammonium sulfate.[17] Nitroaromatic compounds (e.g., nitrophenols and nitrocatechols) have been proposed to be produced from nitration of polycyclic aromatic hydrocarbons.[15, 18] Recently, formation of nitro-heterocyclic compounds (e.g., nitropyrrole) has also been identified as a source of BrC from the NO_3-initiated oxidation of heterocyclic VOC precursors.[12]

To better understand the molecular composition and light absorption of BrC, analytical methods with liquid chromatography (LC) coupled to UV/Vis spectroscopy and high-resolution mass spectrometry (HRMS) have been widely used, and have shown promising results to resolve the light absorption properties and chemical composition of BrC constituents at molecular level.[19-21] However, challenges remain in understanding the BrC molecular composition, as lack of authentic standards makes it difficult to confirm the presence of chromophores in BrC from molecular characterization. To aid in the interpretation of measured molecular composition, computational chemistry approaches using time-dependent density functional theory (TD-DFT) can be useful to evaluate the light absorption properties of potential BrC chromophores when authentic standards are not available. TD-DFT is a widely used *ab initio* approach for modelling electronic spectra.[22-28] The DFT component of TD-DFT models the electronic structures of atoms, molecules, and solids at ground state,[29] while the TD component accounts for the electronically excited-states of matter when interacting with light.[30] Numerous studies have used TD-DFT to examine optical properties of organic and inorganic dyes in industrial applications such as dye-sensitized solar cells,[31, 32] textile tinting,[27] and photosensitizers.[33] Studies have shown that the UV-Vis spectra calculated by TD-DFT approaches are often

in good agreement with experiment data, indicating the capability of TD-DFT in predicting light-absorbing properties of organic carbonaceous materials.[27, 30, 34]

Currently, applications of TD-DFT to study light absorption of BrC chromophores have only been reported in a few studies.[20, 35, 36] Preat et al. used TD-DFT to predict theoretical UV-Vis spectra of pH-sensitive dyes, including 4-nitrocatechol, in solvation, and observed satisfactory results between theoretical and experimental data.[33] Magalhães et al. used TD-DFT methods to characterize the maximum absorption wavelengths and oscillator strengths of catechol and its oxidation products (e.g., polyphenol and phenyl derivatives), and reported that oxidation products of catechol such as biphenyl and terphenyl compounds yield significantly stronger absorption than the parent compound.[35] In comparison with experimental UV-Vis measurements, TD-DFT has been proved to be an effective and efficient tool to predict theoretical UV-Vis spectra of chromophores in various BrC sources.[33, 35] A comprehensive TD-DFT study will complement the molecular characterization and will add to the current understanding of less studied BrC constituents such as nitro-heterocyclic compounds and organonitrates.

In this study, we investigated light-absorbing properties of known and potential BrC chromophores using both computational chemistry and experimental UV-Vis measurement approaches. We focused on organic nitrogen-containing compounds that contain lone-pair electrons as potential BrC chromophores. Effects of chemical composition, structure, solvation environment, and pH on UV-Vis spectra were examined. By using a combination of experimental and computational chemistry methods, results from this study will help to identify potential BrC chromophores and characterize the

optical properties associated with chemical composition, structure and environmental effects. Moreover, results from this study could be used in global climate models to better predict BrC radiative forcing and compare with observed BrC absorption.

2.2 Methods

2.2.1 Chemical Standards

A list of studied organonitrogen compounds is provided in Table 2.1. Authentic standards of commercially available chemical compounds were purchased for experimental UV-Vis measurements and to compare with computational results, including 2-nitrophenol (99%, Arcos Organics), 3-nitrophenol (99.9%, MP Biomedicals, LLC), 4-nitrophenol (>99%, TCI America), 4-nitrocatechol (>98%, TCI America), 2-nitropyrrole (97%, Ark Pharm, Inc.), 3-nitropyrrole (97%, Accela ChemBio Co. Ltd), 2-nitrofuran (97%, Sigma Aldrich), 2-nitrothiophene (>80%, TCI America), and 2-ethylhexyl nitrate (97%, Sigma Aldrich).

Table 2.1. List of selected organonitrogen compounds, including nitrophenols, nitrocatechols, nitro-heterocyclic compounds, organonitrates, and Maillard-type reaction products[α]

Nitrophenols

2-Nitrophenol*

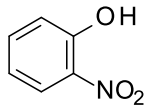

3-Nitrophenol*

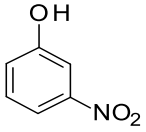

4-Nitrophenol*

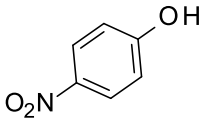

Nitrocatechols

3-Nitrocatechol

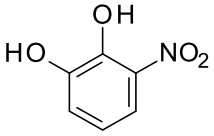

4-Nitrocatechol*

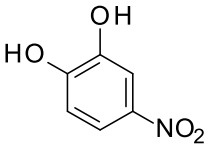

Nitro-heterocyclic compounds

2-Nitropyrrole*

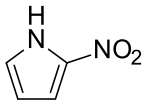

3-Nitropyrrole*

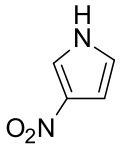

2-Nitrofuran*

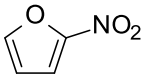

2-Nitrothiophene*

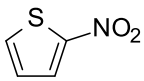

3-Nitrothiophene

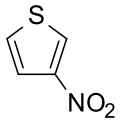

Organonitrates

2-Ethylhexyl nitrate

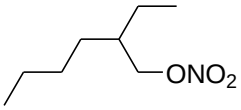

2-Nitratepyrrole

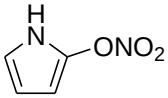

2-Nitratefuran

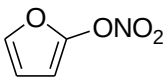

2-Nitratethiophene

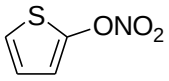

Maillard-type reaction products

2-Acetyl-1-pyrroline

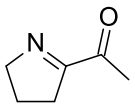

6-Acethyl-2,3,4,5-tetrahydropyridine

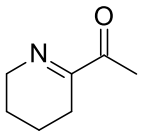

[α]Asterisks (*) indicate chemicals with authentic standards available.

2.2.2 UV-Vis Spectrometric Measurements

The UV-Vis spectra of selected organonitrogen compounds (Table 2.1) were measured in water and methanol using a UV-Vis spectrophotometer (Beckman DU-640) with wavelength scan of 200−700 nm. Prior to measurement, the spectrophotometer was blanked with water or methanol solvent. The reference wavelength was 700 nm. The final absorbance (A) was converted to the molar absorption coefficient (ε, L mol^{-1} cm^{-1}) based on the Beer-Lambert law, in which light path (b) is 1 cm and solution concentration (c) in mol L^{-1}.[37]

$$A = \varepsilon \times b \times c \tag{2.1}$$

The effect of pH on light absorption of acidic compounds was investigated using buffer solutions with pH 2 (potassium chloride-hydrochloric acid, Fisher Scientifics), pH 7.4 (potassium phosphate monobasic-sodium hydroxide, Fisher Scientifics), and pH 11 (sodium phosphate dibasic-sodium hydroxide, LabChem). Nitrophenols are weak acids (pKa=7.2 − 8.4)[38] which can be deprotonated and form nitrophenolates in water. Using buffer solutions with low, medium, and high levels of pH can help to examine how different fractions of protonated and deprotonated forms of nitrophenols in solution may lead to different absorption spectra. With known pH and pKa, fractions of protonated [HA] and deprotonated [A^-] forms of nitrophenols can be estimated based on the equilibrium relationship and mass balance of this species.[39, 40] Given the total concentration of the series of acidic species is equal to the sum of the protonated acid and its conjugated base (C_T), the fraction of each species ($a_0 = \frac{[H_nA]}{C_T}$, $a_1 = \frac{[H_{(n-1)}A^-]}{C_T}$, $a_2 = \frac{[H_{(n-2)}A^{2-}]}{C_T}$, etc.) can be calculated using the equations below.

$$C_T = [H_nA] + \left[H_{(n-1)}A^-\right] + \left[H_{(n-2)}A^{2-}\right] + \cdots \quad (2.2)$$

$$a_0 = \frac{[H_nA]}{C_T} = \frac{[H_nA]}{[H_nA]+\left[H_{(n-1)}A^-\right]+\left[H_{(n-2)}A^{2-}\right]} + \cdots \quad (2.3)$$

For nitrophenols which are monoprotic acids, the fractions of each species are shown below.

$$a_0 = \frac{[HA]}{[HA]+[A^-]} = \frac{[H^+]}{[H^+]+K_a} \quad (2.4)$$

$$a_1 = \frac{[A^-]}{[HA]+[A^-]} = \frac{K_a}{[H^+]+K_a} \quad (2.5)$$

Using a buffer with pH 2 can simulate nearly 100% [HA], since a high level of $[H^+]$ can keep nitrophenols protonated in the solution. On the other hand, using a buffer with pH 11 can simulate almost 100% $[A^-]$, since a high level of $[OH^-]$ can keep nitrophenols deprotonated in the solution. In the pH 7.4 buffer solution, a mixture of nitrophenols and nitrophenolates is present. As the absorbance is additive, theoretical UV-Vis spectra of mixtures can be constructed based on the species formed in the solution.

2.2.3 Quantum-chemical calculations of UV-Vis spectra

All calculations for light-absorbing properties were performed with the Gaussian 09 (Revision E.01) program.[41] All the computed UV-Vis spectra were visualized in GaussView 05 software, and optimized geometries of selected compounds are available in Table S2.1. To compare the computed absorption wavelengths at different levels of theory, four functionals, namely PBE (PBEPBE),[42] PBE0 (PBE1PBE),[43] B3LYP,[44, 45] and CAM-B3LYP, were selected to optimize geometries and perform respective excited states .[46] These four functionals were used as examples of widely used generalized gradient approximation (GGA), hybrid, and range-separated hybrid functionals. PBE is the 1996

functional of Perdew, Burke and Ernzerhof,[42] and PBE was made into a hybrid functional, PBE0, by Adamo and Barone in 1999.[43] B3LYP (Becke, 3-parameter, Lee-Yang-Parr) is also a hybrid functional,[44, 45] and CAM-B3LYP is a range-corrected version of B3LYP by Yanai and coworkers.[46] Different from PBE, hybrid functionals contain a portion of Hartree Fock (exact) exchange. For example, PBE0 and B3LYP contain 25%[46] and 20%[44, 45] of exact exchange, respectively.

Basis set 6-311++G(d,p) was used to calculate both geometry optimizations and excited states. To examine how basis sets with different levels of diffuse and polarization function affect absorption, UV-Vis spectra of 2-nitropyrrole were calculated with PBE in methanol solvation and these basis sets: 6-311++G, 6-311G(d,p), 6-311+G(d,p), 6-311++G(d), and 6-311++G(d,p). The selected 6-311G split valence basis set variants differ by additional diffuse ("+" and "++") and polarization ("d" and "p") functionals. Symbols "+" represents one additional diffuse function on non-hydrogen atoms, and "++" includes a diffuse function on hydrogen atoms. Symbols "d" and "p" represent one additional polarization function on non-hydrogen and hydrogen atoms, respectively.

To investigate bulk solvent effects on light absorption, all calculations were computed in the gas phase (vacuum), water, and methanol environments. Water and methanol are common extraction solvents used for offline analysis in laboratory settings.[12, 47-50] For example, Bones et al. used water as either humidified air or extraction solvent for limonene secondary organic aerosol (SOA), and observed a significant increase in absorption when the SOA was dissolved in aqueous solutions.[48] In this study, the integral

equation formalism extension of the polarizable continuum model (IEFPCM), an implicit solvent model is used in TD-DFT approaches.

2.3 Results and Discussion

2.3.1 Effects of Basis Sets on absorption

Basis sets with different diffuse and polarization functions can affect light absorption computed by TD-DFT. Thus, before comparing theoretical TD-DFT with experimental UV-Vis results, effects of basis sets on UV-Vis prediction are examined. Figure 2.1 shows UV-Vis of 2-nitropyrrole derived from TD-DFT/PBE level of theory with methanol solvation, and basis sets differing in levels of diffuse and polarization functions. Basis sets comprising a combination of diffuse and polarization functions (i.e., 6-311+G(d,p), 6-311++G(d,p), and 6-311++G(d)) have similar wavelengths of maximal absorbance (λ_{max}) of 324−325 nm, and their maximum molar absorption coefficients range from 14,185−14,387 L mol^{-1} cm^{-1}. In contrast, basis sets with only diffuse functions (i.e., 6-311++G) and polarization functions (6-311G(d,p)) have the longest (332 nm) and shortest (311 nm) λ_{max} values. Also, 6-311++G and 6-311G(d,p) have the largest and smallest maximum absorption coefficients of 15,434 and 12,864 L mol^{-1} cm^{-1}, respectively.

This study only tested the larger basis sets, the triple-zeta 6-311G derivatives with different diffuse and polarization functions, and their effects on light absorption. Smaller basis sets such as the double-zeta 6-31G and 6-31G(d) were not tested due to large variations in results as reported by previous studies.[51, 52] Jacqueline et al. reported that basis sets such as 6-311G(d,p) and 6-311+G(2d,p) can yield λ_{max} in good agreement with

experimental results;[52] especially that 6-311+G(2d,p) yields consistent and accurate results for thioindigo dyes.[52, 53] Moreover, basis sets (e.g., 6-311G(d,p), 6-311++G(d,p), 6-311+G(2d,p), and 6-311++G(2d,2p)) with additional diffuse or polarization function yield slight variations in λ_{max}.[52] Similarily, λ_{max} of 2-nitropyrrole computed with PBE using basis sets 6-311+G(d,p), 6-311++G(d,p), and 6-311++G(d) only varied by 1 nm (0.001 eV). Based on its adequate size and accuracy balance, 6-311++G(d,p) was therefore selected for both ground state and excited state calculations in the current study.

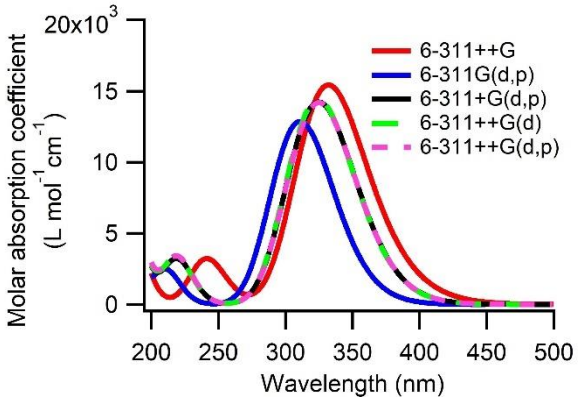

Figure 2.1. UV-Vis spectra of 2-nitropyrrole calculated from TD-DFT/PBE level of theory with basis sets varying in diffuse and polarization functions: 6-311++G, 6-311G(d,p), 6-311+G(d,p), 6-311++G(d), and 6-311++G(d,p). The spectra were calculated in methanol solvation using the IEFPCM solvent model.

2.3.2 Effects of Functionals on absorption

In addition to basis sets, functionals used in TD-DFT calculations can also affect light absorption. Four density functionals, PBE (pure),[42] PBE0 (hybrid),[43] B3LYP (hybrid),[44, 45] and CAM-B3LYP (range-corrected),[46] were used for the computations along with basis set 6-311++G(d,p). IEFPCM[54] solvation model was included to study bulk solvent effects (e.g., water and methanol) on light absorption.

The TD-DFT-derived λ_{max} were compared with experimental measurements in both water and methanol. For 2-, 3-, 4-nitrophenols and 4-nitrocatechol, λ_{max} computed in methanol are generally closer with experimental data (309−346 nm) than λ_{max} computed in water (Table 2.2). This difference could be attributed to that nitrophenols and 4-nitrocatechol are weakly acidic compounds, whose absorption can be affected by pH, which is discussed in Section 3.4.

For nitrophenols in methanol solvation, the λ_{max} obtained from PBE (342−469 nm) and B3LYP (308−378 nm) are larger than experimentally measured values (309−346 nm), with overestimations of 51−140 nm (57−1.13 eV) and 11−49 nm (0.13−0.49 eV), respectively. In contrast, the λ_{max} obtained from PBE0 (292−348 nm) and CAM-B3LYP (277−307 nm) have slight underestimations of 6−11 nm (0.08−0.12 eV) and 22−38 nm (0.27−0.47 eV) than the measured data. 3-Nitrophenol has a slight overestimation of λ_{max} (19 nm/0.21 eV) obtained from PBE0. Regarding 4-nitrocatehol, the computed λ_{max} are slightly underestimated by PBE0 (17 nm/0.19 eV), B3LYP (18 nm/0.20 eV), and CAM-B3LYP (44 nm/0.52 eV). The λ_{max} obtained from PBE has a slight overestimation of 12 nm (0.12 eV) than the experimental data. As for both nitrophenols and 4-nitrocethol, hybrid and range-corrected functionals derived comparable λ_{max} with experimental data in methanol solvation.

The TD-DFT-derived λ_{max} for nitro-heterocyclic compounds (e.g., 2-nitropyrrole, 3-nitropyrrole, 2-nitrofuran, and 2-nitrothiophene) are comparable with experimental measurements in both water and methanol (Table 2.2). In bulk solvents, the λ_{max} obtained by PBE0 (290−329 nm) was slightly overestimated by 10−21 nm (0.12−0.32 eV) for the

selected nitro-heterocyclic compounds, except 2-nitropyrrole that was underestimated by 11−25 nm (0.12−0.53 eV). Meanwhile, the λ_{max} obtained by PBE0 (270−301 nm) and CAM-B3LYP (251−298 nm) was underestimated by 10−49 nm (0.14−0.58 eV) and 18−52 nm (0.26−0.62 eV), respectively. For 2-nitroyrrole, the λ_{max} obtained by B3LYP (313 nm) in bulk solvents were underestimated by 23−37 nm (0.27−42 eV). For 3-nitropyrrole, 2-nitrofuran and 2-nitrothiophene, the λ_{max} by B3LYP in water and methanol were underestimated and overestimated by 6−8 nm (0.08−0.13 eV) and 2−3 nm (0.03−0.04 eV), respectively. Both TD-DFT calculations and experimental measurements show that nitro-heterocyclic compounds absorb light within the near UV range, consistent with Jiang et al. who reported the enhanced light absorption SOA at 375 nm from NO_3-initiated oxidation of heterocyclic VOCs (e.g., furan, pyrrole and thiophene), confirming nitro-heterocyclic compounds as potential BrC chromophores.[12]

Organonitrogen compounds such as organonitrates have been reported as potential chromophores in SOA,[12, 55] but less is known about their light absorbing properties owing to the lack of authentic standards. The computed UV-Vis spectra of heterocyclic organonitrates (e.g., 2-nitratepyrrole, 2-nitratefuran, and 2-nitratethiophene) in bulk solvents generally have larger λ_{max} values (232−476 nm) than their nitro-heterocyclic counterparts (237−329 nm). The λ_{max} values of heterocyclic organonitrates follow this sequence: PBE > B3LYP > PBE0 > CAM-B3LYP. This sequence is comparable with absorptions calculated using TD-DFT for organic dyes reported by Jacquemin et al.[56] PBE is a pure functional with no exact exchange, which often have overestimations or larger variations in computed λ_{max} vs. experimental data.[23, 56] Comparison between experimental

λ_{max} and the values obtained by hybrid functionals (e.g., B3LYP and PBE0) is generally better than the values obtained by the pure functional.[56]

In contrast, the aliphatic organonitrate, 2-ethylhexylnitrate, has much lower λ_{max} range from 189−268 nm in bulk solvents. Absorptions of 2-ethyhexylnitrate are comparable with the Maillard-type reaction products: 2-acetyl-1-pyrroline (λ_{max}=212−279 nm) and 6-acetyl-2,3,4,5-tetrahydropyridine (λ_{max}=205−256 nm). As only solar radiation with wavelengths ≥290 nm can reach the Earth's surface, 2-ethylhexyl nitrate, 2-acetyl-1-pyrroline and 6-acetyl-2,3,4,5-tetrahydropyridine may not be tropospherically relevant components of BrC.

Notably, organonitrates are known to contribute to a large fraction of ambient organic aerosol mass and have been associated with enhanced light absorption in SOA. A model simulation by Camredon et al. predicted that 18% of SOA contain organonitrate groups.[57] Liu et al. detected ~5−20% of organonitrate mass fraction in total secondary organic mass produced from high-NO_x-initiated oxidation of 1,2,4-trimethylbeneze.[55] However, when relative humidity was > 20%, the mass fraction of organonirates decreased due to hydrolysis.[55] Under dry and low-NO_x conditions, Liu et al. detected an increase of light absorption by organonitrate groups at 467 nm.[55] Similarly, SOA formed from the photooxidation of toluene and *m*-xylene, in the presence of NO_x, have enhanced light absorption from organonitrogen compounds including organonitrates.[58]

In terms of nitro-heterocyclic compounds, λ_{max} calculated with hybrid functionals (PBE0 and B3LYP) and range-corrected functional (CAM-B3LYP) compared better with experimental data than pure functional (PBE). Generally, results obtained with hybrid

functionals tend to be in better agreement with experimental values than computed with pure functionals.[56] Ang and coworkers studied optical absorption spectra of thiophene dyes using TD-DFT approach, and observed that the PBE functional results in redshift (longer λ_{max}) vs. the experimental data,[23] while B3LYP provides a quantitatively accurate result.[23] In addition, the functional PBE0 has been found to be an efficient functional to evaluate absorption spectra of organic dyes by many studies.[59-62] For example, Perpete et al. evaluated λ_{max} of anthraquinone dyes, and found that the PBE0 provides accurate λ_{max} compared to experimental data.[60] Also, PBE0 provides accurate correlation between computed and experimental λ_{max} for nitro-diphenylaniline dyes, with absolute deviations of 8 nm.[61] Jaquemin et al. reported that the PBE0 functional produces reasonable color of industrial organic dyes (e.g., azobenzenes, anthraquinones, indigoes, and diarylethenes), while PBE is well suited for low-lying excited states of conjugated organic compounds.[56] It has also been reported that PBE0 and CAM-B3LYP give the best estimates of the experimental transition energies for organic dyes.[56] As a range-corrected functional, CAM-B3LYP is well suited for studying dyes with a very delocalized excited state.[56]

Table 2. 2. Experimental and TD-DFT predicted λ_{max} (nm) of selected nitrogen-containing compounds. TD-DFT/6-311++g(d,p) level of theory was separately performed with PBE, PBE0, B3LYP, and CAM-B3LYP functionals. Water (W) and methanol (M) solvation effects were calculated using IEFPCM model, in addition to gas phase (G) or vacuum calculations.

Compound	Experimental		PBE			PBE0			B3LYP			CAM-B3LYP		
	W	M	G	W	M	G	W	M	G	W	M	G	W	M
2-Nitrophenol	411	338	364	412	410	296	328	327	312	352	350	275	301	300
3-Nitrophenol	328	329	409	471	469	315	349	348	336	379	378	284	308	307
4-Nitrophenol	401	309	331	361	360	277	304	303	292	321	320	260	285	285
3-Nitrocatechol	n.d.	n.d.	330	343	342	280	292	292	294	308	308	265	277	277
4-Nitrocatechol	423	346	351	358	358	300	330	329	315	328	328	277	303	302
2-Nitropyrrole	350	336	309	325	325	281	301	301	292	313	313	274	298	298
3-Nitropyrrole	280	270	270	291	290	237	259	258	249	272	272	227	251	250
2-Nitrofuran	313	302	302	323	322	269	293	292	280	305	305	259	284	284
2-Nitrothiophene	318	308	310	329	329	276	297	296	289	312	311	265	288	288
3-Nitrothiophene	n.d.	n.d.	291	312	311	252	270	271	264	287	287	239	260	260
2-Ethylhexyl nitrate	198	218	254	268	268	195	201	201	207	213	212	184	190	189
2-Nitratepyrrole	n.d.	n.d.	371	420	418	254	254	254	331	412	412	232	232	232
2-Nitratefuran	n.d.	n.d.	371	407	407	252	259	259	320	381	377	231	234	234
2-Nitratethiophene	n.d.	n.d.	469	476	476	316	327	326	357	368	368	275	285	285
2-Acetyl-1-pyrroline	n.d.	n.d.	257	279	279	217	231	230	221	235	235	202	213	212
6-Acetyl-2,3,4,5-tetrahydropyridine	n.d.	n.d.	241	255	256	209	218	218	213	218	218	197	205	205

2.3.3 Effects of Solvation on absorption

Light absorption of molecules may differ in both gas and solvated environments. To examine light absorption of BrC aerosols in atmospheric solvated environments (e.g., fog and cloud droplets) and laboratory setups (using solvents to extract filter samples), experimental measurements and TD-DFT absorption calculations of organonitrogen compounds are intercompared (Table 2.2 and Figure 2.2). Experimental UV-Vis spectra of compounds with commercially available standards were measured in water and in methanol separately. Generally, compounds dissolved in water have spectral redshifts compared to compounds dissolved in methanol. The difference between water and methanol absorption maximums ($\Delta\lambda_{max(aq.\text{-}meth.)}$) for 2-nitrophenol, 4-nitrophenol, and 4-

nitrocatechol is up to 92 nm (0.92 eV) (Table 2.2). On the other hand, the highest $\Delta\lambda_{max(aq.-meth.)}$ for nitro-heterocyclic compounds (e.g., 2- and 3-nitropyrrole, 2-nitrofuran, and 2-nitrothiophene) is 14 nm (0.15 eV). As weak acidic compounds, 2-nitrophenol, 4-nitrophenol, and 4-nitrocatechol, have greater $\Delta\lambda_{max(aq.-meth.)}$ variation than the nitro-heterocyclic compounds, which could be attributed to larger protonation/deprotonation levels in water and methanol.

Light absorbing properties of BrC compounds in gas phase and in solvents were predicted using TD-DFT/6-311++G(d,p) level of theory with PBE, PBE0, B3LYP, and CAM-B3LYP functionals. The solvation model used for water and methanol calculations is the IEFPCM, which allows the solute to lie inside a cavity.[52, 54] In Table 2.2, for the all calculations, there is a very small variation of λ_{max} up to 2 nm (0.03 eV) between water and methanol solvation, which could be attributed to the solvation model used for absorption calculations. IEFPCM is a variant solvation model of the Polarizable Continuum Model, which allows solute to lie inside a cavity, and the solvent acts as a structureless material.[63] The continuum schemes lack solute-solvent interactions (e.g., hydrogen bonds, ion pairing, etc.), which may be a cause for the very slight difference in absorptions calculated in water and methanol.

UV-Vis absorption spectra calculated in gas phase show a blueshift when compared with absorption spectra calculated in both water and methanol (Table 2.2). The average λ_{max} variations between water/methanol solvation vs. gas phase for different classes of selected organonitrogen-containing BrC are: nitrophenols (34 nm/0.39 eV), nitrocatechols (16 nm/0.21 eV), nitro-heterocyclics (22 nm/0.34 eV), organonitrates (19 nm/0.22 eV), and

Maillard-type reaction products (12 nm/0.28 eV). As reported by Magalhães et al, the absorption of a molecule in the condensed phase (e.g., cloud droplets and fog) has an enhancement compared to the gas phase, which is due to a higher degree of electron delocalization in the condensed phase.[35] Among the organonitrates, 2-ethylhexyl nitrate in water/methanol solvation is the only compound with a slightly shorter λ_{max} (-4−-7 nm) than in gas phase. Large variations in λ_{max} are observed for 2-nitratepyrrole for different functionals. Both PBE0 and CAM-B3LYP yields no variations between gas phase and water/methanol solvation. The variation increased by +49 nm and +81 nm in water/methanol for PBE and B3LYP, respectively.

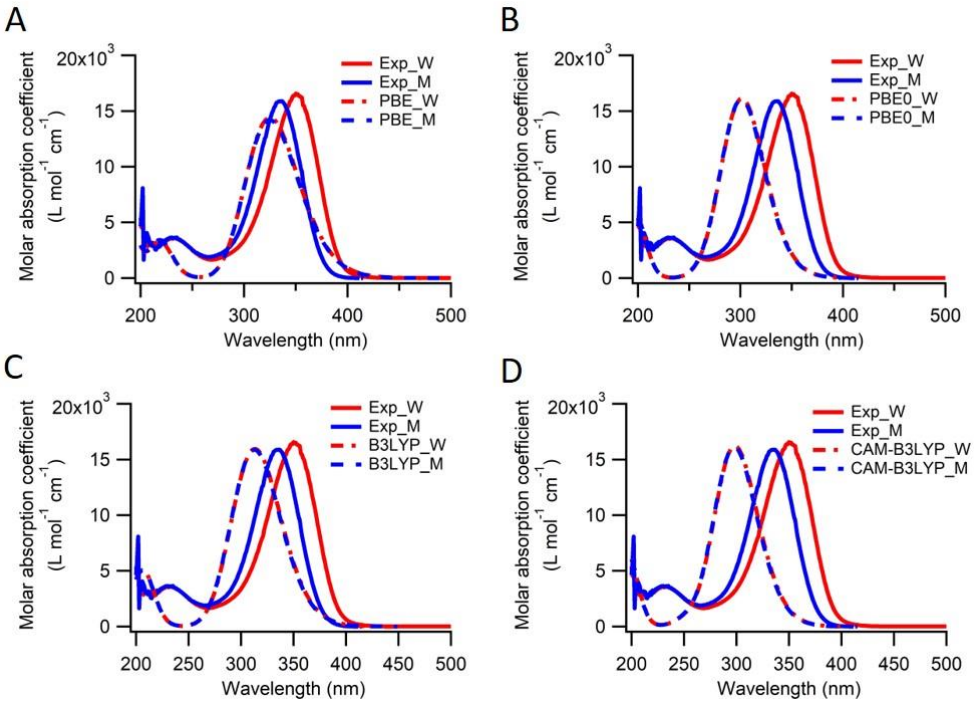

Figure 2.2. Comparison of 2-nitropyrrole UV-Vis spectra between experimental measurements and TD-DFT calculations in water and methanol bulk solvents. Solid lines represent experimental measurements in methanol and water. TD-DFT calculations included basis set 6-311++G(d,p) with different functionals: (A) PBE, (B) PBE0, (C) B3LYP, and (D) CAM-B3LYP. Solvation model IEFPCM was applied in TD-DFT work to examine UV-Vis spectra in water and methanol.

2.3.4 Effects of pH on absorption

Effects of pH on light absorption are important for acidic compounds such as nitrophenols and nitrocatechols. The absorption spectra of 2-, 3-, and 4-nitrophenol and 4-nitrocatechol were measured using buffer solutions with pH 2, 11, and 7.4 (Figure 2.3 and Figures S2.1−S2.3). Figure 2.3 shows absorption spectra of protonated and deprotonated forms of 4-nitrophenol in pH 2 and pH 11 buffer, respectively. Overall, the absorptions of nitrophenols and 4-nitrocatechol in the basic buffer solution (pH 11) are stronger and at longer wavelengths than in the acidic buffer solution (pH 2). Under these conditions, the nitrophenol and nitrocatehcol compounds were mostly in protonated (at pH 2) and deprotonated (at pH 11) forms, respectively (Figure 2.3 and Figures S2.1−S2.3).

As supported by Alif et al., the absorptions of deprotonated or ionic forms of 2-, 3-, and 4-nitrophenols are stronger and at longer λ_{max} than the protonated forms of these compounds.[64-66] Meanwhile, in the pH 7.4 buffer, a combination of protonated and deprotonated species of nitrophenols and 4-nitrocatechol result in two unique peaks in the spectrum (Figure S2.1−S2.3). To assess UV-Vis spectra of protonated and deprotonated forms of 4-nitrophenol, the PBE and B3LYP functionals with basis set 6-311++G(d,p) were used to calculated light absorption in water solvation in TD-DFT. The calculated UV-Vis spectra for the deprotonated form of 4-nitrophenol have stronger absorption and a redshift when comparing with deprotonated form, which is consistent with the experimental data (Figure 2.3).

Different absorption characteristics were observed for the nitrophenol and nitrocatechol compounds in low to high pH buffer solutions.The final measured absorbance

was corrected with absorbance from buffer solutions. Jacobson reported similar patterns for dimethylnitrophenols dissolved in basic solutions, whose absorptions peaked at wavelengths ≥ 400 nm.[15] Also in the basic buffer, the absorption of phenolic aldehydes was stronger and shifted to longer wavelengths.[67] Guo et al. predicted pH values of fine particles in the southeastern United States to be between 0.5 to 3 during summer and winter.[68] In norther China, Shi et al investigated acidity of $PM_{2.5}$ and calculated bulk pH values ranging from 0.33 to 13.6.[69] These studies imply that the acidity of atmospheric aerosols or droplets varies significantly. Regions with high aerosol pH could likely enhance aerosol absorption and contribute greater to the positive climate forcing.

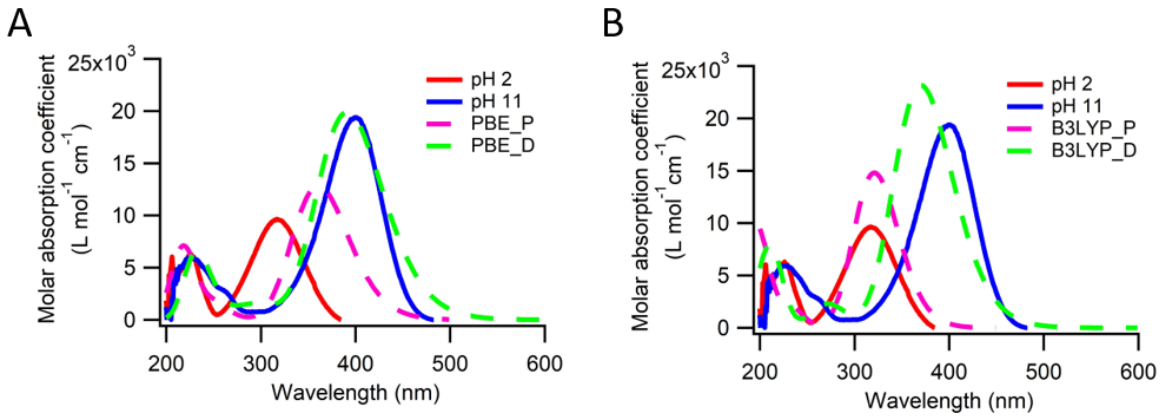

Figure 2.3. Effects of pH of UV-Vis absorption of 4-nitrophenol. Comparison between the measured and TD-DFT-derived UV-Vis. Experimental measurements used buffer solutions of pH=2 and 11. UV-Vis of 4-nitrophenol in protonated ("_P") and deprotonated ("_D") forms were obtained by (A) PBE and (B) B3LYP functionals in water using the IEFPCM solvent model.

To estimate the fractions of protonated and deprotonated species of 2-nitrophenol (pK_a=7.2), 3-nitrophenol (pK_a=8.4), and 4-nitrophenol (pK_a=7.2) at pH=7.4, equations 2.3 and 2.4 were applied. The resulting fractions of protonated ([HA]) and deprotonated ($[A^-]$) species are 38% and 62% for 2-, and 4-nitrophenol, and 91% and 9% for 3-nitrophenol,

respectively. Assuming the selected nitrophenol compounds were completely protonated and deprotonated in pH 2 and pH 11 buffer solutions, respectively, the UV-Vis spectra of nitrophenols in pH 7.4 can be constructed. By multiplying the fraction (%) of protonated and deprotonated forms of 4-nitrophenol by their measured absorbance at pH 2 and pH 11, and sum of the final absorbance provides a satisfactory estimate of UV-Vis spectrum as the actual measured absorbance in pH 7.4 buffer (Figure 2.4). This method is useful to predict absorbance of nitrophenols at different pH levels when combined with accurate spectrum predictions of protonated and deprotonated species of the compound.

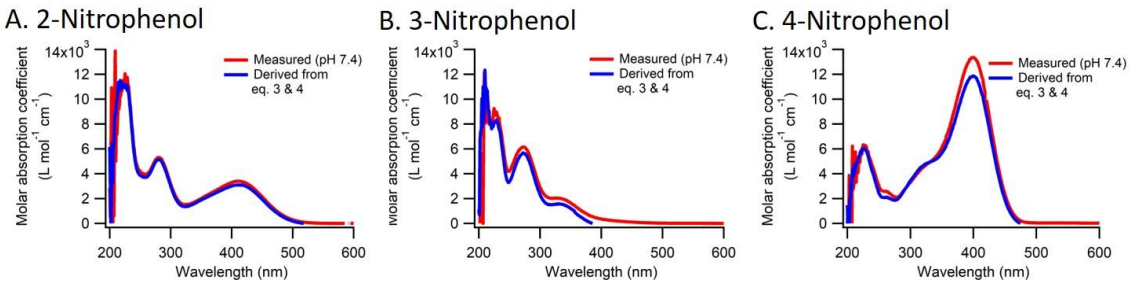

Figure 2.4. Comparisons between measured and the predicted UV-Vis spectra of (A) 2-nitrophenol, (B) 3-nitrophenol, and (C) 4-nitrophenol in pH 7.4 based on the fractions of each species (eq. 3 & 4).

2.4 Atmospheric Implications

The ability of BrC to absorb light within tropospheric-relevant solar radiation (290-700 nm) imply BrC can potentially contribute to climate warming. This study examines the light-absorbing properties of organonitrogen chromophores in BrC using both TD-DFT calculations and experimental measurements. Absorption spectra derived from functionals using TD-DFT generally have the λ_{max} sequence that follows PBE > B3LYP > PBE0 > CAM-B3LYP. Hybrid functionals B3LYP and PBE0 overall provide λ_{max} values with

smaller variations with experimental data. Different UV-Vis absorbance patterns were measured in water and methanol, and resulted in blueshift and redshift in spectrum, respectively. UV-Vis spectra computed using IEFPCM model with water and methanol only result in a maximum variation of 2 nm (0.03 eV). However, UV-Vis calculated in gas phase show a blue spectrum shift in comparison to both water and methanol calculations. This observation implies that BrC in the condensed phase (e.g., fog and cloud droplets, and aerosols) with intermolecular interactions involved may have more influence on climate warming.

Absorbance spectra of nitrophenol compounds display solvent driven changes between water and methanol. These changes are likely driven by shifting fractions of protonated and deprotonated forms of compounds under various pH levels. Supporting this hypothesis, in the pH 11 buffer solution, the absorption of 4-nitrophenol has a redshift or longer λ_{max} compared to the spectrum measured in the pH 2 buffer. This observation indicates that acidity of aerosol can change light absorbing properties of acidic constituents in the atmospheric aerosols or droplets. Moreover, as BrC compounds exist as mixtures in the environment, if major species of chromophores can be identified, the UV-Vis spectra of BrC mixtures can be theoretically constructed.

This study evaluates the UV-Vis absorption of known and potential organonitrogen chromophores in BrC by using experimental and TD-DFT approaches. In general, results obtained from TD-DFT calculations are comparable with experimental data. A limitation to this study is that the selected implicit solvent model, IEFPCM, could not accurately account for the interactions between solute and solvent. A use of explicit solvent model in

TD-DFT and molecular dynamic studies will be needed to better predict effects of bulk solvent on absorption. Overall, the TD-DFT approaches used here exhibit good applicability to predict light absorption of BrC in aerosols. More importantly, results from this study could be used in global climate models to improve prediction of aerosol radiative forcing.

2.5 Supporting Information

Table S2.1. Cartesian coordinates of optimized geometries of studied organonitrogen chromophores in BrC obtained from DFT methods. IEFPCM solvent model was used to model effects of bulk solvents (e.g., water and methanol) on light absorption.

2-Nitrophenol

PBE (Gas)				***PBE (Water)***				***PBE (Methanol)***			
O	1.68459	-1.39283	0.	O	1.68748	-1.38968	0.	O	1.6874	-1.38971	0.
C	-0.64606	-1.98678	0.	C	-0.6377	-1.99003	0.	C	-0.63798	-1.98998	0.
C	-1.98979	-1.62242	0.	C	-1.98068	-1.62743	0.	C	-1.98098	-1.62728	0.
C	-2.35386	-0.26779	0.	C	-2.35206	-0.27162	0.	C	-2.35211	-0.27151	0.
C	-1.35626	0.70171	0.	C	-1.36209	0.70174	0.	C	-1.36188	0.70171	0.
C	0.	0.34411	0.	C	0.	0.34708	0.	C	0.	0.34695	0.
C	0.38021	-1.0207	0.	C	0.3853	-1.02047	0.	C	0.38514	-1.02051	0.
N	0.98686	1.4487	0.	N	0.97301	1.44153	0.	N	0.97345	1.44176	0.
O	0.53996	2.60496	0.	O	0.53627	2.60717	0.	O	0.53634	2.60708	0.
O	2.18624	1.16151	0.	O	2.18328	1.17156	0.	O	2.18337	1.17132	0.
H	1.71699	-2.36652	0.	H	1.72856	-2.36512	0.	H	1.72838	-2.36507	0.
H	-0.36452	-3.04505	0.	H	-0.35229	-3.04592	0.	H	-0.35271	-3.04597	0.
H	-2.75628	-2.40064	0.	H	-2.74457	-2.4077	0.	H	-2.74499	-2.40744	0.
H	-3.40418	0.02706	0.	H	-3.40369	0.01748	0.	H	-3.40368	0.01784	0.
H	-1.59182	1.76639	0.	H	-1.61185	1.76244	0.	H	-1.6112	1.76254	0.

PBE0 (Gas)				***PBE0 (Water)***				***PBE0 (Methanol)***			
O	1.67755	-1.3725	0.	O	-1.67814	-1.37276	0.	O	1.67776	-1.37317	0.
C	-0.62782	-1.97305	0.	C	0.6237	-1.97545	0.	C	-0.6246	-1.97495	0.
C	-1.96401	-1.61752	0.	C	1.95862	-1.61902	0.	C	-1.95943	-1.61824	0.
C	-2.33425	-0.27508	0.	C	2.33357	-0.27477	0.	C	-2.33379	-0.27381	0.
C	-1.3481	0.69237	0.	C	1.35279	0.69441	0.	C	-1.35246	0.6949	0.
C	0.	0.34191	0.	C	0.	0.344	0.	C	0.	0.34373	0.
C	0.38661	-1.00912	0.	C	-0.38944	-1.00983	0.	C	0.38883	-1.00968	0.
N	0.97133	1.44083	0.	N	-0.96181	1.43356	0.	N	0.96253	1.43315	0.
O	0.52479	2.5745	0.	O	-0.52681	2.57578	0.	O	0.52794	2.57555	0.
O	2.15166	1.16641	0.	O	-2.15093	1.1731	0.	O	2.15148	1.17175	0.
H	1.72658	-2.33286	0.	H	-1.7322	-2.33529	0.	H	1.73126	-2.33565	0.
H	-0.34364	-3.02253	0.	H	0.3376	-3.02326	0.	H	-0.33881	-3.02291	0.
H	-2.7209	-2.3948	0.	H	2.71451	-2.39695	0.	H	-2.71555	-2.39589	0.
H	-3.37887	0.01216	0.	H	3.37904	0.00875	0.	H	-3.37908	0.0103	0.
H	-1.58909	1.74792	0.	H	1.60531	1.74673	0.	H	-1.6043	1.74734	0.

B3LYP (Gas)				***B3LYP (Water)***				***B3LYP (Methanol)***			
O	1.67376	-1.39082	0.	O	1.67541	-1.39006	0.	O	1.6754	-1.39001	0.
C	-0.6463	-1.97732	0.	C	-0.64065	-1.97963	0.	C	-0.64083	-1.97962	0.
C	-1.98334	-1.61136	0.	C	-1.97651	-1.61396	0.	C	-1.97672	-1.61391	0.

C	-2.34416	-0.26245	0.	C	-2.34314	-0.26326	0.	C	-2.34316	-0.26327	0.
C	-1.35015	0.70183	0.	C	-1.35561	0.70331	0.	C	-1.35541	0.70321	0.
C	0.	0.34157	0.	C	0.	0.34408	0.	C	0.	0.34394	0.
C	0.37604	-1.0167	0.	C	0.37951	-1.01676	0.	C	0.37942	-1.0168	0.
N	0.98589	1.44006	0.	N	0.97427	1.43214	0.	N	0.97463	1.43241	0.
O	0.54567	2.58751	0.	O	0.54623	2.58915	0.	O	0.54613	2.58908	0.
O	2.17466	1.15854	0.	O	2.17331	1.16605	0.	O	2.17334	1.16594	0.
H	1.72279	-2.35406	0.	H	1.7288	-2.35542	0.	H	1.72886	-2.35527	0.
H	-0.36947	-3.02754	0.	H	-0.36138	-3.02796	0.	H	-0.36169	-3.02804	0.
H	-2.74565	-2.38188	0.	H	-2.73712	-2.3856	0.	H	-2.73743	-2.38547	0.
H	-3.38597	0.03147	0.	H	-3.38597	0.02592	0.	H	-3.38594	0.02612	0.
H	-1.58812	1.75629	0.	H	-1.60545	1.75438	0.	H	-1.60489	1.75439	0.

CAM-B3LYP (Gas) ***CAM-B3LYP (Water)*** ***CAM-B3LYP (Methanol)***

O	1.66185	-1.38956	0.	O	-1.66129	-1.39151	0.	O	-1.66144	-1.39132	0.
C	-0.65006	-1.96551	0.	C	0.6481	-1.96703	0.	C	0.64804	-1.96709	0.
C	-1.98001	-1.59552	0.	C	1.97625	-1.59509	0.	C	1.97627	-1.59524	0.
C	-2.33577	-0.25114	0.	C	2.33553	-0.24848	0.	C	2.3355	-0.24872	0.
C	-1.34189	0.70533	0.	C	1.34623	0.7087	0.	C	1.34609	0.70847	0.
C	0.	0.33919	0.	C	0.	0.34108	0.	C	0.	0.34095	0.
C	0.37115	-1.01214	0.	C	-0.37263	-1.01282	0.	C	-0.37268	-1.01285	0.
N	0.98756	1.42929	0.	N	-0.97957	1.42122	0.	N	-0.97973	1.42156	0.
O	0.55557	2.57008	0.	O	-0.56103	2.57068	0.	O	-0.56055	2.57068	0.
O	2.16582	1.14405	0.	O	-2.16639	1.14837	0.	O	-2.16629	1.14854	0.
H	1.71224	-2.35084	0.	H	-1.71387	-2.35525	0.	H	-1.71423	-2.35494	0.
H	-0.37698	-3.01581	0.	H	0.37437	-3.01611	0.	H	0.37434	-3.01624	0.
H	-2.74464	-2.36277	0.	H	2.7405	-2.36234	0.	H	2.74054	-2.36247	0.
H	-3.37586	0.04593	0.	H	3.37626	0.04561	0.	H	3.3762	0.04546	0.
H	-1.57406	1.76059	0.	H	1.58862	1.76108	0.	H	1.58819	1.76093	0.

3-Nitrophenol

PBE (Gas) ***PBE (Water)*** ***PBE (Methanol)***

O	-0.90278	2.92269	0.	O	-0.90273	2.92123	0.	O	-0.90269	2.92134	0.
C	1.28672	1.85271	0.	C	1.28712	1.8529	0.	C	1.287	1.85289	0.
C	2.03225	0.66841	0.	C	2.03189	0.66813	0.	C	2.03187	0.66819	0.
C	1.39774	-0.57585	0.	C	1.39915	-0.57748	0.	C	1.3991	-0.57739	0.
C	0.	-0.59296	0.	C	0.	-0.59525	0.	C	0.	-0.59516	0.
C	-0.77501	0.56521	0.	C	-0.77582	0.56548	0.	C	-0.77586	0.56544	0.
C	-0.11766	1.80237	0.	C	-0.11894	1.80287	0.	C	-0.11898	1.80283	0.
N	-0.70091	-1.90787	0.	N	-0.69619	-1.89954	0.	N	-0.69629	-1.89983	0.
O	-0.00058	-2.92539	0.	O	-0.00527	-2.92795	0.	O	-0.00505	-2.92788	0.
O	-1.93566	-1.89857	0.	O	-1.93516	-1.90092	0.	O	-1.93512	-1.90092	0.
H	-0.33451	3.71151	0.	H	-0.33904	3.71579	0.	H	-0.33872	3.71563	0.
H	1.79732	2.82074	0.	H	1.79715	2.81987	0.	H	1.79699	2.81991	0.
H	3.12284	0.72044	0.	H	3.12203	0.72063	0.	H	3.12203	0.7207	0.
H	1.95179	-1.51349	0.	H	1.96214	-1.50939	0.	H	1.96184	-1.50946	0.

H	-1.86318	0.50667	0.	H	-1.86401	0.51119	0.	H	-1.86404	0.51101	0.

PBE0 (Gas)

O	-0.89947	2.89542	0.
C	1.27092	1.83878	0.
C	2.01441	0.66442	0.
C	1.38724	-0.57271	0.
C	0.	-0.59074	0.
C	-0.77203	0.55714	0.
C	-0.12242	1.78701	0.
N	-0.6912	-1.89282	0.
O	-0.001	-2.8918	0.
O	-1.90495	-1.88502	0.
H	-0.34814	3.68152	0.
H	1.77628	2.80104	0.
H	3.09742	0.7186	0.
H	1.94014	-1.50235	0.
H	-1.85269	0.49877	0.

PBE0 (Water)

O	-0.89774	2.89535	0.
C	1.27246	1.83864	0.
C	2.01456	0.66357	0.
C	1.38789	-0.57479	0.
C	0.	-0.5921	0.
C	-0.7725	0.55823	0.
C	-0.12247	1.7877	0.
N	-0.68843	-1.8859	0.
O	-0.00705	-2.89425	0.
O	-1.90546	-1.88791	0.
H	-0.34907	3.68613	0.
H	1.77757	2.7998	0.
H	3.09721	0.71755	0.
H	1.94879	-1.49932	0.
H	-1.85319	0.50412	0.

PBE0 (Methanol)

O	-0.89783	2.89539	0.
C	1.27225	1.83866	0.
C	2.0145	0.66369	0.
C	1.38787	-0.57466	0.
C	0.	-0.59203	0.
C	-0.77258	0.55815	0.
C	-0.1226	1.78766	0.
N	-0.68841	-1.88615	0.
O	-0.00667	-2.89415	0.
O	-1.90532	-1.88797	0.
H	-0.34898	3.68596	0.
H	1.7773	2.79988	0.
H	3.09715	0.71774	0.
H	1.94855	-1.49932	0.
H	-1.85326	0.50387	0.

B3LYP (Gas)

O	-0.89885	2.91062	0.
C	1.2806	1.84495	0.
C	2.02324	0.66546	0.
C	1.39141	-0.57337	0.
C	0.	-0.59092	0.
C	-0.77068	0.56285	0.
C	-0.11588	1.79356	0.
N	-0.69754	-1.90036	0.
O	-0.0056	-2.91041	0.
O	-1.92133	-1.89348	0.
H	-0.35033	3.70225	0.
H	1.78702	2.80531	0.
H	3.10536	0.71652	0.
H	1.94489	-1.50093	0.
H	-1.85008	0.51045	0.

B3LYP (Water)

O	-0.89662	2.9108	0.
C	1.28208	1.84434	0.
C	2.02332	0.66441	0.
C	1.39238	-0.57545	0.
C	0.	-0.59266	0.
C	-0.7713	0.564	0.
C	-0.11609	1.79406	0.
N	-0.6943	-1.89237	0.
O	-0.01241	-2.91341	0.
O	-1.92213	-1.89589	0.
H	-0.34953	3.70609	0.
H	1.78842	2.80341	0.
H	3.105	0.71535	0.
H	1.95368	-1.49792	0.
H	-1.85066	0.51549	0.

B3LYP (Methanol)

O	-0.89663	2.91086	0.
C	1.28193	1.84435	0.
C	2.02329	0.66449	0.
C	1.39234	-0.57535	0.
C	0.	-0.59258	0.
C	-0.77135	0.56394	0.
C	-0.11617	1.79404	0.
N	-0.69435	-1.89266	0.
O	-0.01212	-2.91334	0.
O	-1.92204	-1.8959	0.
H	-0.34934	3.70595	0.
H	1.7882	2.8035	0.
H	3.10498	0.71548	0.
H	1.95343	-1.49795	0.
H	-1.85071	0.51529	0.

CAM-B3LYP (Gas)

O	-0.89227	2.89858	0.
C	1.27506	1.8353	0.
C	2.01457	0.66058	0.
C	1.38462	-0.5731	0.
C	0.	-0.58737	0.
C	-0.76811	0.55992	0.
C	-0.11485	1.78484	0.
N	-0.69579	-1.89198	0.
O	-0.00916	-2.89458	0.
O	-1.91048	-1.88405	0.
H	-0.34732	3.69059	0.

CAM-B3LYP (Water)

O	-0.88775	2.90004	0.
C	1.27826	1.83403	0.
C	2.01532	0.65844	0.
C	1.3849	-0.57608	0.
C	0.	-0.58858	0.
C	-0.76794	0.56179	0.
C	-0.11321	1.78547	0.
N	-0.69485	-1.88491	0.
O	-0.01871	-2.89789	0.
O	-1.91286	-1.88542	0.
H	-0.34294	3.69507	0.

CAM-B3LYP (Methanol)

O	-0.88784	2.90006	0.
C	1.27806	1.83407	0.
C	2.01527	0.65856	0.
C	1.3849	-0.57595	0.
C	0.	-0.58852	0.
C	-0.76801	0.56171	0.
C	-0.11334	1.78544	0.
N	-0.69483	-1.88516	0.
O	-0.01834	-2.89781	0.
O	-1.91273	-1.88547	0.
H	-0.34289	3.69491	0.

H	1.78087 2.79517 0.	H	1.78473 2.79241 0.	H	1.78445 2.79252 0.
H	3.09598 0.71109 0.	H	3.09643 0.70787 0.	H	3.09638 0.70806 0.
H	1.93559 -1.50158 0.	H	1.9432 -1.49986 0.	H	1.943 -1.49985 0.
H	-1.8471 0.5081 0.	H	-1.84696 0.51463 0.	H	-1.84703 0.5144 0.

4-Nitrophenol

PBE (Gas)

O	0.09139 -3.44642 0.	O	0.09163 -3.43929 0.	O	0.09178 -3.43955 0.
C	-1.20659 -1.39084 0.	C	-1.20991 -1.3905 0.	C	-1.20977 -1.39055 0.
C	-1.21639 0.00188 0.	C	-1.2186 -0.00046 0.	C	-1.2185 -0.00041 0.
C	0. 0.69165 0.	C	0. 0.69373 0.	C	0. 0.69366 0.
C	1.22513 0.01216 0.	C	1.22795 0.01248 0.	C	1.22787 0.0125 0.
C	1.23397 -1.37814 0.	C	1.23579 -1.37574 0.	C	1.23575 -1.37579 0.
C	0.01753 -2.08457 0.	C	0.01707 -2.08441 0.	C	0.01713 -2.08443 0.
N	-0.0091 2.16563 0.	N	-0.00914 2.15223 0.	N	-0.00921 2.15268 0.
O	-1.10922 2.73391 0.	O	-1.1075 2.73619 0.	O	-1.10763 2.73608 0.
O	1.08374 2.74689 0.	O	1.0821 2.74933 0.	O	1.082 2.74935 0.
H	-0.80763 -3.81795 0.	H	-0.80503 -3.82252 0.	H	-0.80487 -3.82261 0.
H	-2.1508 -1.94359 0.	H	-2.15217 -1.9436 0.	H	-2.15216 -1.94353 0.
H	-2.14994 0.56517 0.	H	-2.15767 0.55261 0.	H	-2.15741 0.55295 0.
H	2.152 0.58637 0.	H	2.15977 0.57766 0.	H	2.15955 0.57794 0.
H	2.17096 -1.93725 0.	H	2.17543 -1.93031 0.	H	2.17531 -1.9305 0.

PBE0 (Gas)

O	0.08821 -3.41487 0.	O	0.08885 -3.40935 0.	O	0.08895 -3.40955 0.
C	-1.1973 -1.3791 0.	C	-1.19972 -1.37959 0.	C	-1.19961 -1.37961 0.
C	-1.20727 0.00466 0.	C	-1.2092 0.00187 0.	C	-1.20912 0.00194 0.
C	0. 0.68821 0.	C	0. 0.68934 0.	C	0. 0.6893 0.
C	1.21658 0.01506 0.	C	1.21933 0.01566 0.	C	1.21925 0.01566 0.
C	1.22483 -1.36602 0.	C	1.22716 -1.36388 0.	C	1.2271 -1.36394 0.
C	0.01751 -2.06761 0.	C	0.01796 -2.0677 0.	C	0.01798 -2.06771 0.
N	-0.00887 2.14856 0.	N	-0.00955 2.13765 0.	N	-0.00959 2.138 0.
O	-1.08983 2.70654 0.	O	-1.08852 2.7089 0.	O	-1.08863 2.70881 0.
O	1.06526 2.71869 0.	O	1.06215 2.72234 0.	O	1.06214 2.72231 0.
H	-0.79564 -3.79127 0.	H	-0.79388 -3.79483 0.	H	-0.79374 -3.79493 0.
H	-2.13487 -1.9279 0.	H	-2.13504 -1.92968 0.	H	-2.13507 -1.92955 0.
H	-2.13511 0.56289 0.	H	-2.14262 0.54996 0.	H	-2.14238 0.55031 0.
H	2.13765 0.58442 0.	H	2.14511 0.57659 0.	H	2.14489 0.57682 0.
H	2.15488 -1.92208 0.	H	2.16029 -1.91485 0.	H	2.16014 -1.91506 0.

B3LYP (Gas)

O	0.08968 -3.43196 0.	O	0.08969 -3.42586 0.	O	0.0898 -3.42609 0.
C	-1.20083 -1.38531 0.	C	-1.20374 -1.38513 0.	C	-1.20363 -1.38516 0.
C	-1.21066 0.0022 0.	C	-1.21282 -0.0004 0.	C	-1.21273 -0.00033 0.
C	0. 0.68869 0.	C	0. 0.69021 0.	C	0. 0.69015 0.
C	1.21986 0.01231 0.	C	1.2227 0.01272 0.	C	1.22261 0.01272 0.

C	1.2276 -1.3724 0.	C	1.22973 -1.36998 0.	C	1.22967 -1.37005 0.
C	0.01708 -2.07506 0.	C	0.01707 -2.07455 0.	C	0.01709 -2.07457 0.
N	-0.00895 2.15771 0.	N	-0.0092 2.14519 0.	N	-0.00924 2.14562 0.
O	-1.09787 2.72301 0.	O	-1.09585 2.72544 0.	O	-1.09596 2.72535 0.
O	1.07273 2.73582 0.	O	1.07041 2.73837 0.	O	1.07037 2.73836 0.
H	-0.79421 -3.81573 0.	H	-0.79326 -3.81796 0.	H	-0.7931 -3.81809 0.
H	-2.13767 -1.93315 0.	H	-2.13849 -1.93376 0.	H	-2.13849 -1.93368 0.
H	-2.13891 0.5567 0.	H	-2.14607 0.54474 0.	H	-2.14583 0.54509 0.
H	2.14152 0.57771 0.	H	2.1487 0.57012 0.	H	2.14849 0.57035 0.
H	2.15729 -1.92703 0.	H	2.16196 -1.92025 0.	H	2.16182 -1.92046 0.

CAM-B3LYP (Gas) ***CAM-B3LYP (Water)*** ***CAM-B3LYP (Methanol)***

O	0.08812 -3.41618 0.	O	0.08889 -3.41151 0.	O	0.08897 -3.41168 0.
C	-1.19569 -1.37942 0.	C	-1.19741 -1.38026 0.	C	-1.19733 -1.38026 0.
C	-1.20543 0.0032 0.	C	-1.20717 0.00011 0.	C	-1.2071 0.00018 0.
C	0. 0.68393 0.	C	0. 0.68465 0.	C	0. 0.68462 0.
C	1.21517 0.01341 0.	C	1.21785 0.01429 0.	C	1.21777 0.01428 0.
C	1.22278 -1.36612 0.	C	1.22535 -1.3639 0.	C	1.22529 -1.36396 0.
C	0.01719 -2.06454 0.	C	0.01829 -2.06439 0.	C	0.01829 -2.06441 0.
N	-0.00884 2.14941 0.	N	-0.00993 2.13906 0.	N	-0.00995 2.1394 0.
O	-1.08935 2.70976 0.	O	-1.08827 2.7121 0.	O	-1.08836 2.71202 0.
O	1.06474 2.72197 0.	O	1.06079 2.72611 0.	O	1.06081 2.72607 0.
H	-0.79271 -3.80252 0.	H	-0.79183 -3.80466 0.	H	-0.79167 -3.80479 0.
H	-2.13121 -1.92787 0.	H	-2.13071 -1.9301 0.	H	-2.13075 -1.92997 0.
H	-2.13217 0.55933 0.	H	-2.13946 0.54611 0.	H	-2.13923 0.54646 0.
H	2.13525 0.58056 0.	H	2.14234 0.57344 0.	H	2.14214 0.57365 0.
H	2.15057 -1.92257 0.	H	2.15645 -1.91488 0.	H	2.15629 -1.91511 0.

3-Nitrocatechol

PBE (Gas) ***PBE (Water)*** ***PBE (Methanol)***

O	1.61303 -1.1568 0.	O	1.61993 -1.15264 0.	O	1.61971 -1.15278 0.
O	-0.36552 -2.96475 0.	O	-0.35709 -2.96957 0.	O	-0.3574 -2.96942 0.
C	-2.01589 -1.23404 0.	C	-2.00812 -1.24185 0.	C	-2.00838 -1.2416 0.
C	-2.34244 0.13564 0.	C	-2.34181 0.12713 0.	C	-2.34184 0.12739 0.
C	-1.34736 1.10279 0.	C	-1.35113 1.09748 0.	C	-1.35101 1.09765 0.
C	0. 0.69286 0.	C	0. 0.69373 0.	C	0. 0.69373 0.
C	0.35351 -0.67707 0.	C	0.3608 -0.6773 0.	C	0.36055 -0.67728 0.
C	-0.6853 -1.64195 0.	C	-0.67605 -1.64483 0.	C	-0.67634 -1.64473 0.
N	1.04293 1.7015 0.	N	1.03122 1.70275 0.	N	1.03159 1.70273 0.
O	0.73972 2.89113 0.	O	0.72329 2.89682 0.	O	0.72388 2.89667 0.
O	2.24632 1.30347 0.	O	2.24036 1.32164 0.	O	2.24055 1.32102 0.
H	2.20054 -0.33964 0.	H	2.21245 -0.34384 0.	H	2.21208 -0.34373 0.
H	0.60958 -3.03188 0.	H	0.61752 -3.04947 0.	H	0.61723 -3.04902 0.
H	-2.79447 -1.99933 0.	H	-2.78701 -2.00695 0.	H	-2.78724 -2.00674 0.
H	-3.39093 0.43722 0.	H	-3.39152 0.42337 0.	H	-3.39151 0.42384 0.
H	-1.56888 2.16943 0.	H	-1.5839 2.16141 0.	H	-1.58347 2.16166 0.

PBE0 (Gas)

O	1.60826	-1.1503	0.
O	-0.34162	-2.93978	0.
C	-1.98879	-1.23623	0.
C	-2.32381	0.12078	0.
C	-1.33941	1.08468	0.
C	0.	0.68457	0.
C	0.36036	-0.6693	0.
C	-0.66548	-1.63179	0.
N	1.02654	1.70098	0.
O	0.70394	2.86466	0.
O	2.20624	1.32666	0.
H	2.20973	-0.37411	0.
H	0.6205	-3.01338	0.
H	-2.75535	-2.00314	0.
H	-3.36666	0.4149	0.
H	-1.56581	2.14271	0.

PBE0 (Water)

O	1.61345	-1.14768	0.
O	-0.33437	-2.94388	0.
C	-1.98261	-1.2422	0.
C	-2.32361	0.11433	0.
C	-1.34257	1.08045	0.
C	0.	0.68498	0.
C	0.36662	-0.66954	0.
C	-0.65826	-1.6336	0.
N	1.01691	1.70155	0.
O	0.69115	2.86905	0.
O	2.20122	1.34221	0.
H	2.22131	-0.37937	0.
H	0.62775	-3.02745	0.
H	-2.75034	-2.00818	0.
H	-3.36746	0.40397	0.
H	-1.57868	2.1361	0.

PBE0 (Methanol)

O	1.61329	-1.14779	0.
O	-0.33465	-2.94376	0.
C	-1.98281	-1.242	0.
C	-2.32362	0.11454	0.
C	-1.34247	1.0806	0.
C	0.	0.68498	0.
C	0.36641	-0.66954	0.
C	-0.6585	-1.63354	0.
N	1.01723	1.70154	0.
O	0.69161	2.86893	0.
O	2.20139	1.3417	0.
H	2.22097	-0.37926	0.
H	0.62745	-3.02712	0.
H	-2.75049	-2.00802	0.
H	-3.36743	0.40435	0.
H	-1.57828	2.13632	0.

B3LYP (Gas)

O	1.61497	-1.15856	0.
O	-0.35009	-2.95569	0.
C	-1.9966	-1.2408	0.
C	-2.33155	0.11997	0.
C	-1.34441	1.08609	0.
C	0.	0.68661	0.
C	0.35925	-0.67286	0.
C	-0.6698	-1.63664	0.
N	1.03116	1.71011	0.
O	0.70599	2.88364	0.
O	2.22315	1.33741	0.
H	2.22535	-0.38841	0.
H	0.61345	-3.04091	0.
H	-2.763	-2.00633	0.
H	-3.37324	0.41449	0.
H	-1.57403	2.14184	0.

B3LYP (Water)

O	1.62014	-1.155	0.
O	-0.34253	-2.95989	0.
C	-1.99016	-1.24642	0.
C	-2.33112	0.11388	0.
C	-1.34779	1.08208	0.
C	0.	0.68736	0.
C	0.36527	-0.67319	0.
C	0.66263	-1.63822	0.
N	1.02071	1.70935	0.
O	0.69393	2.88781	0.
O	2.21796	1.35189	0.
H	2.23523	-0.39097	0.
H	0.62096	-3.05412	0.
H	-2.75779	-2.01083	0.
H	-3.3738	0.40366	0.
H	-1.58692	2.13538	0.

B3LYP (Methanol)

O	1.61999	-1.15513	0.
O	-0.3428	-2.95976	0.
C	-1.99037	-1.24624	0.
C	-2.33114	0.11405	0.
C	-1.34769	1.0822	0.
C	0.	0.68736	0.
C	0.36507	-0.67319	0.
C	-0.66285	-1.63817	0.
N	1.02104	1.7094	0.
O	0.69433	2.8877	0.
O	2.21813	1.35144	0.
H	2.23495	-0.39094	0.
H	0.62068	-3.0538	0.
H	-2.75792	-2.01071	0.
H	-3.37377	0.40401	0.
H	-1.58656	2.13557	0.

CAM-B3LYP (Gas)

O	1.60497	-1.16094	0.
O	-0.34876	-2.93939	0.
C	-1.99023	-1.23137	0.
C	-2.32241	0.12465	0.
C	-1.33665	1.08399	0.
C	0.	0.68124	0.
C	0.35617	-0.6692	0.
C	-0.67061	-1.62668	0.
N	1.03175	1.7024	0.
O	0.70794	2.86635	0.
O	2.21118	1.33027	0.

CAM-B3LYP (Water)

O	1.60959	-1.1584	0.
O	-0.34152	-2.94354	0.
C	-1.9848	-1.23651	0.
C	-2.3224	0.11909	0.
C	-1.33952	1.08006	0.
C	0.	0.68155	0.
C	0.36164	-0.66942	0.
C	-0.66445	-1.62765	0.
N	1.02266	1.70222	0.
O	0.69706	2.87021	0.
O	2.20646	1.34419	0.

CAM-B3LYP (Methanol)

O	1.60944	-1.1585	0.
O	-0.3418	-2.94341	0.
C	-1.98499	-1.23634	0.
C	-2.3224	0.11928	0.
C	-1.33943	1.08019	0.
C	0.	0.68155	0.
C	0.36145	-0.66942	0.
C	-0.66465	-1.62762	0.
N	1.02296	1.70224	0.
O	0.69745	2.87011	0.
O	2.20662	1.34373	0.

H	2.22513 -0.40346 0.	H	2.2351 -0.40748 0.	H	2.23481 -0.40742 0.
H	0.61349 -3.0244 0.	H	0.62095 -3.03587 0.	H	0.62066 -3.03561 0.
H	-2.75606 -1.99661 0.	H	-2.75228 -2.00032 0.	H	-2.75239 -2.00021 0.
H	-3.36274 0.42128 0.	H	-3.36357 0.41178 0.	H	-3.36353 0.41211 0.
H	-1.56224 2.14015 0.	H	-1.57432 2.13395 0.	H	-1.57396 2.13416 0.

4-Nitrocatechol

PBE (Gas)

O	1.44875 2.46394 0.	O	1.45203 2.45984 0.	O	1.45186 2.45999 0.
O	-1.16364 3.02777 0.	O	-1.151 3.02529 0.	O	-1.15155 3.02534 0.
C	-1.74774 0.71368 0.	C	-1.74486 0.71725 0.	C	-1.74499 0.71707 0.
C	-1.36204 -0.62671 0.	C	-1.36456 -0.62272 0.	C	-1.36448 -0.62291 0.
C	0. -0.93965 0.	C	0. -0.9398 0.	C	0. -0.93981 0.
C	0.99 0.05388 0.	C	0.99669 0.0518 0.	C	0.99642 0.05191 0.
C	0.59379 1.3841 0.	C	0.60691 1.38393 0.	C	0.60641 1.38396 0.
C	-0.78091 1.7257 0.	C	-0.77207 1.72524 0.	C	-0.77243 1.72522 0.
O	1.64033 -2.58492 0.	O	1.62661 -2.59802 0.	O	1.62717 -2.59747 0.
O	-0.46023 -3.21698 0.	O	-0.47489 -3.21492 0.	O	-0.4742 -3.21506 0.
N	0.42271 -2.34984 0.	N	0.40907 -2.3394 0.	N	0.4096 -2.33972 0.
H	2.37192 2.16147 0.	H	2.38298 2.17538 0.	H	2.3826 2.175 0.
H	-0.35553 3.57702 0.	H	-0.34406 3.57985 0.	H	-0.34463 3.57981 0.
H	-2.80129 0.99793 0.	H	-2.79845 1.00106 0.	H	-2.79859 1.00086 0.
H	-2.0962 -1.43188 0.	H	-2.1081 -1.41855 0.	H	-2.10773 -1.41903 0.
H	2.04187 -0.24018 0.	H	2.04956 -0.23368 0.	H	2.04929 -0.23372 0.

PBE0 (Gas)

O	1.4375 2.43997 0.	O	1.43948 2.43751 0.	O	1.43937 2.4376 0.
O	-1.15197 3.00012 0.	O	-1.14168 2.99846 0.	O	-1.1421 2.99849 0.
C	-1.73411 0.70683 0.	C	-1.73181 0.70973 0.	C	-1.73191 0.7096 0.
C	-1.3512 -0.62549 0.	C	-1.35327 -0.62245 0.	C	-1.35321 -0.62258 0.
C	0. -0.93339 0.	C	0. -0.93268 0.	C	0. -0.9327 0.
C	0.98276 0.0528 0.	C	0.98886 0.05145 0.	C	0.98864 0.05153 0.
C	0.58903 1.37332 0.	C	0.60019 1.37385 0.	C	0.59979 1.37385 0.
C	-0.77479 1.7112 0.	C	-0.76739 1.71046 0.	C	-0.76768 1.71047 0.
O	1.61604 -2.56031 0.	O	1.60409 -2.57304 0.	O	1.60456 -2.57257 0.
O	-0.44757 -3.18275 0.	O	-0.45894 -3.18156 0.	O	-0.45843 -3.18166 0.
N	0.41983 -2.33105 0.	N	0.40871 -2.32275 0.	N	0.40912 -2.323 0.
H	2.35241 2.14981 0.	H	2.36159 2.16346 0.	H	2.36129 2.16312 0.
H	-0.35998 3.55112 0.	H	-0.35052 3.55404 0.	H	-0.35097 3.554 0.
H	-2.78036 0.98929 0.	H	-2.77847 0.9907 0.	H	-2.77856 0.9906 0.
H	-2.08106 -1.42452 0.	H	-2.09191 -1.41278 0.	H	-2.09159 -1.41317 0.
H	2.02805 -0.23622 0.	H	2.0353 -0.22922 0.	H	2.03506 -0.22929 0.

B3LYP (Gas)

O	1.44665 2.45137 0.	O	1.4493 2.44834 0.	O	1.44914 2.44846 0.
O	-1.16245 3.01392 0.	O	-1.15232 3.01189 0.	O	-1.15277 3.01193 0.
C	-1.73908 0.71066 0.	C	-1.73687 0.71322 0.	C	-1.73698 0.71308 0.
C	-1.35528 -0.62497 0.	C	-1.35764 -0.62184 0.	C	-1.35757 -0.62199 0.

C	0. -0.93528 0.	C	0. -0.93495 0.	C	0. -0.93497 0.
C	0.98465 0.05506 0.	C	0.99056 0.05392 0.	C	0.99033 0.054 0.
C	0.58948 1.37902 0.	C	0.60056 1.37914 0.	C	0.60014 1.37916 0.
C	-0.77742 1.71781 0.	C	-0.77004 1.71672 0.	C	-0.77036 1.71673 0.
O	1.62761 -2.57605 0.	O	1.61583 -2.58795 0.	O	1.61632 -2.58746 0.
O	-0.45118 -3.20215 0.	O	-0.46241 -3.20087 0.	O	-0.46184 -3.20099 0.
N	0.42181 -2.34137 0.	N	0.4104 -2.33149 0.	N	0.41085 -2.33179 0.
H	2.36482 2.16181 0.	H	2.37398 2.17293 0.	H	2.37366 2.17269 0.
H	-0.37467 3.57518 0.	H	-0.36533 3.57744 0.	H	-0.3658 3.5774 0.
H	-2.78461 0.99181 0.	H	-2.78263 0.99316 0.	H	-2.78274 0.99303 0.
H	-2.08682 -1.42035 0.	H	-2.09755 -1.40876 0.	H	-2.09722 -1.40918 0.
H	2.02943 -0.22946 0.	H	2.03624 -0.22298 0.	H	2.036 -0.22303 0.

CAM-B3LYP (Gas) ***CAM-B3LYP (Water)*** ***CAM-B3LYP (Methanol)***

O	1.43458 2.44317 0.	O	1.436 2.44143 0.	O	1.43591 2.4415 0.
O	-1.15516 2.99994 0.	O	-1.1462 2.99896 0.	O	-1.14658 2.99896 0.
C	-1.73333 0.70567 0.	C	-1.73151 0.70785 0.	C	-1.7316 0.70774 0.
C	-1.34859 -0.62539 0.	C	-1.35042 -0.62304 0.	C	-1.35037 -0.62315 0.
C	0. -0.92949 0.	C	0. -0.92847 0.	C	0. -0.9285 0.
C	0.98102 0.05537 0.	C	0.98635 0.05461 0.	C	0.98615 0.05467 0.
C	0.58436 1.3726 0.	C	0.59378 1.37306 0.	C	0.59344 1.37306 0.
C	-0.77654 1.70772 0.	C	-0.7702 1.70623 0.	C	-0.77046 1.70626 0.
O	1.61908 -2.56284 0.	O	1.60844 -2.57449 0.	O	1.60887 -2.57405 0.
O	-0.443 -3.18654 0.	O	-0.45204 -3.18584 0.	O	-0.45159 -3.18593 0.
N	0.42254 -2.33233 0.	N	0.41298 -2.32445 0.	N	0.41335 -2.32469 0.
H	2.35404 2.16324 0.	H	2.36183 2.1751 0.	H	2.36156 2.17481 0.
H	-0.36752 3.55914 0.	H	-0.3583 3.56104 0.	H	-0.35874 3.56102 0.
H	-2.77817 0.98672 0.	H	-2.77696 0.98659 0.	H	-2.77703 0.98653 0.
H	-2.07711 -1.42295 0.	H	-2.08708 -1.41247 0.	H	-2.08679 -1.41282 0.
H	2.0254 -0.22861 0.	H	2.03196 -0.22105 0.	H	2.03174 -0.22113 0.

2-Nitropyrrole

PBE (Gas) ***PBE (Water)*** ***PBE (Methanol)***

N 1.436 0.02031 -0.00011	N 1.42391 0.01738 0.	N 1.424307 0.017483 0.000000
O 1.93621 -1.12479 -0.00023	O 1.95217 -1.11954 -0.00001	O 1.951672 -1.119700 -0.000009
O 2.07675 1.07993 0.00008	O 2.07072 1.08462 0.00001	O 2.070914 1.084444 0.000005
C 0.01259 0.10033 -0.00012	C 0.01505 0.08853 -0.00001	C 0.014965 0.088892 -0.000008
N -0.73538 -1.05267 0.0003	N -0.74339 -1.06011 0.00001	N -0.743157 -1.059882 0.000008
C -2.05919 -0.71676 0.00007	C -2.05888 -0.7133 0.	C -2.058923 -0.713386 0.000004
C -2.15458 0.67679 -0.00041	C -2.1478 0.68557 -0.00001	C -2.148015 0.685306 -0.000010

C	-0.84128	1.19971	0.00039	C	-0.83598	1.19843	0.00001	C	-0.836107	1.198461	0.000009
H	-0.31513	-1.97931	0.00075	H	-0.35436	-2.00119	0.00003	H	-0.353204	-2.000539	0.000025
H	-2.83193	-1.48002	-0.00004	H	-2.83596	-1.47217	-0.00001	H	-2.835906	-1.472347	-0.000003
H	-3.08002	1.24605	-0.00088	H	-3.0704	1.25933	-0.00002	H	-3.070669	1.258979	-0.000023
H	-0.52617	2.23835	0.00051	H	-0.52041	2.23712	0.	H	-0.520470	2.237116	0.000006

PBE0 (Gas)

N	1.42664	0.01904	0.00001
O	1.91754	-1.10442	-0.00001
O	2.05433	1.06069	-0.00002
C	0.01195	0.09725	0.
N	-0.72925	-1.04545	0.00001
C	-2.04109	-0.70884	-0.00001
C	-2.13631	0.67239	-0.00001
C	-0.82766	1.1902	0.00002
H	-0.32021	-1.96744	0.00005
H	-2.81135	-1.46465	-0.00003
H	-3.05461	1.23951	-0.00003
H	-0.51183	2.22141	0.00003

PBE0 (Water)

N	1.41541	0.01636	0.0001
O	1.93278	-1.09897	-0.00006
O	2.04881	1.06456	-0.00004
C	0.01456	0.08601	0.00003
N	-0.73726	-1.0524	0.00002
C	-2.04091	-0.70573	-0.00002
C	-2.1299	0.68094	-0.00002
C	-0.82291	1.1888	0.00001
H	-0.35708	-1.98776	0.00005
H	-2.81515	-1.45762	-0.00004
H	-3.04549	1.25254	-0.00005
H	-0.50707	2.22028	0.00002

PBE0 (Methanol)

N	-1.4158	0.01644	-0.00011
O	-1.93237	-1.09912	0.00006
O	-2.04897	1.06442	0.00005
C	-0.01446	0.08633	-0.00004
N	0.73706	-1.0522	-0.00002
C	2.04099	-0.70578	0.00002
C	2.13011	0.68069	0.00003
C	0.823	1.18882	-0.00002
H	0.35609	-1.98719	-0.00005
H	2.81515	-1.45775	0.00005
H	3.04573	1.25224	0.00006
H	0.5071	2.22027	-0.00002

B3LYP (Gas)

N	1.43131	0.0191	0.00001
O	1.9302	-1.11305	-0.00001
O	2.06664	1.06885	-0.00001
C	0.01193	0.09714	0.
N	-0.73608	-1.05058	0.00001
C	-2.05352	-0.70895	-0.00001
C	-2.14478	0.67605	-0.00001
C	-0.83159	1.19284	0.00002
H	-0.33062	-1.97511	0.00005
H	-2.82478	-1.46205	-0.00003
H	-3.06051	1.24532	-0.00003
H	-0.51768	2.22331	0.00002

B3LYP (Water)

N	1.41819	0.01654	-0.00001
O	1.94523	-1.10793	-0.00001
O	2.06128	1.07323	0.00001
C	0.01519	0.08587	-0.00001
N	-0.74385	-1.05771	0.00002
C	-2.05212	-0.70633	0.
C	-2.13771	0.68477	-0.00001
C	-0.82757	1.19171	0.
H	-0.36691	-1.99527	0.00003
H	-2.82763	-1.45507	0.
H	-3.05105	1.25769	-0.00002
H	-0.51362	2.2223	-0.00001

B3LYP (Methanol)

N	1.41863	0.01663	-0.00001
O	1.94479	-1.10807	-0.00001
O	2.06144	1.07306	0.00001
C	0.01507	0.0862	-0.00001
N	-0.74364	-1.0575	0.00001
C	-2.05221	-0.70637	0.
C	-2.13793	0.68451	-0.00001
C	-0.82764	1.19172	0.
H	-0.36589	-1.99468	0.00003
H	-2.82764	-1.45519	0.
H	-3.0513	1.25739	-0.00002
H	-0.51362	2.22228	-0.00001

CAM-B3LYP (Gas)

N	1.42823	0.01855	-0.00001
O	1.92088	-1.10425	0.00001
O	2.05806	1.05914	-0.00001
C	0.00889	0.09703	-0.00001
N	-0.73334	-1.04676	0.00001
C	-2.04584	-0.7039	-0.00001
C	-2.13661	0.67293	0.
C	-0.82455	1.18807	0.00002
H	-0.32949	-1.97123	0.00004

CAM-B3LYP (Water)

N	1.41672	0.01595	0.00003
O	1.93541	-1.0987	-0.00002
O	2.05271	1.06261	0.
C	0.01189	0.08608	0.
N	-0.74127	-1.05341	0.00001
C	-2.04503	-0.70111	-0.00001
C	-2.12996	0.68142	-0.00001
C	-0.82029	1.18669	0.
H	-0.3655	-1.99088	0.00004

CAM-B3LYP (Methanol)

N	1.41712	0.01604	0.00004
O	1.93502	-1.09884	-0.00003
O	2.05287	1.06248	-0.00001
C	0.01176	0.08639	0.
N	-0.74107	-1.05322	0.00002
C	-2.04512	-0.70115	-0.00001
C	-2.13017	0.68117	-0.00001
C	-0.82037	1.18671	0.
H	-0.36451	-1.99033	0.00004

H	-2.8178	-1.45575	-0.00003	H	-2.82095	-1.44905	-0.00001	H	-2.82097	-1.44916	-0.00002
H	-3.05115	1.24305	-0.00001	H	-3.04188	1.25576	-0.00002	H	-3.04213	1.25545	-0.00002
H	-0.5086	2.21762	0.00002	H	-0.50442	2.21651	-0.00001	H	-0.50444	2.2165	0.

3-Nitropyrrole

PBE (Gas)

N	1.4731	-0.00059	-0.00001
O	2.03412	-1.10828	0.
O	2.05925	1.09149	0.
C	0.03202	0.02009	0.
C	-0.76878	-1.11652	0.
N	-2.05843	-0.66898	0.
C	-2.09597	0.71725	0.
C	-0.79642	1.17882	0.00001
H	-0.50007	-2.16694	0.00001
H	-2.87551	-1.27123	0.
H	-3.04072	1.25187	-0.00001
H	-0.45845	2.20977	0.00001

PBE (Water)

N	1.45916	-0.00194	-0.00001
O	2.03934	-1.10736	0.00001
O	2.06315	1.08934	0.
C	0.03516	0.02093	0.
C	-0.77394	-1.11898	0.
N	-2.05352	-0.66871	0.
C	-2.09238	0.71771	0.
C	-0.79531	1.18317	0.
H	-0.51912	-2.17286	0.
H	-2.87388	-1.27057	-0.00001
H	-3.03959	1.24757	0.00001
H	-0.46805	2.21758	0.

PBE (Methanol)

N	1.45961	-0.00187	-0.00001
O	2.03913	-1.10738	0.
O	2.06313	1.08934	0.
C	0.03503	0.02094	0.
C	-0.77376	-1.11888	0.
N	-2.05369	-0.66871	0.
C	-2.09253	0.71767	0.
C	-0.79536	1.18304	0.
H	-0.51853	-2.17264	0.
H	-2.87393	-1.27061	0.
H	-3.03963	1.24772	-0.00001
H	-0.46778	2.21734	0.00001

PBE0 (Gas)

N	-1.46299	-0.00025	-0.00005
O	-2.01366	-1.08867	0.00002
O	-2.03825	1.07275	0.00003
C	-0.03297	0.0199	-0.00003
C	0.75933	-1.10648	-0.00001
N	2.03891	-0.66539	0.00001
C	2.0781	0.70883	0.00001
C	0.7908	1.17164	-0.00001
H	0.48939	-2.1496	-0.00002
H	2.84771	-1.26403	0.00003
H	3.01668	1.24011	0.00003
H	0.45839	2.19705	-0.00002

PBE0 (Water)

N	1.45057	-0.0015	0.00007
O	2.01892	-1.08717	-0.00004
O	2.04236	1.07013	-0.00004
C	0.03562	0.02072	0.00003
C	-0.76443	-1.10882	0.00001
N	-2.03437	-0.66505	-0.00002
C	-2.0753	0.70917	-0.00001
C	-0.79007	1.1758	0.00001
H	-0.50803	-2.15541	0.00002
H	-2.84624	-1.26384	-0.00004
H	-3.01642	1.2357	-0.00003
H	-0.46786	2.20459	0.00002

PBE0 (Methanol)

N	-1.45096	-0.00145	-0.0001
O	-2.01878	-1.08717	0.00006
O	-2.04225	1.07016	0.00005
C	-0.03549	0.02068	-0.00005
C	0.76426	-1.10877	-0.00002
N	2.03452	-0.66504	0.00002
C	2.07539	0.70915	0.00003
C	0.7901	1.17566	-0.00002
H	0.50752	-2.15526	-0.00003
H	2.84629	-1.26383	0.00004
H	3.01639	1.23589	0.00006
H	0.46758	2.20435	-0.00003

B3LYP (Gas)

N	-1.46754	-0.00005	-0.0001
O	-2.02718	-1.09588	0.00005
O	-2.04908	1.08159	0.00006
C	-0.03139	0.01865	-0.00005
C	0.76321	-1.1109	-0.00002
N	2.04943	-0.66891	0.00002
C	2.08722	0.7136	0.00003
C	0.79656	1.17445	-0.00002
H	0.49513	-2.15306	-0.00003
H	2.85916	-1.26841	0.00005
H	3.02434	1.24495	0.00006
H	0.46472	2.1987	-0.00004

B3LYP (Water)

N	1.45356	-0.00133	-0.00002
O	2.03211	-1.09491	0.00001
O	2.05338	1.07916	0.00001
C	0.03476	0.01988	-0.00001
C	-0.76865	-1.11318	0.
N	-2.04406	-0.66886	0.
C	-2.08397	0.71401	0.00001
C	-0.79591	1.17891	0.
H	-0.51306	-2.15849	0.
H	-2.8569	-1.26833	0.
H	-3.02377	1.24014	0.00001
H	-0.47401	2.20634	0.

B3LYP (Methanol)

N	1.45402	-0.00127	-0.00002
O	2.03195	-1.09492	0.
O	2.0533	1.07917	0.00001
C	0.03462	0.01985	-0.00001
C	-0.76849	-1.11309	0.
N	-2.04426	-0.66884	0.00001
C	-2.08409	0.71398	0
C	-0.79593	1.17876	0.
H	-0.51254	-2.1583	0.
H	-2.85701	-1.26832	0.00001
H	-3.02378	1.24034	0.
H	-0.4737	2.20608	0.

CAM-B3LYP (Gas)

N	-1.46337	0.00025	-0.00002
O	-2.0178	-1.08726	0.00001
O	-2.04007	1.07332	0.00002
C	-0.02972	0.01835	-0.00001
C	0.75809	-1.10527	-0.00001
N	2.0406	-0.66728	0.00001
C	2.07851	0.70931	0.00001
C	0.79462	1.17072	-0.00001
H	0.48627	-2.14636	-0.00001
H	2.84902	-1.26707	0.00002
H	3.01518	1.24075	0.00001
H	0.46293	2.19469	-0.00001

CAM-B3LYP (Water)

N	1.45093	-0.00098	0.00003
O	2.02286	-1.08557	-0.00001
O	2.04432	1.07049	-0.00002
C	0.03254	0.01938	0.00001
C	-0.76321	-1.10743	0.00001
N	-2.03566	-0.667	-0.00001
C	-2.07597	0.70952	0.
C	-0.79415	1.1748	0.
H	-0.5046	-2.15197	0.00001
H	-2.84702	-1.26723	-0.00002
H	-3.01537	1.23594	-0.00001
H	-0.47262	2.20211	0.00001

CAM-B3LYP (Methanol)

N	-1.45133	-0.00093	-0.00004
O	-2.02274	-1.08557	0.00002
O	-2.04422	1.07053	0.00002
C	-0.0324	0.01933	-0.00002
C	0.76306	-1.10737	-0.00001
N	2.03584	-0.66698	0.00001
C	2.07606	0.70951	0.00001
C	0.79416	1.17466	-0.00001
H	0.50412	-2.15182	-0.00002
H	2.84712	-1.2672	0.00002
H	3.01533	1.23616	0.00002
H	0.47231	2.20186	-0.00001

2-Nitrofuran

PBE (Gas)

N	1.43356	-0.00179	0.00008
O	2.03982	1.08066	-0.00033
O	1.94778	-1.12498	0.00019
C	-0.00138	0.08756	0.
O	-0.69893	-1.07954	0.00025
C	-2.01476	-0.72311	0.00019
C	-2.15332	0.64442	-0.00066
C	-0.83346	1.18065	0.00034
H	-2.71914	-1.54895	0.0002
H	-3.08918	1.1962	-0.00127
H	-0.51847	2.21911	0.00044

PBE (Water)

N	1.4197	0.0019	0.00005
O	2.04819	1.07723	-0.00024
O	1.94474	-1.12521	0.00002
C	0.00118	0.09148	-0.00001
O	-0.69313	-1.08014	0.00005
C	-2.00982	-0.72649	0.00008
C	-2.15202	0.64268	-0.00037
C	-0.83848	1.18354	0.00051
H	-2.71392	-1.55273	-0.00007
H	-3.08977	1.19072	-0.00077
H	-0.53771	2.22637	0.00072

PBE (Methanol)

N	1.42013	0.00179	0.00004
O	2.04805	1.07727	-0.00025
O	1.94467	-1.12524	0.00003
C	0.00109	0.09146	-0.00002
O	-0.69323	-1.08003	0.00004
C	-2.00991	-0.72643	0.00008
C	-2.1521	0.64267	-0.00038
C	-0.83838	1.1835	0.00052
H	-2.71392	-1.55276	-0.00007
H	-3.08983	1.19077	-0.00077
H	-0.53727	2.22623	0.00075

PBE0 (Gas)

N	1.42238	-0.00243	0.00004
O	2.01822	1.06045	-0.0002
O	1.92637	-1.10606	-0.00006
C	-0.00326	0.08477	0.00003
O	-0.69193	-1.06532	0.00007
C	-1.99295	-0.71771	0.00013
C	-2.13563	0.63716	-0.00046
C	-0.82028	1.17162	0.00052
H	-2.69481	-1.53628	0.00004
H	-3.06622	1.18337	-0.00093
H	-0.50421	2.20236	0.00076

PBE0 (Water)

N	1.41004	0.00108	0.00002
O	2.02685	1.05658	-0.00021
O	1.92358	-1.10581	0.00002
C	-0.00094	0.0888	-0.00001
O	-0.68664	-1.06589	0.00003
C	-1.98864	-0.72099	0.00009
C	-2.13493	0.6354	-0.00036
C	-0.82543	1.17438	0.00048
H	-2.69029	-1.53999	-0.00003
H	-3.06722	1.17834	-0.00073
H	-0.5235	2.20958	0.00067

PBE0 (Methanol)

N	1.41043	0.00097	0.00002
O	2.02669	1.05664	-0.00022
O	1.92353	-1.10585	0.00003
C	-0.00102	0.08877	-0.00001
O	-0.68673	-1.0658	0.00002
C	-1.98872	-0.72094	0.00009
C	-2.13499	0.63539	-0.00035
C	-0.82532	1.17434	0.00048
H	-2.69029	-1.54	-0.00003
H	-3.06726	1.17838	-0.00072
H	-0.52305	2.20944	0.00067

B3LYP (Gas)

N	1.42831	-0.00285	0.00012
O	2.03287	1.0676	-0.00031

B3LYP (Water)

N	1.41458	0.00097	0.00006
O	2.04146	1.06398	-0.00022

B3LYP (Methanol)

N	1.41502	0.00085	0.00006
O	2.0413	1.06403	-0.00023

O	1.93849	-1.1149	0.00013	O	1.93566	-1.11487	0.	O	1.9356	-1.1149	0.00001
C	-0.00261	0.08627	0.00003	C	0.00029	0.09017	0.	C	0.00018	0.09015	0.
O	-0.69912	-1.07052	0.00025	O	-0.69361	-1.07151	0.00005	O	-0.6937	-1.07139	0.00005
C	-2.0086	-0.71754	0.00015	C	-2.00387	-0.72077	0.00006	C	-2.00397	-0.72072	0.00006
C	-2.14479	0.64055	-0.00065	C	-2.14357	0.63903	-0.00034	C	-2.14365	0.63901	-0.00034
C	-0.82426	1.17424	0.00035	C	-0.82963	1.17698	0.00045	C	-0.82951	1.17695	0.00046
H	-2.71084	-1.53401	0.00015	H	-2.70619	-1.53736	-0.00008	H	-2.70618	-1.5374	-0.00008
H	-3.07198	1.19057	-0.00126	H	-3.07245	1.18561	-0.00069	H	-3.07252	1.18563	-0.00069
H	-0.51175	2.20478	0.00045	H	-0.53083	2.21173	0.00063	H	-0.5304	2.2116	0.00064

CAM-B3LYP (Gas) ***CAM-B3LYP (Water)*** ***CAM-B3LYP (Methanol)***

N	1.42474	-0.00348	0.00014	N	1.41273	0.0002	0.00006	N	1.4131	0.00009	0.00006
O	2.02439	1.05793	0.00002	O	2.03325	1.05347	-0.00033	O	2.03309	1.05355	-0.00033
O	1.92898	-1.10699	0.00034	O	1.92574	-1.10666	0.00021	O	1.9257	-1.1067	0.00022
C	-0.00591	0.08624	-0.00003	C	-0.00358	0.09046	-0.00001	C	-0.00367	0.09042	-0.00002
O	-0.69607	-1.06395	0.0001	O	-0.69091	-1.06466	0.00022	O	-0.69099	-1.06457	0.00022
C	-2.00002	-0.71378	-0.00014	C	-1.99602	-0.7167	0.00017	C	-1.99609	-0.71666	0.00017
C	-2.13716	0.6365	-0.00023	C	-2.13633	0.63478	-0.00054	C	-2.13639	0.63478	-0.00055
C	-0.81741	1.16993	-0.00023	C	-0.82233	1.1726	0.00028	C	-0.82223	1.17257	0.00028
H	-2.70242	-1.52968	-0.00014	H	-2.69852	-1.53279	0.00017	H	-2.69849	-1.53282	0.00017
H	-3.06417	1.18559	-0.00034	H	-3.06482	1.18103	-0.00105	H	-3.06487	1.18105	-0.00106
H	-0.50203	2.19923	-0.00035	H	-0.52087	2.20632	0.00031	H	-0.52044	2.20618	0.00031

2-Nitrothiophene

PBE (Gas) ***PBE (Water)*** ***PBE (Methanol)***

N	1.61991	0.04815	-0.00006	N	1.60788	0.04945	-0.00018	N	1.60827	0.04939	-0.00018
O	2.30265	1.08006	-0.00001	O	2.30671	1.07737	0.0001	O	2.30657	1.07744	0.0001
O	2.06373	-1.11093	0.00011	O	2.06734	-1.11013	0.00013	O	2.06725	-1.11014	0.00012
C	0.18424	0.20313	-0.00006	C	0.18652	0.20226	-0.00011	C	0.18643	0.20227	-0.00011
S	-0.84036	-1.20186	-0.00003	S	-0.84192	-1.20347	-0.00003	S	-0.84189	-1.20342	-0.00003
C	-2.23493	-0.18175	0.00002	C	-2.23219	-0.18153	0.00008	C	-2.23228	-0.18151	0.00008
C	-1.91657	1.16343	0.00005	C	-1.91324	1.16555	0.00005	C	-1.91334	1.1655	0.00005
C	-0.5177	1.39152	0.	C	-0.51758	1.39431	-0.00005	C	-0.51756	1.3942	-0.00005
H	-3.22395	-0.63577	0.00003	H	-3.22024	-0.63769	0.00014	H	-3.22037	-0.6376	0.00013
H	-2.66552	1.95494	0.00009	H	-2.66298	1.95579	0.00011	H	-2.66302	1.95581	0.00011
H	-0.02544	2.36259	0.	H	-0.0347	2.3699	-0.00008	H	-0.03437	2.36965	-0.00008

PBE0 (Gas) ***PBE0 (Water)*** ***PBE0 (Methanol)***

N	1.60867	0.04655	-0.00002	N	1.59801	0.04784	0.00001	N	1.59835	0.04779	0.00001
O	2.27698	1.06199	-0.00007	O	2.28139	1.05874	-0.00006	O	2.28125	1.05883	-0.00006
O	2.04628	-1.09083	0.00013	O	2.04983	-1.08939	0.00008	O	2.04975	-1.08942	0.00008
C	0.18213	0.19678	-0.00004	C	0.18388	0.19606	-0.00002	C	0.18381	0.19607	-0.00002
S	-0.83469	-1.19104	-0.00006	S	-0.8362	-1.19255	-0.00004	S	-0.83617	-1.1925	-0.00004
C	-2.21514	-0.1789	0.00003	C	-2.2129	-0.17882	0.00002	C	-2.21298	-0.17881	0.00002
C	-1.9003	1.15466	0.00005	C	-1.8975	1.1565	0.00003	C	-1.89757	1.15645	0.00003

C	-0.506	1.37808	0.00002	C	-0.50622	1.38073	0.00001	C	-0.50619	1.38064	0.00001
H	-3.19946	-0.62632	0.00003	H	-3.19642	-0.62826	0.00002	H	-3.19653	-0.62817	0.00002
H	-2.64211	1.94271	0.0001	H	-2.63981	1.94369	0.00006	H	-2.63984	1.9437	0.00006
H	-0.0142	2.34142	0.00003	H	-0.02401	2.3488	0.00003	H	-0.02368	2.34856	0.00003

B3LYP (Gas)

N	1.61646	0.04625	-0.00003
O	2.29364	1.06862	-0.00006
O	2.06104	-1.09992	0.00012
C	0.18421	0.19746	-0.00004
S	-0.84591	-1.19957	-0.00004
C	-2.23056	-0.17016	0.00001
C	-1.90543	1.1631	0.00005
C	-0.50569	1.38132	0.00002
H	-3.21669	-0.61037	0.
H	-2.64102	1.95573	0.0001
H	-0.01567	2.34415	0.00004

B3LYP (Water)

N	1.60444	0.04758	-0.00003
O	2.29833	1.06546	-0.00004
O	2.0646	-1.09885	0.0001
C	0.18648	0.19651	-0.00004
S	-0.84762	-1.20118	-0.00004
C	-2.22779	-0.16997	0.00003
C	-1.90206	1.16535	0.00004
C	-0.50599	1.3842	0.00001
H	-3.21308	-0.61204	0.00004
H	-2.63819	1.95692	0.00007
H	-0.0252	2.35146	0.00002

B3LYP (Methanol)

N	1.60483	0.04753	-0.00003
O	2.29818	1.06554	-0.00004
O	2.06452	-1.09886	0.0001
C	0.18639	0.19652	-0.00004
S	-0.84759	-1.20113	-0.00004
C	2.22789	-0.16996	0.00003
C	-1.90216	1.16528	0.00004
C	-0.50596	1.3841	0.00001
H	-3.21321	-0.61195	0.00003
H	-2.63824	1.95692	0.00007
H	-0.02487	2.35121	0.00002

CAM-B3LYP (Gas)

N	1.61127	0.04555	-0.00006
O	2.28159	1.06042	-0.00007
O	2.05209	-1.09118	0.00017
C	0.17959	0.19455	-0.00005
S	-0.84228	-1.19244	-0.00007
C	-2.21884	-0.16973	0.00004
C	-1.89868	1.15672	0.00007
C	-0.49982	1.37373	0.00002
H	-3.20507	-0.6085	0.00004
H	-2.63372	1.94866	0.00013
H	-0.00671	2.33444	0.00004

CAM-B3LYP (Water)

N	1.60079	0.04678	0.00001
O	2.28619	1.05676	-0.00009
O	2.05565	-1.08954	0.00011
C	0.18145	0.1937	-0.00002
S	-0.84409	-1.19372	-0.00005
C	-2.2167	-0.16941	0.00002
C	-1.89572	1.15852	0.00004
C	-0.49997	1.37604	0.00003
H	-3.20216	-0.61002	0.00001
H	-2.63089	1.9499	0.00008
H	-0.01631	2.34137	0.00006

CAM-B3LYP (Methanol)

N	1.60113	0.04673	0.00001
O	2.28606	1.05685	-0.00009
O	2.05557	-1.08957	0.00011
C	0.18138	0.19371	-0.00002
S	-0.84406	-1.19368	-0.00005
C	-2.21678	-0.1694	0.00002
C	-1.8958	1.15847	0.00004
C	-0.49994	1.37595	0.00003
H	-3.20228	-0.60994	0.00001
H	-2.63094	1.9499	0.00007
H	-0.01598	2.34114	0.00005

3-Nitrothiophene

PBE (Gas)

S	-2.14714	-0.54238	-0.00005
O	2.2653	-1.21481	-0.00014
O	2.44714	0.98623	-0.00016
N	1.78442	-0.06717	0.00026
C	0.3335	0.05997	0.00014
C	-0.3433	1.31875	0.00007
C	-0.50112	-1.0427	0.00006
C	-1.70684	1.14454	-0.00005
H	0.16978	2.28001	0.0001
H	-0.21343	-2.09212	0.00009
H	-2.486	1.9057	-0.00012

PBE (Water)

N	1.7748	-0.06681	0.00018
O	2.2671	-1.20696	-0.00009
O	2.44544	0.9793	-0.00012
C	0.33172	0.05969	0.0001
C	-0.50281	-1.04262	0.00005
S	-2.14175	-0.54222	-0.00004
C	-1.70236	1.14409	-0.00003
C	-0.34393	1.3181	0.00005
H	-0.228	-2.09354	0.00007
H	-2.4836	1.90036	-0.00007
H	0.16004	2.28214	0.00007

PBE (Methanol)

S	-2.14185	-0.54213	-0.00002
O	2.26692	-1.20713	-0.00004
O	2.44544	0.97939	-0.00007
N	1.77522	-0.06653	0.00009
C	0.33171	0.05968	0.00005
C	-0.34402	1.31787	0.00003
C	-0.50253	-1.04259	0.00002
C	-1.70259	1.14389	-0.00002
H	0.16028	2.2817	0.00005
H	-0.22786	-2.0935	0.00002
H	-2.48359	1.90037	-0.00004

PBE0 (Gas)

S	-2.12559	-0.53883	0.00001
O	2.2437	-1.19368	0.00002
O	2.41922	0.97026	0.00001
N	1.77016	-0.06623	-0.00002
C	0.33115	0.05791	-0.00001
C	-0.34112	1.30993	0.
C	-0.49432	-1.03476	-0.00002
C	-1.69292	1.13244	0.
H	0.16711	2.26504	0.
H	-0.20385	-2.07575	-0.00003
H	-2.46514	1.88985	0.

PBE0 (Water)

N	1.76238	-0.06547	0.00003
O	2.24611	-1.18524	-0.00001
O	2.41826	0.96304	-0.00003
C	0.32928	0.05786	0.00002
C	-0.49546	-1.03489	0.00001
S	-2.1208	-0.53891	-0.00001
C	-1.69008	1.13159	0.
C	-0.34249	1.30942	0.00002
H	-0.2178	-2.07801	0.00001
H	-2.46488	1.88452	-0.00001
H	0.15637	2.26802	0.00002

PBE0 (Methanol)

S	-2.12092	-0.53877	0.00001
O	2.24586	-1.18535	0.00005
O	2.41814	0.96315	0.00003
N	1.76276	-0.06548	-0.00007
C	0.32926	0.05775	-0.00003
C	-0.34238	1.30924	-0.00001
C	-0.49547	-1.03492	-0.00003
C	-1.69003	1.13163	0.00001
H	0.15735	2.26738	-0.00001
H	-0.21754	-2.07796	-0.00005
H	-2.4647	1.88468	0.00003

B3LYP (Gas)

S	-2.13865	-0.54131	0.
O	2.25822	-1.19586	-0.00001
O	2.43022	0.97311	-0.00003
N	1.78015	-0.0667	0.00003
C	0.32904	0.05571	0.00002
C	-0.3451	1.31082	0.00002
C	-0.495	-1.0365	-0.00001
C	-1.69575	1.14083	-0.00001
H	0.16399	2.26275	0.00003
H	-0.20849	-2.07561	-0.00001
H	-2.46482	1.89758	-0.00002

B3LYP (Water)

N	1.76895	-0.06627	0.00009
O	2.26206	-1.19391	-0.00004
O	2.4331	0.97016	-0.00007
C	0.32977	0.0565	0.00005
C	-0.49738	-1.03823	0.00002
S	-2.13547	-0.54209	-0.00002
C	-1.6946	1.14158	-0.00001
C	-0.34508	1.31372	0.00003
H	-0.22153	-2.08011	0.00003
H	-2.46608	1.89583	-0.00003
H	0.15494	2.27019	0.00004

B3LYP (Methanol)

S	-2.13564	-0.54199	0.00001
O	2.26182	-1.19406	0.00004
O	2.433	0.97029	0.00002
N	1.76927	-0.06618	-0.00005
C	0.32968	0.05639	-0.00002
C	-0.34497	1.31353	0.
C	-0.49721	-1.03831	-0.00003
C	-1.69456	1.14167	0.00001
H	0.15588	2.26956	0.
H	-0.2209	-2.08006	-0.00004
H	-2.46587	1.8961	0.00002

CAM-B3LYP (Gas)

S	-2.12627	-0.5396	0.00001
O	2.24737	-1.18629	0.00003
O	2.41727	0.96638	0.00001
N	1.77309	-0.06577	-0.00004
C	0.32573	0.05518	-0.00002
C	-0.34604	1.30673	0.
C	-0.49186	-1.03113	-0.00003
C	-1.68998	1.13162	0.
H	0.16197	2.25856	0.
H	-0.19949	-2.06839	-0.00004
H	-2.45807	1.88873	0.00001

CAM-B3LYP (Water)

N	1.76345	-0.06517	0.00001
O	2.25167	-1.18382	0.
O	2.42034	0.96351	-0.00002
C	0.32588	0.05591	0.00001
C	-0.49368	-1.03297	0.
S	-2.12349	-0.54037	-0.00001
C	-1.68969	1.13206	0.
C	-0.34649	1.30922	0.00001
H	-0.21239	-2.07324	0.
H	-2.46028	1.88672	0.
H	0.15215	2.26582	0.00001

CAM-B3LYP (Methanol)

S	-2.12365	-0.54027	0.00002
O	2.25145	-1.18393	0.00006
O	2.42022	0.9636	0.00004
N	1.76385	-0.0652	-0.00009
C	0.32587	0.05581	-0.00004
C	-0.34641	1.3091	-0.00001
C	-0.49367	-1.03296	-0.00004
C	-1.68963	1.1321	0.00002
H	0.15307	2.26527	-0.00001
H	-0.21184	-2.0731	-0.00006
H	-2.46003	1.88694	0.00004

2-Ethylhexylnitrate

PBE (Gas)

C	2.29339	-0.59757	-0.52385
H	1.61875	-1.35821	-0.95546
H	2.42024	0.17764	-1.30096

PBE (Water)

C	2.29961	-0.59328	-0.52162
H	1.62925	-1.35577	-0.95649
H	2.42553	0.18458	-1.29601

PBE (Methanol)

C	2.29943	-0.59327	-0.52159
H	1.62889	-1.35577	-0.95616
H	2.42517	0.18449	-1.29613

C	3.65575	-1.25998	-0.25296	C	3.66441	-1.24978	-0.2488	C	3.66424	-1.24985	-0.24907
H	3.52944	-2.04547	0.51465	H	3.54072	-2.03239	0.52219	H	3.5407	-2.03258	0.52181
H	3.97798	-1.78311	-1.16971	H	3.98908	-1.77388	-1.16426	H	3.9887	-1.77382	-1.16468
C	4.7609	-0.29028	0.18256	C	4.76523	-0.27312	0.1833	C	4.76521	-0.27331	0.18287
H	5.72294	-0.81308	0.29792	H	5.72909	-0.79203	0.30396	H	5.7289	-0.79243	0.30386
H	4.90464	0.50894	-0.56365	H	4.90596	0.52175	-0.56834	H	4.90631	0.52123	-0.56903
H	4.53493	0.19143	1.14664	H	4.53339	0.21412	1.14336	H	4.53341	0.21431	1.14272
C	1.64461	0.01657	0.72709	C	1.6468	0.01243	0.73147	C	1.64692	0.01275	0.73152
H	1.56304	-0.76563	1.50486	H	1.56343	-0.77408	1.50399	H	1.56379	-0.77358	1.50429
H	2.30793	0.79268	1.14497	H	2.30471	0.78977	1.15491	H	2.30492	0.79023	1.15455
C	0.25056	0.66163	0.52496	C	0.251	0.65423	0.52918	C	0.25104	0.65445	0.52933
H	-0.08843	0.99727	1.52304	H	-0.09	0.97931	1.52994	H	-0.08974	0.98009	1.53001
C	0.30807	1.89668	-0.40023	C	0.30884	1.89566	-0.38619	C	0.3086	1.89546	-0.38671
H	1.2125	2.47176	-0.13229	H	1.18323	2.49442	-0.07584	H	1.18369	2.49388	-0.07765
H	0.46125	1.56354	-1.44236	H	0.51357	1.57383	-1.42242	H	0.51198	1.57304	-1.42303
C	-0.90701	2.82967	-0.33256	C	-0.93533	2.79169	-0.36635	C	-0.93503	2.79226	-0.36557
H	-1.077	3.18287	0.69748	H	-1.16877	3.12295	0.65887	H	-1.16651	3.12437	0.65978
H	-0.75032	3.71533	-0.96789	H	-0.77224	3.69155	-0.97995	H	-0.77237	3.69157	-0.98007
H	-1.83034	2.3339	-0.66383	H	-1.8238	2.27538	-0.75867	H	-1.82452	2.27623	-0.75583
C	-0.74483	-0.41083	0.06013	C	-0.7355	-0.41827	0.04988	C	-0.73559	-0.41835	0.05091
H	-0.67513	-0.59679	-1.02419	H	-0.69945	-0.56275	-1.04088	H	-0.69828	-0.56473	-1.0396
H	-0.57667	-1.3628	0.59098	H	-0.55293	-1.38303	0.54929	H	-0.5534	-1.38243	0.55188
O	-2.07789	0.06974	0.37638	O	-2.0761	0.03614	0.41756	O	-2.07604	0.03709	0.41656
N	-3.13665	-0.86372	-0.00477	N	-3.12464	-0.8477	-0.00033	N	-3.12493	-0.84819	-0.00036
O	-2.79482	-1.90584	-0.52937	O	-2.81373	-1.85618	-0.60707	O	-2.81313	-1.85795	-0.60455
O	-4.23578	-0.44385	0.26827	O	-4.22625	-0.4496	0.3237	O	-4.2266	-0.44884	0.3212

PBE0 (Gas)

C	2.27583	-0.57731	-0.52704
H	1.61092	-1.33109	-0.96686
H	2.39904	0.20355	-1.28808
C	3.63225	-1.23035	-0.26272
H	3.50988	-2.02469	0.48514
H	3.96228	-1.72987	-1.18072
C	4.71802	-0.26325	0.19324
H	5.67981	-0.77344	0.29672
H	4.85082	0.54886	-0.52986
H	4.48636	0.1898	1.16143
C	1.62688	0.01288	0.72334
H	1.55221	-0.77356	1.48665
H	2.2794	0.78415	1.14675
C	0.23802	0.64194	0.52478
H	-0.1067	0.96439	1.5166
C	0.29042	1.87536	-0.38525
H	1.1722	2.4611	-0.09738
H	0.46867	1.55488	-1.4193
C	-0.93534	2.77967	-0.33595
H	-1.13879	3.10991	0.68768
H	-0.77733	3.67219	-0.94812
H	-1.83453	2.27868	-0.69966
C	-0.73768	-0.42656	0.04925
H	-0.67154	-0.59733	-1.0289

PBE0 (Water)

C	2.28237	-0.57169	-0.52669
H	1.62027	-1.32412	-0.97292
H	2.40773	0.21369	-1.28248
C	3.63907	-1.2234	-0.26055
H	3.51618	-2.01684	0.48822
H	3.97134	-1.72201	-1.1784
C	4.72263	-0.25368	0.19623
H	5.68469	-0.76305	0.30467
H	4.85542	0.55596	-0.52986
H	4.48524	0.20273	1.1616
C	1.6293	0.00818	0.72653
H	1.55091	-0.78433	1.4825
H	2.2774	0.77848	1.15788
C	0.23993	0.6366	0.52843
H	-0.10765	0.94551	1.52341
C	0.29471	1.87931	-0.36744
H	1.14406	2.48724	-0.03344
H	0.52657	1.57446	-1.39496
C	0.95936	2.74527	-0.367
H	-1.2274	3.04945	0.65018
H	-0.79624	3.65362	-0.95429
H	-1.81983	2.22454	-0.79374
C	-0.72913	-0.42853	0.03451
H	-0.6927	-0.55717	-1.04974

PBE0 (Methanol)

C	2.28204	-0.57218	-0.52638
H	1.61987	-1.32497	-0.97191
H	2.40701	0.21274	-1.28271
C	3.63893	-1.22356	-0.26039
H	3.51645	-2.01668	0.48877
H	3.97094	-1.72258	-1.17811
C	4.7225	-0.25348	0.19555
H	5.68469	-0.76264	0.30379
H	4.85493	0.5559	-0.53089
H	4.4855	0.20325	1.16085
C	1.62933	0.00843	0.72669
H	1.55121	-0.78364	1.48317
H	2.27766	0.7789	1.15742
C	0.23994	0.6368	0.52862
H	-0.10755	0.94622	1.52348
C	0.29456	1.87914	-0.36779
H	1.1444	2.4869	-0.03465
H	0.52573	1.57381	-1.39535
C	-0.95914	2.74563	-0.36687
H	-1.22637	3.05043	0.65031
H	-0.79609	3.6536	-0.95477
H	-1.82026	2.22512	-0.79249
C	-0.72928	-0.42852	0.03535
H	-0.69227	-0.55815	-1.0488

H	-0.56566	-1.37645	0.56408	H	-0.54512	-1.39131	0.518	H	-0.5453	-1.39105	0.51944
O	-2.06468	0.03346	0.36948	O	-2.06221	0.00792	0.40169	O	-2.06217	0.00829	0.40173
N	-3.07982	-0.84	0.00225	N	-3.0716	-0.82795	0.00741	N	-3.07174	-0.82813	0.0072
O	-2.76331	-1.86868	-0.53209	O	-2.784	-1.8274	-0.59615	O	-2.78333	-1.82774	-0.59575
O	-4.16809	-0.4342	0.27763	O	-4.16214	-0.44097	0.32787	O	-4.1622	-0.44102	0.32694

B3LYP (Gas)

C	2.30368	-0.58608	-0.5274
H	1.64444	-1.34222	-0.9692
H	2.43107	0.1918	-1.28922
C	3.66717	-1.24249	-0.25284
H	3.54333	-2.02582	0.50529
H	3.99332	-1.75456	-1.16468
C	4.76739	-0.27146	0.19014
H	5.72262	-0.79089	0.305
H	4.91072	0.52469	-0.54785
H	4.5382	0.20164	1.14864
C	1.63881	0.00959	0.72346
H	1.55815	-0.77522	1.48638
H	2.28668	0.78098	1.15077
C	0.24092	0.64396	0.51883
H	-0.09971	0.96795	1.51008
C	0.29319	1.8854	-0.39707
H	1.18715	2.45885	-0.12619
H	0.44474	1.56546	-1.43449
C	-0.92292	2.81624	-0.3226
H	-1.09532	3.15546	0.70335
H	-0.76192	3.70228	-0.94297
H	-1.83788	2.32925	-0.66277
C	-0.74376	-0.43079	0.04682
H	-0.67979	-0.61066	-1.02814
H	-0.58126	-1.37458	0.57203
O	-2.08241	0.04246	0.36311
N	-3.12137	-0.84797	0.0005
O	-2.80792	-1.89015	-0.52655
O	-4.2124	-0.42917	0.27649

B3LYP (Water)

C	2.31125	-0.57906	-0.52762
H	1.65522	-1.33357	-0.97674
H	2.44113	0.20412	-1.28333
C	3.67484	-1.23414	-0.25085
H	3.55	-2.01775	0.50681
H	4.00435	-1.74376	-1.16302
C	4.77217	-0.26096	0.19564
H	5.72758	-0.77958	0.31582
H	4.91629	0.53377	-0.54389
H	4.53609	0.21387	1.15171
C	1.64133	0.00514	0.72603
H	1.55737	-0.78594	1.48134
H	2.28387	0.77605	1.16158
C	0.24246	0.63782	0.52136
H	-0.10118	0.94873	1.51561
C	0.29662	1.88807	-0.38101
H	1.15972	2.484	-0.06437
H	0.50112	1.58245	-1.41296
C	-0.94903	2.78155	-0.35439
H	-1.1858	3.09654	0.66674
H	-0.7817	3.68303	-0.95056
H	-1.82811	2.27478	-0.7573
C	-0.7344	-0.43459	0.03153
H	-0.70359	-0.57083	-1.04994
H	-0.55857	-1.39224	0.52386
O	-2.08085	0.01314	0.39986
N	-3.11169	-0.83485	0.00625
O	-2.82888	-1.84519	-0.59736
O	-4.20568	-0.43703	0.33135

B3LYP (Methanol)

C	2.3109	-0.5796	-0.5273
H	1.6548	-1.33452	-0.97566
H	2.44032	0.20309	-1.2836
C	3.67472	-1.23429	-0.25072
H	3.55036	-2.01749	0.50744
H	4.00391	-1.74442	-1.1627
C	4.77208	-0.26068	0.19473
H	5.72762	-0.77906	0.31478
H	4.91581	0.53366	-0.54528
H	4.53641	0.21464	1.15066
C	1.64138	0.00538	0.72621
H	1.55775	-0.78522	1.48207
H	2.28414	0.77649	1.16109
C	0.24247	0.63796	0.52159
H	-0.10094	0.94964	1.51568
C	0.29634	1.88761	-0.38168
H	1.16042	2.48305	-0.06672
H	0.49922	1.58118	-1.41374
C	-0.94848	2.78221	-0.35381
H	-1.18334	3.09824	0.6674
H	-0.78135	3.68302	-0.95102
H	-1.82875	2.27591	-0.75462
C	-0.73459	-0.4348	0.03284
H	-0.70277	-0.57282	-1.04841
H	-0.55909	-1.39185	0.52657
O	-2.08087	0.01379	0.39946
N	-3.11195	-0.83502	0.00593
O	-2.82821	-1.84611	-0.596
O	-4.20589	-0.43657	0.32946

CAM-B3LYP (Gas)

C	2.28748	-0.56855	-0.5308
H	1.62522	-1.31491	-0.98192
H	2.41817	0.21869	-1.28065
C	3.64242	-1.22853	-0.26391
H	3.51534	-2.0239	0.479
H	3.97459	-1.72266	-1.18168
C	4.73071	-0.26437	0.20124
H	5.68932	-0.77709	0.30397
H	4.86627	0.54963	-0.51665
H	4.49679	0.18276	1.16954
C	1.63049	0.01032	0.7237
H	1.55355	-0.78182	1.47768

CAM-B3LYP (Water)

C	2.29489	-0.56076	-0.53169
H	1.63495	-1.30385	-0.99146
H	2.42967	0.23235	-1.27433
C	3.64882	-1.22185	-0.26279
H	3.51904	-2.01827	0.47853
H	3.98405	-1.7128	-1.18131
C	4.73535	-0.25789	0.20779
H	5.6934	-0.77142	0.31538
H	4.873	0.55567	-0.51037
H	4.49475	0.18984	1.17429
C	1.63302	0.00602	0.72587
H	1.55187	-0.79324	1.47117

CAM-B3LYP (Methanol)

C	2.29458	-0.56103	-0.53134
H	1.63456	-1.30436	-0.99063
H	2.42906	0.23179	-1.27434
C	3.64864	-1.22195	-0.26266
H	3.51924	-2.0181	0.47902
H	3.98353	-1.71326	-1.18111
C	4.73534	-0.25776	0.20704
H	5.69329	-0.77135	0.31497
H	4.87309	0.55517	-0.51179
H	4.49494	0.19078	1.17321
C	1.63299	0.00624	0.72615
H	1.55208	-0.7927	1.47185

H	2.27794	0.77778	1.15557	H	2.27596	0.77165	1.16718	H	2.27607	0.77202	1.16701
C	0.23906	0.63782	0.52288	C	0.24134	0.6332	0.52566	C	0.24129	0.63338	0.52596
H	-0.10988	0.95316	1.51273	H	-0.11168	0.93197	1.51902	H	-0.11174	0.93249	1.5192
C	0.29184	1.87811	-0.38092	C	0.29684	1.8855	-0.35979	C	0.29676	1.88546	-0.35985
H	1.1626	2.46966	-0.08021	H	1.12975	2.50111	-0.00636	H	1.12976	2.50113	-0.00669
H	0.48235	1.56638	-1.41307	H	0.5479	1.59369	-1.38414	H	0.54782	1.59338	-1.38414
C	-0.94475	2.77281	-0.33978	C	-0.97103	2.73596	-0.37354	C	-0.97103	2.7361	-0.37371
H	-1.16327	3.09294	0.6821	H	-1.26088	3.02606	0.63988	H	-1.26081	3.02643	0.63962
H	-0.78642	3.6693	-0.94304	H	-0.80912	3.65007	-0.94896	H	-0.80907	3.65003	-0.94938
H	-1.83301	2.26684	-0.71759	H	-1.81461	2.20783	-0.81992	H	-1.81484	2.20806	-0.81971
C	-0.73539	-0.42874	0.03674	C	-0.72657	-0.4278	0.01681	C	-0.72681	-0.4277	0.01746
H	-0.67974	-0.58461	-1.04141	H	-0.70469	-0.53383	-1.0675	H	-0.70439	-0.53426	-1.06684
H	-0.56463	-1.38231	0.53884	H	-0.54137	-1.39699	0.48004	H	-0.54135	-1.39687	0.48076
O	-2.06705	0.02892	0.37214	O	-2.06384	0.00134	0.40717	O	-2.0637	0.00143	0.40751
N	-3.08713	-0.83734	0.00569	N	-3.07839	-0.82612	0.01203	N	-3.07848	-0.82631	0.01185
O	-2.77903	-1.86353	-0.54282	O	-2.80079	-1.81785	-0.61242	O	-2.80004	-1.81796	-0.61241
O	-4.17472	-0.43435	0.29344	O	-4.16776	-0.44616	0.35084	O	-4.16779	-0.44629	0.35011

2-Nitratepyrrole

PBE (Gas)

N	-2.02605	0.07371	0.206
O	-1.57023	0.49968	1.23578
O	-0.66291	-0.32547	-1.07779
C	0.48931	-0.09624	-0.5616
N	1.2253	-1.09838	0.10368
C	2.42607	-0.60326	0.50428
C	2.49273	0.75004	0.13602
C	1.29252	1.07411	-0.51245
O	-3.1406	-0.14107	-0.18052
H	0.90245	-2.05652	0.20081
H	3.15983	-1.22593	1.00954
H	3.33519	1.4085	0.33013
H	0.99383	2.03365	-0.9255

PBE (Water)

N	-2.06295	0.09147	0.18068
O	-1.57324	0.62933	1.15092
O	-0.57976	-0.46476	-1.13994
C	0.52463	-0.17758	-0.59603
N	1.24449	-1.09345	0.21447
C	2.40352	-0.53589	0.61726
C	2.4773	0.78538	0.11168
C	1.3193	1.01984	-0.62241
O	-3.22323	-0.13996	-0.08619
H	0.93597	-2.04288	0.41405
H	3.11877	-1.08536	1.22434
H	3.30452	1.46881	0.28368
H	1.03131	1.92589	-1.14939

PBE (Methanol)

N	-2.06201	0.09071	0.18199
O	-1.57636	0.62523	1.15574
O	-0.5835	-0.45821	-1.13612
C	0.5233	-0.17367	-0.59406
N	1.24462	-1.09391	0.20978
C	2.40582	-0.53947	0.61173
C	2.47914	0.78369	0.11219
C	1.3187	1.02269	-0.61734
O	-3.21955	-0.14185	-0.0925
H	0.93521	-2.04364	0.40599
H	3.12269	-1.09227	1.21383
H	3.30724	1.46589	0.28494
H	1.03005	1.93148	-1.13918

PBE0 (Gas)

N	-1.88825	0.00755	-0.18289
O	-1.48614	0.02254	-1.29675
O	-0.8227	0.02399	0.91874
C	0.42983	0.08825	0.44722
N	1.14124	-1.05586	0.19185
C	2.39509	-0.71894	-0.2163
C	2.48424	0.65636	-0.23346
C	1.23657	1.17198	0.18292
O	-2.97491	-0.02375	0.27866
H	0.79152	-1.9887	0.33338
H	3.1286	-1.47378	-0.45333
H	3.35732	1.22573	-0.51389
H	0.94718	2.20679	0.28371

PBE0 (Water)

N	-1.87997	0.00696	0.17669
O	-1.49005	0.01985	1.2957
O	-0.82925	0.04282	-0.90771
C	0.43117	0.09213	-0.4393
N	1.13578	-1.05582	-0.19724
C	2.39099	-0.72675	0.20732
C	2.48857	0.65039	0.23265
C	1.24022	1.17535	-0.17396
O	-2.97067	-0.03139	-0.28359
H	0.78335	-1.99132	-0.32873
H	3.11918	-1.48977	0.43503
H	3.36708	1.21396	0.50964
H	0.95377	2.21216	-0.26753

PBE0 (Methanol)

N	-1.88055	0.00712	0.17683
O	-1.49062	0.02158	1.29562
O	-0.82868	0.04114	-0.90801
C	0.43112	0.09145	-0.43889
N	1.13607	-1.05606	-0.19536
C	2.39153	-0.72618	0.20789
C	2.48874	0.65095	0.2315
C	1.24005	1.17503	-0.17496
O	-2.97092	-0.03162	-0.28399
H	0.78444	-1.99162	-0.32825
H	3.12009	-1.48853	0.43661
H	3.36715	1.21483	0.50812
H	0.95281	2.21157	-0.26895

B3LYP (Gas)

N	-1.96507	0.06041	0.00467
O	-1.79824	1.24851	0.02901
O	-0.79274	-0.77907	-0.02003
C	0.46215	-0.1975	-0.01073
N	1.47358	-1.11957	0.01157
C	2.6824	-0.4541	0.01401
C	2.41484	0.89146	-0.00529
C	0.99737	1.07015	-0.02137
O	-2.96611	-0.59611	-0.00637
H	1.33471	-2.11702	0.02222
H	3.61252	-0.99673	0.02922
H	3.14846	1.68178	-0.00784
H	0.46093	1.99947	-0.03795

B3LYP (Water)

N	-2.13713	-0.02198	-0.05799
O	-1.11428	0.70568	0.01879
O	0.11612	-1.95268	-0.12701
C	0.64616	-0.87835	-0.11759
N	1.20003	-0.25586	1.09403
C	1.91458	0.78136	0.76333
C	1.90833	0.97194	-0.67405
C	1.13654	0.00687	-1.21131
O	-3.23362	0.52979	0.11696
H	1.04577	-0.60513	2.03311
H	2.4199	1.38827	1.50242
H	2.42574	1.77492	-1.17326
H	0.88885	-0.16645	-2.24673

B3LYP (Methanol)

N	-2.13304	-0.02052	-0.05937
O	-1.10917	0.7062	0.01531
O	0.11394	-1.95401	-0.12313
C	0.64434	-0.87964	-0.11597
N	1.19676	-0.25409	1.09476
C	1.90997	0.78402	0.76257
C	1.90653	0.97014	-0.67471
C	1.13611	0.00266	-1.21068
O	-3.22861	0.53088	0.1167
H	1.03809	-0.59923	2.03452
H	2.41183	1.39446	1.50109
H	2.4232	1.77254	-1.17561
H	0.88986	-0.17319	-2.24602

CAM-B3LYP (Gas)

N	-1.87844	-0.00147	0.17338
O	-1.48684	-0.0595	1.29349
O	-0.83876	0.06992	-0.8969
C	0.43154	0.1114	-0.42865
N	1.13754	-1.04548	-0.23268
C	2.39882	-0.72433	0.17853
C	2.48921	0.64373	0.24999
C	1.23519	1.17914	-0.13395
O	-2.97049	0.00352	-0.28512
H	0.78415	-1.9718	-0.40697
H	3.1313	-1.48801	0.38034
H	3.36335	1.20106	0.54481
H	0.94774	2.21622	-0.19042

CAM-B3LYP (Water)

N	-1.87136	0.00124	0.16724
O	-1.49358	-0.03382	1.29381
O	-0.84358	0.07248	-0.88723
C	0.43348	0.10742	-0.42247
N	1.13405	-1.04925	-0.22253
C	2.39574	-0.72907	0.18032
C	2.49349	0.64188	0.24014
C	1.23898	1.17942	-0.14165
O	-2.9675	-0.01358	-0.29148
H	0.77826	-1.98124	-0.37268
H	3.12412	-1.49656	0.38327
H	3.3725	1.19835	0.52343
H	0.9535	2.21703	-0.2059

CAM-B3LYP (Methanol)

N	-1.87141	0.00169	0.16737
O	-1.49317	-0.02969	1.29381
O	-0.84356	0.06993	-0.88773
C	0.43339	0.10622	-0.4228
N	1.1342	-1.04992	-0.22004
C	2.39595	-0.7284	0.182
C	2.49321	0.6426	0.23874
C	1.23854	1.17895	-0.14433
O	-2.96754	-0.01494	-0.29113
H	0.77894	-1.98207	-0.37
H	3.12465	-1.49521	0.38638
H	3.37184	1.19999	0.52128
H	0.95261	2.21632	-0.21019

2-Nitratefuran

PBE (Gas)

C	-0.49151	-0.10235	-0.56966
C	-1.33034	1.023	-0.57622
C	-2.50433	0.6824	0.12627
C	-2.33161	-0.62179	0.55668
O	-1.14164	-1.12261	0.17314
H	-1.08565	1.96287	-1.06308
H	-3.37822	1.30292	0.30561
H	-2.97292	-1.2918	1.12386
N	2.01052	0.09455	0.2018
O	3.10746	-0.22499	-0.1485
O	1.55542	0.63947	1.16972
O	0.64249	-0.3573	-1.06953

PBE (Water)

C	-0.51367	-0.24156	-0.55784
C	-1.32868	0.89332	-0.76283
C	-2.48744	0.73213	0.0116
C	-2.34274	-0.47464	0.68545
O	-1.17944	-1.07941	0.39064
H	-1.07196	1.71453	-1.42663
H	-3.34015	1.40133	0.08576
H	-2.99644	-0.99631	1.38057
N	2.03899	0.12746	0.17373
O	3.1623	-0.23333	-0.06254
O	1.57102	0.87615	0.99282
O	0.59247	-0.62183	-1.01018

PBE (Methanol)

C	-0.51278	-0.2383	-0.55809
C	-1.32842	0.89677	-0.75876
C	-2.48799	0.73097	0.01387
C	-2.34266	-0.47832	0.6828
O	-1.17871	-1.08101	0.38548
H	-1.07151	1.72092	-1.41873
H	-3.34145	1.3989	0.09036
H	-2.99619	-1.0037	1.37514
N	2.03826	0.12711	0.1745
O	3.16041	-0.23411	-0.06456
O	1.57055	0.8718	0.99707
O	0.5943	-0.61576	-1.01139

PBE0 (Gas)

C	-0.43766	0.23299	-0.40775
C	-1.30009	1.17657	0.05961
C	-2.50845	0.48225	0.34595
C	-2.2746	-0.82284	0.04407
O	-1.01904	-0.99139	-0.41759
H	-1.08727	2.22813	0.17113
H	-3.42961	0.89536	0.72712
H	-2.88162	-1.71235	0.09603
N	1.86716	-0.03247	0.18274
O	2.94622	-0.01102	-0.28853
O	1.45613	-0.25798	1.26802
O	0.79835	0.31068	-0.8775

PBE0 (Water)

C	-0.43865	0.20281	-0.4192
C	-1.28695	1.17901	0.00443
C	-2.50339	0.51347	0.32522
C	-2.28949	-0.80818	0.08438
O	-1.03428	-1.0153	-0.37001
H	-1.06145	2.23225	0.06776
H	-3.4183	0.95679	0.68741
H	-2.90987	-1.68536	0.17663
N	1.86754	-0.02322	0.18232
O	2.94931	-0.01851	-0.28864
O	1.46375	-0.18855	1.28054
O	0.79968	0.23939	-0.89402

PBE0 (Methanol)

C	-0.43864	0.20417	-0.41868
C	-1.2875	1.17897	0.00702
C	-2.50366	0.51215	0.32615
C	-2.28891	-0.80885	0.08261
O	-1.03367	-1.01429	-0.37222
H	-1.06259	2.2322	0.07255
H	-3.41885	0.95418	0.68918
H	-2.90873	-1.6866	0.17306
N	1.86753	-0.02364	0.1823
O	2.94923	-0.01805	-0.28866
O	1.46354	-0.19181	1.28005
O	0.79962	0.24253	-0.89336

B3LYP (Gas)

C	-0.46371	0.09125	-0.51391
C	-1.31124	1.14511	-0.24554
C	-2.50882	0.58378	0.26539
C	-2.31109	-0.7696	0.29858
O	-1.08447	-1.09395	-0.15981
H	-1.08069	2.18412	-0.41679
H	-3.40202	1.10453	0.5712
H	-2.93644	-1.59174	0.60561
N	1.94216	0.02491	0.20975
O	3.01406	-0.1473	-0.25662
O	1.52198	0.19964	1.30559
O	0.72257	0.01981	-1.02107

B3LYP (Water)

C	-0.49415	-0.17154	-0.5569
C	-1.30909	0.95932	-0.66568
C	-2.47889	0.70255	0.06657
C	-2.32446	-0.55349	0.61166
O	-1.14774	-1.09791	0.27174
H	-1.05583	1.84129	-1.23215
H	-3.33631	1.34394	0.19105
H	-2.97109	-1.15229	1.23328
N	1.99312	0.10933	0.18534
O	3.0945	-0.23637	-0.10617
O	1.54985	0.76144	1.07806
O	0.63475	-0.47957	-1.02157

B3LYP (Methanol)

C	-0.49138	-0.15395	-0.5566
C	-1.30824	0.9754	-0.64209
C	-2.48132	0.6965	0.07917
C	-2.32472	-0.57107	0.59379
O	-1.14363	-1.1024	0.24487
H	-1.05582	1.8719	-1.18565
H	-3.34141	1.33199	0.21515
H	-2.97079	-1.18816	1.19775
N	1.98919	0.10481	0.18863
O	3.087	-0.23454	-0.11925
O	1.54873	0.73048	1.10049
O	0.64261	-0.44739	-1.02527

CAM-B3LYP (Gas)

C	-0.43844	0.2539	-0.38151
C	-1.30253	1.17445	0.10363
C	-2.51521	0.46264	0.35023
C	-2.27662	-0.82463	0.00431
O	-1.00945	-0.96998	-0.44937
H	-1.09608	2.22034	0.25709
H	-3.43986	0.85924	0.73594
H	-2.87788	-1.71725	0.01595
N	1.85597	-0.03892	0.17105
O	2.94121	0.00901	-0.29289
O	1.45472	-0.3309	1.24847
O	0.81588	0.35588	-0.83949

CAM-B3LYP (Water)

C	-0.43926	0.22531	-0.39115
C	-1.28736	1.17877	0.05499
C	-2.51034	0.49487	0.33222
C	-2.29415	-0.80985	0.04067
O	-1.0265	-0.99414	-0.40701
H	-1.06636	2.22734	0.16613
H	-3.4283	0.92246	0.70075
H	-2.91042	-1.69128	0.0876
N	1.85516	-0.031	0.16919
O	2.9442	0.00672	-0.29434
O	1.4643	-0.27105	1.26304
O	0.8187	0.28644	-0.8566

CAM-B3LYP (Methanol)

C	-0.43925	0.22651	-0.39073
C	-1.28802	1.17865	0.05702
C	-2.51059	0.49354	0.33296
C	-2.29345	-0.81053	0.03919
O	-1.02577	-0.99319	-0.40875
H	-1.06773	2.22717	0.16989
H	-3.42885	0.91987	0.70218
H	-2.90909	-1.69247	0.08466
N	1.85516	-0.03129	0.16923
O	2.9441	0.00677	-0.29431
O	1.46399	-0.27348	1.26251
O	0.81861	0.28933	-0.85594

2-Nitratethiophene

PBE (Gas)

O	1.687	2.79872	0.
O	-0.49385	2.45859	0.
N	0.67238	2.16014	0.
O	1.01075	0.66065	0.
C	-1.01038	-2.53477	0.
C	-1.94337	-1.52951	0.
C	-1.37921	-0.21669	0.
C	0.	-0.26253	0.
S	0.61269	-1.91095	0.
H	-1.16154	-3.61133	0.
H	-3.01776	-1.71378	0.
H	-1.96398	0.69666	0.

PBE (Water)

O	1.65389	2.81583	0.
O	-0.52212	2.45145	0.
N	0.64536	2.16149	0.
O	0.99985	0.67827	0.
C	-0.97727	-2.54758	0.
C	-1.92474	-1.5552	0.
C	-1.37926	-0.23296	0.
C	0.	-0.26144	0.
S	0.63766	-1.9	0.
H	-1.10899	-3.62696	0.
H	-2.99647	-1.75491	0.
H	-1.98002	0.67022	0.

PBE (Methanol)

O	1.65483	2.81538	0.
O	-0.52132	2.45164	0.
N	0.64614	2.16149	0.
O	1.00019	0.67774	0.
C	-0.9782	-2.54722	0.
C	-1.92527	-1.55448	0.
C	-1.37926	-0.2325	0.
C	0.	-0.26149	0.
S	0.63694	-1.90032	0.
H	-1.1105	-3.62652	0.
H	-2.99708	-1.75375	0.
H	-1.97956	0.67098	0.

PBE0 (Gas)

O	1.45819	2.85458	0.
O	-0.64908	2.35402	0.
N	0.52118	2.12568	0.
O	0.93253	0.76295	0.
C	-0.79794	-2.56819	0.
C	-1.80854	-1.65971	0.
C	-1.36232	-0.30608	0.
C	0.	-0.24483	0.
S	0.74763	-1.8091	0.
H	-0.85678	-3.64664	0.
H	-2.85561	-1.93503	0.
H	-2.01829	0.54802	0.

PBE0 (Water)

O	1.41748	2.87287	0.
O	-0.68185	2.34493	0.
N	0.49007	2.12335	0.
O	0.91664	0.78283	0.
C	-0.75711	-2.57999	0.
C	-1.7838	-1.68839	0.
C	-1.36116	-0.32658	0.
C	0.	-0.24409	0.
S	0.77621	-1.79415	0.
H	-0.7942	-3.65968	0.
H	-2.82611	-1.98152	0.
H	-2.03531	0.51343	0.

PBE0 (Methanol)

O	1.41837	2.87249	0.
O	-0.68115	2.34513	0.
N	0.49076	2.12347	0.
O	0.91701	0.78237	0.
C	-0.75799	-2.57974	0.
C	-1.78433	-1.6878	0.
C	-1.36118	-0.32615	0.
C	0.	-0.24411	0.
S	0.77557	-1.79448	0.
H	-0.79556	-3.65941	0.
H	-2.82675	-1.98054	0.
H	-2.03492	0.51418	0.

B3LYP (Gas)

O	1.49827	2.86735	0.
O	-0.63132	2.39427	0.
N	0.54291	2.15229	0.
O	0.94771	0.74912	0.
C	-0.83994	-2.57862	0.
C	-1.83487	-1.65015	0.
C	-1.36525	-0.29898	0.
C	0.	-0.25285	0.
S	0.73353	-1.84189	0.
H	-0.91802	-3.65459	0.
H	-2.88601	-1.90582	0.
H	-2.00969	0.56234	0.

B3LYP (Water)

O	1.45316	2.88747	0.
O	-0.66811	2.38278	0.
N	0.50826	2.1494	0.
O	0.93079	0.77147	0.
C	-0.79488	-2.59185	0.
C	-1.80777	-1.68195	0.
C	-1.36408	-0.32132	0.
C	0.	-0.25208	0.
S	0.76539	-1.82468	0.
H	-0.84865	-3.66947	0.
H	-2.85389	-1.95737	0.
H	-2.02781	0.52534	0.

B3LYP (Methanol)

O	1.45424	2.88699	0.
O	-0.66724	2.38304	0.
N	0.50911	2.14951	0.
O	0.93121	0.77093	0.
C	-0.79597	-2.59155	0.
C	-1.80843	-1.68121	0.
C	-1.36411	-0.3208	0.
C	0.	-0.2521	0.
S	0.76463	-1.82508	0.
H	-0.85035	-3.66912	0.
H	-2.85467	-1.95615	0.
H	-2.02737	0.52623	0.

CAM-B3LYP (Gas)

O	1.41805	2.87942	0.
O	-0.68114	2.34733	0.
N	0.49387	2.13203	0.

CAM-B3LYP (Water)

O	1.38148	2.89567	0.
O	-0.70996	2.33928	0.
N	0.46603	2.12869	0.

CAM-B3LYP (Methanol)

O	1.38217	2.89539	0.
O	-0.70943	2.33941	0.
N	0.46658	2.12883	0.

O 0.9221 0.78008 0.	O 0.90755 0.79841 0.	O 0.90785 0.79804 0.
C -0.76714 -2.57969 0.	C -0.73082 -2.58988 0.	C -0.73151 -2.58968 0.
C -1.78528 -1.68829 0.	C -1.76282 -1.7133 0.	C -1.76324 -1.71282 0.
C -1.35482 -0.3248 0.	C -1.35341 -0.34305 0.	C -1.35343 -0.34272 0.
C 0. -0.24853 0.	C 0. -0.24812 0.	C 0. -0.24812 0.
S 0.77374 -1.8011 0.	S 0.79909 -1.78783 0.	S 0.7986 -1.78811 0.
H -0.81658 -3.65688 0.	H -0.76081 -3.668 0.	H -0.7619 -3.66779 0.
H -2.82753 -1.97469 0.	H -2.8007 -2.01531 0.	H -2.80121 -2.01454 0.
H -2.0216 0.51825 0.	H -2.03654 0.48695 0.	H -2.03621 0.48757 0.

2-Acetyl-1-pyrroline

PBE (Gas)

C	-2.19421	0.60602	0.
C	-2.14193	-0.95131	0.
C	-0.62666	-1.26678	0.
C	0.	0.12331	0.
N	-0.82102	1.11123	0.
O	1.96205	1.50117	0.
C	2.38874	-0.86075	0.
C	1.50128	0.37141	0.
H	-2.71204	1.02304	0.88074
H	-2.71204	1.02304	-0.88074
H	-2.64167	-1.3713	0.88432
H	-2.64167	-1.3713	-0.88432
H	-0.30804	-1.84708	0.88226
H	-0.30804	-1.84708	-0.88226
H	3.44143	-0.55417	0.
H	2.18476	-1.48724	0.8844
H	2.18476	-1.48724	-0.8844

PBE (Water)

C	-2.20315	0.57356	0.
C	-2.12582	-0.97968	0.
C	-0.60677	-1.27557	0.
C	0.	0.11588	0.
N	-0.83261	1.09717	0.
O	1.93285	1.53342	0.
C	2.40054	-0.82057	0.
C	1.4955	0.38592	0.
H	-2.72596	0.98289	0.88124
H	-2.72596	0.98289	-0.88124
H	-2.61785	-1.40409	0.88564
H	-2.61785	-1.40409	-0.88564
H	-0.27841	-1.84821	0.88279
H	-0.27841	-1.84821	-0.88279
H	3.45097	-0.50667	0.
H	2.19862	-1.44966	0.88273
H	2.19862	-1.44966	-0.88273

PBE (Methanol)

C	-2.20305	0.5738	0.
C	-2.12596	-0.97955	0.
C	-0.60692	-1.27556	0.
C	0.	0.11607	0.
N	-0.83259	1.09729	0.
O	1.93306	1.53315	0.
C	2.40048	-0.82097	0.
C	1.49551	0.38601	0.
H	-2.72585	0.98324	0.88119
H	-2.72585	0.98324	-0.88119
H	-2.61808	-1.404	0.88559
H	-2.61808	-1.404	-0.88559
H	-0.2787	-1.84832	0.88279
H	-0.2787	-1.84832	-0.88279
H	3.45085	-0.50683	0.
H	2.19882	-1.45004	0.88281
H	2.19882	-1.45004	-0.88281

PBE0 (Gas)

C	-2.16844	0.63676	0.
C	-2.14093	-0.90921	0.
C	-0.64203	-1.24875	0.
C	0.	0.12239	0.
N	-0.796	1.11151	0.
O	1.96574	1.4565	0.
C	2.36172	-0.88851	0.
C	1.49707	0.34653	0.
H	-2.67561	1.0572	0.87519
H	-2.67561	1.0572	-0.87519
H	-2.64429	-1.31838	0.87818
H	-2.64429	-1.31838	-0.87818
H	-0.33522	-1.82861	0.87708
H	-0.33522	-1.82861	-0.87708
H	3.41111	-0.59681	0.
H	2.15046	-1.50572	0.8796
H	2.15046	-1.50572	-0.8796

PBE0 (Water)

C	-2.17639	0.61062	0.
C	-2.12813	-0.93254	0.
C	-0.62589	-1.25674	0.
C	0.	0.11544	0.
N	-0.80459	1.10013	0.
O	1.94097	1.48451	0.
C	2.37223	-0.85571	0.
C	1.49314	0.35779	0.
H	-2.68748	1.02442	0.87592
H	-2.68748	1.02442	-0.87592
H	-2.62525	-1.34505	0.87937
H	-2.62525	-1.34505	-0.87937
H	-0.31081	-1.83002	0.87766
H	-0.31081	-1.83002	-0.87766
H	3.42039	-0.56013	0.
H	2.16061	-1.47437	0.87819
H	2.16061	-1.47437	-0.87819

PBE0 (Methanol)

C	-2.1761	0.61149	0.
C	-2.12853	-0.93175	0.
C	-0.62639	-1.25643	0.
C	0.	0.11574	0.
N	-0.80428	1.10058	0.
O	1.9419	1.4835	0.
C	2.37171	-0.85691	0.
C	1.49326	0.35742	0.
H	-2.68707	1.02555	0.87586
H	-2.68707	1.02555	-0.87586
H	-2.62579	-1.34411	0.87937
H	-2.62579	-1.34411	-0.87937
H	-0.31162	-1.82987	0.87768
H	-0.31162	-1.82987	-0.87768
H	3.41994	-0.56161	0.
H	2.16003	-1.47546	0.87825
H	2.16003	-1.47546	-0.87825

B3LYP (Gas)

C	-2.18426	0.63766	0.
C	-2.15417	-0.91779	0.
C	-0.6451	-1.25639	0.
C	0.	0.12431	0.
N	-0.80041	1.11312	0.
O	1.97396	1.46439	0.
C	2.38011	-0.8876	0.
C	1.50429	0.35075	0.
H	-2.6891	1.05661	0.876
H	-2.6891	1.05661	-0.876
H	-2.6558	-1.32687	0.87832
H	-2.6558	-1.32687	-0.87832
H	-0.34022	-1.8358	0.87692
H	-0.34022	-1.8358	-0.87692
H	3.42713	-0.58911	0.
H	2.17451	-1.50569	0.87979
H	2.17451	-1.50569	-0.87979

B3LYP (Water)

C	-2.19236	0.61067	0.
C	-2.14108	-0.94154	0.
C	-0.62872	-1.26442	0.
C	0.	0.11702	0.
N	-0.80893	1.10158	0.
O	1.94858	1.49265	0.
C	2.3908	-0.85373	0.
C	1.49984	0.36189	0.
H	-2.70083	1.02312	0.87674
H	-2.70083	1.02312	-0.87674
H	-2.63621	-1.35386	0.87961
H	-2.63621	-1.35386	-0.87961
H	-0.31571	-1.83697	0.8776
H	-0.31571	-1.83697	-0.8776
H	3.43612	-0.54963	0.
H	2.18617	-1.47327	0.87853
H	2.18617	-1.47327	-0.87853

B3LYP (Methanol)

C	-2.19212	0.61145	0.
C	-2.14146	-0.9409	0.
C	-0.62915	-1.26417	0.
C	0.	0.11733	0.
N	-0.8087	1.10198	0.
O	1.94942	1.49179	0.
C	2.39039	-0.8548	0.
C	1.49995	0.36161	0.
H	-2.70051	1.0241	0.87669
H	-2.70051	1.0241	-0.87669
H	-2.63671	-1.3531	0.87961
H	-2.63671	-1.3531	-0.87961
H	-0.31642	-1.83688	0.87762
H	-0.31642	-1.83688	-0.87762
H	3.43576	-0.55096	0.
H	2.1857	-1.47426	0.8786
H	2.1857	-1.47426	-0.8786

CAM-B3LYP (Gas)

C	-2.17137	0.64874	0.
C	-2.14934	-0.89937	0.
C	-0.64934	-1.24645	0.
C	0.	0.12463	0.
N	-0.78916	1.11289	0.
O	1.97369	1.44531	0.
C	2.36339	-0.89933	0.
C	1.50063	0.33931	0.
H	-2.67234	1.06941	0.87518
H	-2.67234	1.06941	-0.87518
H	-2.65324	-1.30514	0.8771
H	-2.65324	-1.30514	-0.8771
H	-0.34743	-1.82562	0.87628
H	-0.34743	-1.82562	-0.87628
H	3.41124	-0.60762	0.
H	2.15272	-1.51375	0.87924
H	2.15272	-1.51375	-0.87924

CAM-B3LYP (Water)

C	-2.17882	0.62594	0.
C	-2.13814	-0.91953	0.
C	-0.63525	-1.25347	0.
C	0.	0.11789	0.
N	-0.79601	1.10317	0.
O	1.95158	1.4704	0.
C	2.37285	-0.87047	0.
C	1.49735	0.34811	0.
H	-2.68297	1.04042	0.87615
H	-2.68297	1.04042	-0.87615
H	-2.63653	-1.32813	0.87819
H	-2.63653	-1.32813	-0.87819
H	-0.32605	-1.82665	0.8769
H	-0.32605	-1.82665	-0.8769
H	3.41982	-0.57604	0.
H	2.16133	-1.48576	0.87804
H	2.16133	-1.48576	-0.87804

CAM-B3LYP (Methanol)

C	-2.17856	0.62677	0.
C	-2.13851	-0.91879	0.
C	-0.6357	-1.25316	0.
C	0.	0.11823	0.
N	-0.79576	1.1036	0.
O	1.95254	1.46944	0.
C	2.37233	-0.87164	0.
C	1.49748	0.34779	0.
H	-2.68262	1.04149	0.87608
H	-2.68262	1.04149	-0.87608
H	-2.63705	-1.32729	0.87817
H	-2.63705	-1.32729	-0.87817
H	-0.32679	-1.82652	0.8769
H	-0.32679	-1.82652	-0.8769
H	3.41937	-0.57754	0.
H	2.1607	-1.48683	0.8781
H	2.1607	-1.48683	-0.8781

6-Acetyl-tetrahydropyridine

PBE (Gas)

C	0.	0.32773	0.
C	1.03671	-0.77461	0.
C	0.50547	-2.2275	0.
C	-1.03617	-2.41168	0.
C	-1.89426	-1.12067	0.

PBE (Water)

C	0.	0.3265	0.
C	1.04282	-0.76214	0.
C	0.527	-2.21868	0.
C	-1.01128	-2.419	0.
C	-1.88402	-1.14135	0.

PBE (Methanol)

C	0.	0.32651	0.
C	1.04365	-0.76166	0.
C	0.52851	-2.21854	0.
C	-1.00971	-2.41971	0.
C	-1.88307	-1.14239	0.

N	-1.27193	0.18541	0.	N	-1.27406	0.17491	0.	N	-1.27379	0.17396	0.
O	-0.28896	2.71984	0.	O	-0.31645	2.71727	0.	O	-0.31891	2.71668	0.
C	1.99838	2.02993	0.	C	1.97458	2.04611	0.	C	1.97316	2.04792	0.
C	0.49598	1.78721	0.	C	0.48467	1.78738	0.	C	0.48311	1.78787	0.
H	1.69469	-0.61616	0.87197	H	1.69787	-0.59562	0.8721	H	1.69868	-0.59492	0.87211
H	1.69469	-0.61616	-0.87197	H	1.69787	-0.59562	-0.8721	H	1.69868	-0.59492	-0.87211
H	0.92451	-2.74706	0.87418	H	0.95081	-2.73138	0.87535	H	0.95258	-2.73112	0.87532
H	0.92451	-2.74706	-0.87418	H	0.95081	-2.73138	-0.87535	H	0.95258	-2.73112	-0.87532
H	-1.3205	-3.01457	0.87565	H	-1.29055	-3.02224	0.87652	H	-1.28863	-3.02319	0.8765
H	-1.3205	-3.01457	-0.87565	H	-1.29055	-3.02224	-0.87652	H	-1.28863	-3.02319	-0.8765
H	-2.57617	-1.11529	0.86956	H	-2.56559	-1.1445	0.86989	H	-2.56468	-1.14576	0.86985
H	-2.57617	-1.11529	-0.86956	H	-2.56559	-1.1445	-0.86989	H	-2.56468	-1.14576	-0.86985
H	2.18147	3.11111	0.	H	2.15796	3.12718	0.	H	2.1554	3.12918	0.
H	2.47599	1.57802	0.88488	H	2.45218	1.59244	0.8834	H	2.45126	1.59484	0.88347
H	2.47599	1.57802	-0.88488	H	2.45218	1.59244	-0.8834	H	2.45126	1.59484	-0.88347

PBE0 (Gas)

C	0.	0.32451	0.
C	1.02713	-0.77414	0.
C	0.49056	-2.2135	0.
C	-1.04193	-2.38678	0.
C	-1.88903	-1.10165	0.
N	-1.25776	0.18934	0.
O	-0.27185	2.69572	0.
C	1.99372	2.00763	0.
C	0.50102	1.77235	0.
H	1.67926	-0.61931	0.86707
H	1.67926	-0.61931	-0.86707
H	0.90321	-2.73223	0.86832
H	0.90321	-2.73223	-0.86832
H	-1.3269	-2.98448	0.86956
H	-1.3269	-2.98448	-0.86956
H	-2.56359	-1.09285	0.86457
H	-2.56359	-1.09285	-0.86457
H	2.17855	3.0811	0.
H	2.46394	1.55744	0.87998
H	2.46394	1.55744	-0.87998

PBE0 (Water)

C	0.	0.32295	0.
C	1.03294	-0.76319	0.
C	0.51001	-2.20597	0.
C	-1.01968	-2.39358	0.
C	-1.88029	-1.12019	0.
N	-1.25973	0.18069	0.
O	-0.29715	2.69322	0.
C	1.97281	2.02257	0.
C	0.49141	1.77291	0.
H	1.68202	-0.60071	0.86737
H	1.68202	-0.60071	-0.86737
H	0.92686	-2.71842	0.86946
H	0.92686	-2.71842	-0.86946
H	-1.30009	-2.99141	0.87044
H	-1.30009	-2.99141	-0.87044
H	-2.55414	-1.11957	0.86519
H	-2.55414	-1.11957	-0.86519
H	2.15852	3.09584	0.
H	2.44209	1.57034	0.87888
H	2.44209	1.57034	-0.87888

PBE0 (Methanol)

C	0.	0.32294	0.
C	1.03367	-0.76277	0.
C	0.51137	-2.20585	0.
C	-1.01828	-2.39421	0.
C	-1.87945	-1.12111	0.
N	-1.25952	0.17991	0.
O	-0.29927	2.69266	0.
C	1.97152	2.02421	0.
C	0.49003	1.77332	0.
H	1.68271	-0.60008	0.86738
H	1.68271	-0.60008	-0.86738
H	0.92845	-2.7182	0.86943
H	0.92845	-2.7182	-0.86943
H	-1.29838	-2.99227	0.87041
H	-1.29838	-2.99227	-0.87041
H	-2.55335	-1.12069	0.86515
H	-2.55335	-1.12069	-0.86515
H	2.15618	3.09765	0.
H	2.44128	1.57252	0.87893
H	2.44128	1.57252	-0.87893

B3LYP (Gas)

C	0.	0.32694	0.
C	1.0305	-0.78164	0.
C	0.48683	-2.22907	0.
C	-1.05553	-2.40064	0.
C	-1.90369	-1.10503	0.
N	-1.2601	0.19167	0.
O	-0.26423	2.7109	0.
C	2.00965	2.01973	0.
C	0.50801	1.78239	0.
H	1.68208	-0.63242	0.86728
H	1.68208	-0.63242	-0.86728

B3LYP (Water)

C	0.	0.3254	0.
C	1.03645	-0.77029	0.
C	0.50697	-2.22127	0.
C	-1.0324	-2.40784	0.
C	-1.89452	-1.12447	0.
N	-1.26209	0.18293	0.
O	-0.29036	2.70842	0.
C	1.9879	2.03512	0.
C	0.49797	1.78268	0.
H	1.68469	-0.6132	0.86769
H	1.68469	-0.6132	-0.86769

B3LYP (Methanol)

C	0.	0.3254	0.
C	1.03715	-0.76989	0.
C	0.50825	-2.22117	0.
C	-1.03108	-2.40844	0.
C	-1.89372	-1.12532	0.
N	-1.26189	0.18217	0.
O	-0.29236	2.70791	0.
C	1.98668	2.03664	0.
C	0.49664	1.7831	0.
H	1.68538	-0.6126	0.86769
H	1.68538	-0.6126	-0.86769

H	0.89725	-2.74771	0.86858	H	0.92168	-2.73349	0.86973	H	0.92319	-2.73331	0.86969
H	0.89725	-2.74771	-0.86858	H	0.92168	-2.73349	-0.86973	H	0.92319	-2.73331	-0.86969
H	-1.34112	-2.99633	0.86993	H	-1.31322	-3.00369	0.87083	H	-1.31161	-3.00451	0.87079
H	-1.34112	-2.99633	-0.86993	H	-1.31322	-3.00369	-0.87083	H	-1.31161	-3.00451	-0.87079
H	-2.57524	-1.09364	0.8657	H	-2.56514	-1.12097	0.86643	H	-2.56442	-1.12201	0.86638
H	-2.57524	-1.09364	-0.8657	H	-2.56514	-1.12097	-0.86643	H	-2.56442	-1.12201	-0.86638
H	2.19322	3.09294	0.	H	2.17122	3.10836	0.	H	2.16908	3.11003	0.
H	2.48036	1.57116	0.87999	H	2.45799	1.58525	0.87896	H	2.45721	1.58725	0.879
H	2.48036	1.57116	-0.87999	H	2.45799	1.58525	-0.87896	H	2.45721	1.58725	-0.879

CAM-B3LYP (Gas)

C	0.	0.32546	0.
C	1.02308	-0.78187	0.
C	0.47521	-2.2199	0.
C	-1.0612	-2.38359	0.
C	-1.90258	-1.09184	0.
N	-1.25346	0.19713	0.
O	-0.25066	2.6988	0.
C	2.01038	1.99978	0.
C	0.51468	1.77167	0.
H	1.67321	-0.6335	0.86651
H	1.67321	-0.6335	-0.86651
H	0.88268	-2.74036	0.86728
H	0.88268	-2.74036	-0.86728
H	-1.34874	-2.97794	0.86853
H	-1.34874	-2.97794	-0.86853
H	-2.57178	-1.07737	0.86493
H	-2.57178	-1.07737	-0.86493
H	2.19813	3.07118	0.
H	2.4766	1.54929	0.87941
H	2.4766	1.54929	-0.87941

CAM-B3LYP (Water)

C	0.	0.3238	0.
C	1.02875	-0.77137	0.
C	0.49407	-2.21283	0.
C	-1.03966	-2.39041	0.
C	-1.89432	-1.10999	0.
N	-1.25541	0.18941	0.
O	-0.27537	2.69636	0.
C	1.99027	2.01451	0.
C	0.50575	1.77214	0.
H	1.67561	-0.61554	0.86699
H	1.67561	-0.61554	-0.86699
H	0.90555	-2.72717	0.86844
H	0.90555	-2.72717	-0.86844
H	-1.32266	-2.98484	0.86946
H	-1.32266	-2.98484	-0.86946
H	-2.56245	-1.10358	0.86581
H	-2.56245	-1.10358	-0.86581
H	2.17866	3.08576	0.
H	2.45546	1.56233	0.87847
H	2.45546	1.56233	-0.87847

CAM-B3LYP (Methanol)

C	0.	0.32379	0.
C	1.02938	-0.77104	0.
C	0.49522	-2.21277	0.
C	-1.03851	-2.39093	0.
C	-1.8936	-1.11071	0.
N	-1.25522	0.18878	0.
O	-0.27718	2.69582	0.
C	1.98921	2.01591	0.
C	0.50457	1.77248	0.
H	1.67623	-0.61504	0.867
H	1.67623	-0.61504	-0.867
H	0.90689	-2.72703	0.86841
H	0.90689	-2.72703	-0.86841
H	-1.32125	-2.98556	0.86943
H	-1.32125	-2.98556	-0.86943
H	-2.5618	-1.10445	0.86575
H	-2.5618	-1.10445	-0.86575
H	2.17666	3.08733	0.
H	2.45483	1.56421	0.87852
H	2.45483	1.56421	-0.87852

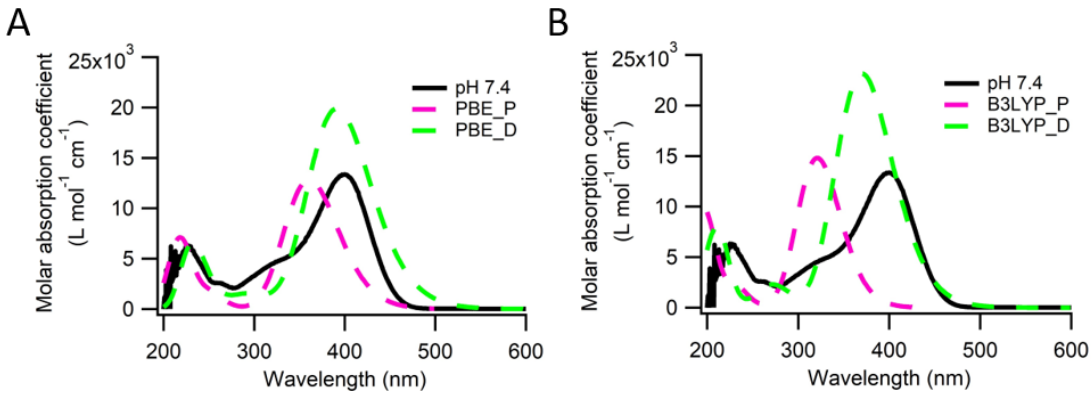

Figure S2.1. Effects of pH on UV-Vis absorption of 4-nitrophenol. Comparison between the measured and TD-DFT-derived UV-Vis. Measured absorbance of 4-nitrophenol was in pH 7.4 buffer. UV-Vis of 4-nitrophenol in protonated ("_P") and deprotonated ("_D") forms were obtained by (A) PBE and (B) B3LYP functionals in water solvation using IEFPCM solvent model.

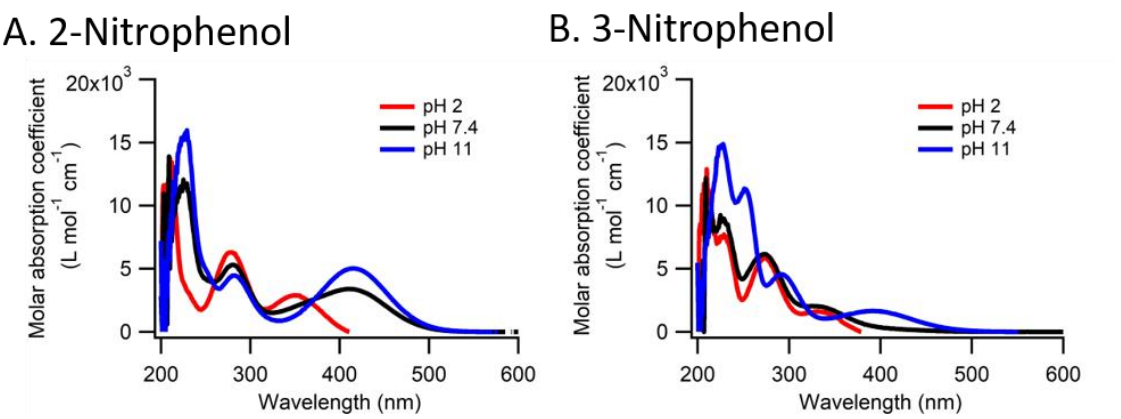

Figure S2.2. Effects of pH on UV-Vis absorption of (A) 2-nitrophenol and (B) 3-nitrophenol. UV-Vis measured for the chemicals dissolved in buffers with pH=2, 7.4 and 11.

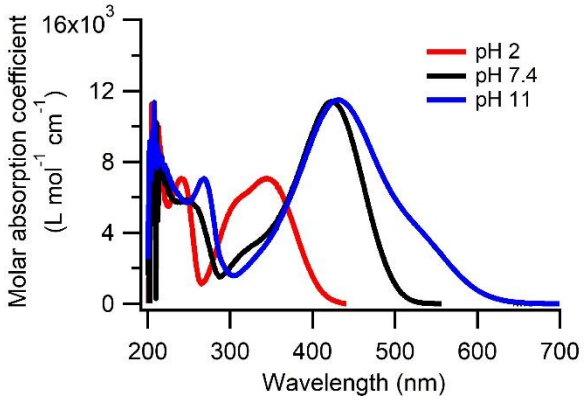

Figure S2.3. Effects of pH on UV-Vis absorption of 4-nitrocatechol, UV-Vis measured in buffers with pH=2, 7.4 and 11.

References

1. Pachauri, R. K.; Allen, M. R.; Barros, V. R.; Broome, J.; Cramer, W.; Christ, R.; Church, J. A.; Clarke, L.; Dahe, Q.; Dasgupta, P., *Climate change 2014: synthesis report. Contribution of Working Groups I, II and III to the fifth assessment report of the Intergovernmental Panel on Climate Change*. IPCC: 2014.

2. Ramanathan, V.; Carmichael, G., Global and regional climate changes due to black carbon. *Nat. Geosci.* **2008,** *1*, 221.

3. Menon, S.; Hansen, J.; Nazarenko, L.; Luo, Y., Climate effects of black carbon aerosols in China and India. *Science* **2002,** *297*, 2250-2253.

4. Washenfelder, R.; Attwood, A.; Brock, C.; Guo, H.; Xu, L.; Weber, R.; Ng, N.; Allen, H.; Ayres, B.; Baumann, K., Biomass burning dominates brown carbon absorption in the rural southeastern United States. *Geophys. Res. Lett.* **2015,** *42*, 653-664.

5. Lack, D. A.; Langridge, J. M.; Bahreini, R.; Cappa, C. D.; Middlebrook, A. M.; Schwarz, J. P., Brown carbon and internal mixing in biomass burning particles. *P. Natl. Acad. Sci.* **2012,** *109*, 14802-14807.

6. Bond, T. C., Spectral dependence of visible light absorption by carbonaceous particles emitted from coal combustion. *Geophys. Res. Lett.* **2001,** *28*, 4075-4078.

7. Andreae, M. O.; Crutzen, P. J., Atmospheric aerosols: Biogeochemical sources and role in atmospheric chemistry. *Science* **1997,** *276*, 1052-1058.

8. Andreae, M. O.; Gelencsér, A., Black carbon or brown carbon? The nature of light-absorbing carbonaceous aerosols. *Atmos. Chem. Phys.* **2006,** *6*, 3131-3148.

9. Sun, H.; Biedermann, L.; Bond, T. C., Color of brown carbon: A model for ultraviolet and visible light absorption by organic carbon aerosol. *Geophys. Res. Lett.* **2007,** *34*.

10. Bahadur, R.; Praveen, P. S.; Xu, Y.; Ramanathan, V., Solar absorption by elemental and brown carbon determined from spectral observations. *P. Natl. Acad. Sci.* **2012,** *109*, 17366-17371.

11. Feng, Y.; Ramanathan, V.; Kotamarthi, V., Brown carbon: a significant atmospheric absorber of solar radiation? *Atmos. Chem. Phys.* **2013,** *13*, 8607-8621.

12. Jiang, H.; Frie, A. L.; Lavi, A.; Chen, J. Y.; Zhang, H.; Bahreini, R.; Lin, Y.-H., Brown carbon formation from nighttime chemistry of unsaturated heterocyclic volatile organic compounds. *Environ. Sci. Tech. Let.* **2019,** *6*.

13. Zhang, X.; Lin, Y.-H.; Surratt, J. D.; Weber, R. J., Sources, composition and absorption Ångstrom exponent of light-absorbing organic components in aerosol extracts from the Los Angeles Basin. *Environ. Sci. Technol.* **2013,** *47*, 3685-3693.

14. Laskin, A.; Laskin, J.; Nizkorodov, S. A., Chemistry of atmospheric brown carbon. *Chem. Rev.* **2015,** *115*, 4335-4382.

15. Jacobson, M. Z., Isolating nitrated and aromatic aerosols and nitrated aromatic gases as sources of ultraviolet light absorption. *J. Geophys. Res-Atmos.* **1999,** *104*, 3527-3542.

16. Hoffer, A.; Gelencsér, A.; Guyon, P.; Kiss, G.; Schmid, O.; Frank, G.; Artaxo, P.; Andreae, M., Optical properties of humic-like substances (HULIS) in biomass-burning aerosols. *Atmos. Chem. Phys.* **2006,** *6*, 3563-3570.

17. Powelson, M. H.; Espelien, B. M.; Hawkins, L. N.; Galloway, M. M.; De Haan, D. O., Brown carbon formation by aqueous-phase carbonyl compound reactions with amines and ammonium sulfate. *Environ. Sci. Technol.* **2013,** *48*, 985-993.

18. Pitts, J. N.; Van Cauwenberghe, K. A.; Grosjean, D.; Schmid, J. P.; Fitz, D. R.; Belser, W. L.; Knudson, G.; Hynds, P. M., Atmospheric reactions of polycyclic aromatic hydrocarbons: facile formation of mutagenic nitro derivatives. *Science* **1978,** *202*, 515-519.

19. Lin, Y.-H.; Budisulistiorini, S. H.; Chu, K.; Siejack, R. A.; Zhang, H.; Riva, M.; Zhang, Z.; Gold, A.; Kautzman, K. E.; Surratt, J. D., Light-absorbing oligomer formation in secondary organic aerosol from reactive uptake of isoprene epoxydiols. *Environ. Sci. Technol.* **2014,** *48*, 12012-12021.

20. Lin, P.; Liu, J.; Shilling, J. E.; Kathmann, S. M.; Laskin, J.; Laskin, A., Molecular characterization of brown carbon (BrC) chromophores in secondary organic aerosol generated from photo-oxidation of toluene. *Phys. Chem. Chem. Phys.* **2015,** *17*, 23312-23325.

21. Lin, P.; Fleming, L. T.; Nizkorodov, S. A.; Laskin, J.; Laskin, A., Comprehensive molecular characterization of atmospheric brown carbon by high resolution mass spectrometry with electrospray and atmospheric pressure photoionization. *Anal. Chem.* **2018,** *90*, 12493-12502.

22. Perdew, J. P.; Ruzsinszky, A.; Tao, J.; Staroverov, V. N.; Scuseria, G. E.; Csonka, G. I., Prescription for the design and selection of density functional approximations: More constraint satisfaction with fewer fits. *J. Chem. Phys.* **2005,** *123*, 062201.

23. Ang, S. T.; Pal, A.; Manzhos, S., Comparison of optical absorption spectra of organic molecules and aggregates computed from real frequency dependent polarizability to TD-DFT and the dipole approximation. *J. Chem. Phys.* **2018,** *149*, 044114.

24. Jacquemin, D.; Preat, J.; Wathelet, V.; Fontaine, M.; Perpète, E. A., Thioindigo dyes: highly accurate visible spectra with TD-DFT. *J. Am. Chem. Soc.* **2006,** *128*, 2072-2083.

25. Jacquemin, D.; Preat, J.; Wathelet, V.; André, J.-M.; Perpète, E. A., Substitution effects on the visible spectra of 1, 4-diNHPh-9, 10-anthraquinones. *Chem. Phys. Lett.* **2005,** *405*, 429-433.

26. Jacquemin, D.; Wathelet, V.; Perpete, E. A.; Adamo, C., Extensive TD-DFT benchmark: singlet-excited states of organic molecules. *J. Chem. Theory Comput.* **2009,** *5*, 2420-2435.

27. Jacquemin, D.; Preat, J.; Perpète, E. A., A TD-DFT study of the absorption spectra of fast dye salts. *Chem. Phys. Lett.* **2005,** *410*, 254-259.

28. Stoïanov, A.; Champion, J.; Maurice, R. m., UV–Vis absorption spectroscopy of polonium (IV) chloride complexes: An electronic structure theory study. *Inorg. Chem.* **2019,** *58*, 7036-7043.

29. Parr, R. G.; Yang, W., Density-functional theory of atoms and molecules. In: Fukui K., Pullman B. (eds) Horizons of Quantum Chemistry. Académie Internationale Des Sciences Moléculaires Quantiques / International Academy of Quantum Molecular Science. *Springer, Dordrecht* **1989,** *3*, 5-15.

30. Adamo, C.; Jacquemin, D., The calculations of excited-state properties with time-dependent density functional theory. *Chem. Soc. Rev.* **2013,** *42*, 845-856.

31. De Angelis, F.; Fantacci, S.; Selloni, A., Alignment of the dye's molecular levels with the TiO2 band edges in dye-sensitized solar cells: a DFT–TDDFT study. *Nanotechnology* **2008,** *19*, 424002.

32. Mehmood, U.; Hussein, I. A.; Harrabi, K.; Reddy, B. V., Density functional theory study on dye-sensitized solar cells using oxadiazole-based dyes. *J. Photon. Energy* **2015,** *5*, 053097.

33. Preat, J.; Jacquemin, D.; Perpète, E. A., A UV/VIS spectra investigation of pH-sensitive dyes using time-dependent density functional theory. *Int. J. Quantum Chem.* **2010,** *110*, 2147-2154.

34. Petit, L.; Quartarolo, A.; Adamo, C.; Russo, N., Spectroscopic properties of porphyrin-like photosensitizers: Insights from theory. *J. Phys. Chem. B* **2006,** *110*, 2398-2404.

35. Magalhães, A. C. O.; Esteves da Silva, J. C.; Pinto da Silva, L. s., Density functional theory calculation of the absorption properties of brown carbon chromophores generated by catechol heterogeneous ozonolysis. *ACS Earth Space Chem.* **2017,** *1*, 353-360.

36. Sousa, J.; da Silva, L. P., Modelling the absorption properties of polycyclic aromatic hydrocarbons and derivatives over three European cities by TD-DFT calculations. *Sci. Total Environ.* **2019,** *695*, 133881.

37. Swinehart, D., The beer-lambert law. *J. Chem. Educ.* **1962,** *39*, 333.

38. Serjeant, E. P.; Dempsey, B., *Ionisation constants of organic acids in aqueous solution*. Pergamon: 1979; Vol. 23.

39. Henderson, L. J., Concerning the relationship between the strength of acids and their capacity to preserve neutrality. *Am. J. Physiol-Legacy Content* **1908,** *21*, 173-179.

40. Hasselbalch, K. A., *Die Berechnung der Wasserstoffzahl des Blutes aus der freien und gebundenen Kohlensäure desselben, und die Sauerstoffbindung des Blutes als Funktion der Wasserstoffzahl*. Julius Springer: 1916.

41. Frisch, M. J.; Trucks, G. W.; Schlegel, H. B.; Scuseria, G. E.; Robb, M. A.; Cheeseman, J. R.; Scalmani, G.; Barone, V.; Petersson, G. A.; Nakatsuji, H.; Li, X.; Caricato, M.; Marenich, A.; Bloino, J.; Janesko, B. G.; Gomperts, R.; Mennucci, B.; Hratchian, H. P.; Ortiz, J. V.; Izmaylov, A. F.; Sonnenberg, J. L.; Williams-Young, D.; Ding, F.; Lipparini, F.; Egidi, F.; Goings, J.; Peng, B.; Petrone, A.; Henderson, T.; Ranasinghe, D.; Zakrzewski, V. G.; Gao, J.; Rega, N.; Zheng, G.; Liang, W.; Hada, M.; Ehara, M.; Toyota, K.; Fukuda, R.; Hasegawa, J.; Ishida, M.; Nakajima, T.; Honda, Y.; Kitao, O.; Nakai, H.; Vreven, T.; Throssell, K.; Montgomery, J. A.; Peralta, J., J. E.; Ogliaro, F.; Bearpark, M.; Heyd, J. J.; Brothers, E.; Kudin, K. N.; Staroverov, V. N.; Keith, T.; Kobayashi, R.; Normand, J.; Raghavachari, K.; Rendell, A.; Burant, J. C.; Iyengar, S. S.; Tomasi, J.; Cossi, M.; Millam, J. M.; Klene, M.; Adamo, C.; Cammi, R.; Ochterski, J. W.; Martin, R. L.; Morokuma, K.; Farkas, O.; Foresman, J. B.; Fox, D. J., Gaussian 09, Revision E. 01. *Gaussian Inc., Wallingford, CT* **2016**.

42. Perdew, J. P.; Burke, K.; Ernzerhof, M., Generalized gradient approximation made simple. *Phys. Rev. Lett.* **1996,** *77*, 3865.

43. Adamo, C.; Barone, V., Toward reliable density functional methods without adjustable parameters: The PBE0 model. *J. Chem. Phys.* **1999,** *110*, 6158-6170.

44. Becke, A. D., A new mixing of Hartree–Fock and local density-functional theories. *J. Chem. Phys.* **1993,** *98*, 1372-1377.

45. Becke, A. D., Density-functional thermochemistry. III. The role of exact exchange. *J. Chem. Phys.* **1993,** *98*, 5648-5652.

46. Yanai, T.; Tew, D. P.; Handy, N. C., A new hybrid exchange–correlation functional using the Coulomb-attenuating method (CAM-B3LYP). *Chem. Phys. Lett.* **2004,** *393*, 51-57.

47. Updyke, K. M.; Nguyen, T. B.; Nizkorodov, S. A., Formation of brown carbon via reactions of ammonia with secondary organic aerosols from biogenic and anthropogenic precursors. *Atmos. Environ.* **2012,** *63*, 22-31.

48. Bones, D. L.; Henricksen, D. K.; Mang, S. A.; Gonsior, M.; Bateman, A. P.; Nguyen, T. B.; Cooper, W. J.; Nizkorodov, S. A., Appearance of strong absorbers and fluorophores in limonene-O3 secondary organic aerosol due to NH4+-mediated chemical aging over long time scales. *J. Geophys. Res-Atmos.* **2010,** *115* (D5).

49. Nguyen, T. B.; Lee, P. B.; Updyke, K. M.; Bones, D. L.; Laskin, J.; Laskin, A.; Nizkorodov, S. A., Formation of nitrogen-and sulfur-containing light-absorbing compounds accelerated by evaporation of water from secondary organic aerosols. *J. Geophys. Res-Atmos.* **2012,** *117* (D1).

50. Laskin, J.; Laskin, A.; Roach, P. J.; Slysz, G. W.; Anderson, G. A.; Nizkorodov, S. A.; Bones, D. L.; Nguyen, L. Q., High-resolution desorption electrospray ionization mass spectrometry for chemical characterization of organic aerosols. *Anal. Chem.* **2010,** *82* (5), 2048-2058.

51. Majumdar, D.; Lee, H. M.; Kim, J.; Kim, K. S.; Mhin, B. J., Photoswitch and nonlinear optical switch: Theoretical studies on 1, 2-bis-(3-thienyl)-ethene derivatives. *J. Chem. Phys.* **1999,** *111*, 5866-5872.

52. Jacquemin, D.; Perpète, E. A., Ab initio calculations of the colour of closed-ring diarylethenes: TD-DFT estimates for molecular switches. *Chem. Phys. Lett.* **2006,** *429*, 147-152.

53. Jacquemin, D.; Preat, J.; Wathelet, V.; Perpète, E. A., Theoretical investigation of the absorption spectrum of thioindigo dyes. *J. Mol. Struct-THEOCHEM* **2005,** *731*, 67-72.

54. Mennucci, B.; Cammi, R.; Tomasi, J., Excited states and solvatochromic shifts within a nonequilibrium solvation approach: A new formulation of the integral equation formalism method at the self-consistent field, configuration interaction, and multiconfiguration self-consistent field level. *J. Chem. Phys.* **1998,** *109*, 2798-2807.

55. Liu, S.; Shilling, J. E.; Song, C.; Hiranuma, N.; Zaveri, R. A.; Russell, L. M., Hydrolysis of organonitrate functional groups in aerosol particles. *Aerosol Sci. Tech.* **2012,** *46*, 1359-1369.

56. Jacquemin, D.; Perpete, E. A.; Scuseria, G. E.; Ciofini, I.; Adamo, C., TD-DFT performance for the visible absorption spectra of organic dyes: conventional versus long-range hybrids. *J. Chem. Theory Comput.* **2008,** *4*, 123-135.

57. Camredon, M.; Aumont, B.; Lee-Taylor, J.; Madronich, S., The SOA/VOC/NOx system: An explicit model of secondary organic aerosol formation. *Atmos. Chem. Phys.* **2007,** *7*, 5599-5610.

58. Liu, P.; Abdelmalki, N.; Hung, H.-M.; Wang, Y.; Brune, W. H.; Martin, S., Ultraviolet and visible complex refractive indices of secondary organic material produced by photooxidation of the aromatic compounds toluene and m-xylene. *Atmospheric Chemistry and Physics* **2015,** *15* (3), 1435-1446.

59. Adamo, C.; Scuseria, G. E.; Barone, V., Accurate excitation energies from time-dependent density functional theory: Assessing the PBE0 model. *J. Chem. Phys.* **1999,** *111*, 2889-2899.

60. Perpète, E. A.; Wathelet, V.; Preat, J.; Lambert, C.; Jacquemin, D., Toward a theoretical quantitative estimation of the λmax of anthraquinones-based dyes. *J. Chem. Theory Comput.* **2006,** *2*, 434-440.

61. Jacquemin, D.; Bouhy, M.; Perpète, E. A., Excitation spectra of nitro-diphenylaniline: Accurate time-dependent density functional theory predictions for charge-transfer dyes. *J. Chem. Phys.* **2006,** *124*, 204321.

62. Jacquemin, D.; Perpète, E. A.; Ciofini, I.; Adamo, C., On the TD-DFT UV/vis spectra accuracy: the azoalkanes. *Theor. Chem. Acc.* **2008,** *120*, 405-410.

63. Cossi, M.; Barone, V., Time-dependent density functional theory for molecules in liquid solutions. *J. Chem. Phys.* **2001,** *115*, 4708-4717.

64. Alif, A.; Pilichowski, J.-F.; Boule, P., Photochemistry and environment XIII: Phototransformation of 2-nitrophenol in aqueous solution. *J. Photoch. Photobio. A* **1991,** *59*, 209-219.

65. Alif, A.; Boule, P.; Lemaire, J., Photochemistry and environment XII: Phototransformation of 3-nitrophenol in aqueous solution. *J. Photoch. Photobio. A* **1990,** *50*, 331-342.

66. Alif, A.; Boule, P.; Lemaire, J., Comportement photochimique du nitro-4 phenol en solution aqueuse. *Chemosphere* **1987,** *16*, 2213-2223.

67. Panossian, A.; Mamikonyan, G.; Torosyan, M.; Gabrielyan, E.; Mkhitaryan, S., Analysis of aromatic aldehydes in brandy and wine by high-performance capillary electrophoresis. *Anal. Chem.* **2001,** *73*, 4379-4383.

68. Guo, H.; Xu, L.; Bougiatioti, A.; Cerully, K. M.; Capps, S. L.; Hite Jr, J.; Carlton, A.; Lee, S.-H.; Bergin, M.; Ng, N., Fine-particle water and pH in the southeastern United States. *Atmos. Chem. Phys.* **2015,** *15*.

69. Shi, G.; Xu, J.; Peng, X.; Xiao, Z.; Chen, K.; Tian, Y.; Guan, X.; Feng, Y.; Yu, H.; Nenes, A., pH of aerosols in a polluted atmosphere: source contributions to highly acidic aerosol. *Environ. Sci. Technol.* **2017,** *51*, 4289-4296.

Chapter III. Characterization of Electrophilicity and Oxidative Potential of Atmospheric Carbonyls

Reproduced from Ref. **Environ. Sci.: Processes Impacts**, 2019,**21**, 856-866, with permission from the Royal Society of Chemistry

3.1 Introduction

Recent epidemiological and toxicological studies have identified a strong association between ambient air pollution and adverse health outcomes, such as allergy, asthma, lung cancer and cardiopulmonary diseases.[1-3] Carbonyl (C=O) compounds are ubiquitous atmospheric pollutants existing in both gas and particle phases. They can either be emitted from primary sources (e.g., incomplete combustion of fossil fuels, cigarette smoking, and cooking),[4-7] or be produced through the oxidation of volatile organic compounds by atmospheric oxidants (e.g., OH radicals and ozone).[8, 9] Toxicological studies have linked carbonyl compounds to pulmonary oxidative stress and inflammatory responses that play key roles in the pathogenesis of chronic obstructive pulmonary disease (COPD).[10, 11] Specifically, formaldehyde and acetaldehyde, the most dominant carbonyls in the urban atmosphere,[5, 6] have been classified as Group 1 and Group 2B human carcinogens, respectively by the International Agency for Research on Cancer (IARC).[12]

From a biochemical point of view, carbonyl compounds represent a group of electrophiles and can react with nucleophilic sites in macromolecules (e.g., DNA, RNA, and proteins), leading to the dysfunctions of macromolecules and eventually cytotoxicity.[13-15] Reactivities of carbonyls toward nucleophiles are determined by their structural and electronic properties. Utilizing the hard soft acid base (HSAB) principle, structurally different carbonyls can be categorized as hard (with low electronic

polarizability) or soft (with high electronic polarizability) electrophiles based on the electron distributions.[16] For example, formaldehyde (the simplest carbonyl) and acrylamide (an α,β-unsaturated carbonyl) are classified as hard and soft compounds due to their low and high electronic polarizability, respectively.

To predict the chemical reactivity and toxicological potency of carbonyl compounds towards the nucleophilic sites of biological macromolecules, the electrophilicity index (ω) proposed by Parr et al.[17] that combines the concepts of hardness (η) and chemical potential (μ), has been widely used as a global reactivity descriptor for carbonyl compounds. For example, a recent study by LoPachin et. al.[18] pointed out that the theoretical ω of an aldehyde compound is positively correlated with the rate constant of aldehyde-nucleophile adduct reaction. A strong consistency between theoretical and experimental ω values of 79 various aldehydes has been reported in the study by Pratihar.[19] Thus, the theoretical ω value can provide an useful insight into the toxicological potency of a carbonyl and the corresponding toxicity mechanism.

With two thiol functional groups, dithiothreitol (DTT) is often used as a surrogate for biological reducing agent such as glutathione (GSH), which is one of the most abundant endogenous antioxidants in cells capable of preventing cellular damage caused by reactive oxygen species (ROS).[20] DTT assay has been developed as a chemical assay to quantitatively assess the redox activity and oxidative potential (i.e., the ability of a chemical species to catalyze the electron transfer between reductants and oxygen molecules) of ambient particulate matter (PM).[21] The rate of DTT consumption corresponds to the amount of redox-active species in PM.[21] In consideration of the various

sources and varied chemical compositions of PM, the identification of contributing components in PM to its oxidative potential is essential to predict their health impacts. So far, DTT activities or consumption rates of DTT have been largely correlated with the concentration of transition metals (e.g., Cu and Zn)[22-25] and soluble organic compounds (e.g., quinones and organic peroxides)[26, 27] from vehicle emissions, biomass burning and secondary organic aerosols. These redox-active chemical species in PM can oxidize the reduced DTT to its disulfide form, and the rate of DTT loss in the reaction is regarded to be associated with the generation of ROS.[28] Despite the wide application of DTT assay to evaluate the toxic potency of PM, the mechanisms leading to the DTT consumption and the actual reaction products have not been well characterized yet. Particularly, the non-redox reactions such as the nucleophilic addition of DTT with carbonyl compounds have been overlooked in interpretation of DTT consumption by PM.

In this study, the global electrophilicity indexes of model carbonyl compounds were calculated using the density functional theory (DFT). To evaluate the validity of using this computational approach to predict DTT consumptions by carbonyl-dominated organic systems, the global electrophilicity indexes were compared to the experimental DTT consumption rates. To elucidate the mechanisms by which carbonyls and DTT interact, the carbonyl-DTT adducts were characterized using gas chromatography/electron ionization-mass spectrometry (GC/EI-MS).

3.2 Methods and materials

3.2.1 Chemicals

Ten atmospheric relevant carbonyls were selected as model compounds for this study, including mesityl oxide (MPO; >95%, TCI America), formaldehyde (FM; 36.5-38% in H_2O, Sigma-Aldrich), citral (Ctr; 95%, Sigma-Aldrich), 2-furaldehyde (2-FA; 99%, Acros Organics), 4-formylbenzoic acid (4-FBA; >95%, Matrix Scientific), benzaldehyde (BA; ≥99%, Sigma-Aldrich), 2-nitrobenzaldehyde (2-NBA; >99%, Chem-Impex Int'l Inc.), 3-nitrobenzaldehyde (3-NBA; >98%, TCI America), 4-nitrobenzaldehyde (4-NBA; >99%, Chem-Impex Int'l Inc.), and *trans*-cinnamaldehyde (*t*-CA; >98%, TCI America). Dithiothreitol (DTT), 5-5'-dithiobis (2-nitrobenzoic acid) (DTNB), ethylenediaminetetraacetic acid disodium salt solution (EDTA, 0.5 M in H_2O) and dimethyl sulfoxide (DMSO) were purchased from Sigma-Aldrich (St. Louis, MO, USA). Potassium phosphate buffer (0.05 M KH_2PO_4, pH 7.4) was purchased from Fisher Scientific.

3.2.2 Computational procedure for calculating electrophilicity index

The global electrophilicity indexes (ω) of carbonyl compounds were calculated with the DFT/B3LYP/6-311+G** level of theory using Gaussian 09W[29] (Gaussian, Inc.). B3LYP (Becke, 3-parameter, Lee-Yang-Parr), a hybrid functional with the Hartree-Fock (exact) exchange energy,[30, 31] was used to calculate for molecular properties such as atomization energies and vibrational frequencies. The standard basis set of 6-311+G** is applied during calculations to incorporate the diffusion and polarization functions as noted by "+" and "**", respectively. The B3LYP functional has been reported to provide results

close to accurate electron correlation methods if basis sets with sufficient quality are used for calculation of DFT-based reactivity indexes.[32]

Avogadro (an open-source molecular editor and visualizer, Version 1.2.0)[33] was used to generate a molecular configuration file of a specified carbonyl molecule. The molecular configuration file was then imported to Gaussian 09W [29] that optimized the molecule's geometry and output the energy values for the highest occupied (E_{HOMO}) and the lowest unoccupied molecular orbitals (E_{LUMO}). Koopmans' theorem in DFT has been used as a convenient method within its limitations to approximate the ionization potential (I) with the negative of the HOMO energy ($-E_{HOMO} = I$).[34, 35] By extension, it is considered that the electron affinity (A) can be approximated by the negative of the LUMO energy ($-E_{LUMO} = A$).[34, 35] Several comparative studies have indicated that the I and A values calculated by HOMO and LUMO energies generally correlate well with I and A calculated by a delta self-consistent field (ΔSCF) procedure (i.e., the difference of total energy upon adding or removing an electron) or experimental I and A values. This semi-quantitative estimate of I and A provides satisfactory linear correlation relationships with molecular properties.[35, 36] The chemical potential (μ), chemical hardness (η) and global electrophilicity index (ω) were calculated using E_{HOMO} and E_{LUMO} values, as shown in the following equations.[17-19] The factor of ½ for η was neglected.[37]

$$\omega = \frac{\mu^2}{2\eta} \tag{3.1}$$

$$\mu = -\frac{I + A}{2} \approx \frac{E_{HOMO} + E_{LUMO}}{2} \tag{3.2}$$

$$\eta = \frac{I-A}{2} \approx E_{LUMO} - E_{HOMO} \quad (3.3)$$

To account for the aqueous environment of DTT assays, a separate set of calculations were performed in water using the conductor-like polarizable continuum model (CPCM)[38] as a solvation model. To compared with the calculations conducted in gas phase by Pratihar,[19] we also performed the calculations of ω in gas phase. The calculated parameters (i.e., E_{HOMO}, E_{LUMO}, μ, η, and ω) in water and in gas phase can be found in Table 3.1 and Table S3.1, respectively. Geometries of selected compounds used for Gaussian 09W was optimized within Gaussian, as shown in Table S3.2.

3.2.3 DTT assay

The DTT assay procedures were modified from those published by Kramer et al.[27] Each of the carbonyl sample was incubated with 2.5 nmol of DTT in potassium phosphate buffer (0.5 M, pH 7.4) and 1 mM EDTA at 37 ºC for 30 min. To ensure the tested compounds to be fully soluble, carbonyl standard solutions were initially prepared in DMSO and diluted with methanol or buffer, except formaldehyde. Varying amounts of each carbonyl reacted with DTT are listed in Table S3.3. After incubation, 10 µl of 1 mM DTNB (in potassium phosphate buffer, pH 7.4) was added to the reaction mixture to titrate the remaining DTT. The final volume of the reaction mixture was 135 µl. The reaction between DTNB and DTT resulted in the production of 5-thio-2-nitrobenzoic acid (TNB) that can be quantified by its absorbance at 412 nm using a UV-Visible spectrophotometer (Beckman DU-640). In equation (3.4), the blank-corrected DTT consumption (ΔDTT, nmol) by the carbonyl compound was calculated using the absorbance of DTT-blank mixture (A_0), the absorbance of DTT-carbonyl mixture (A), and the initial DTT

concentration (DTT_0, nmol). The absorbance of the carbonyl itself was subtracted from that of DTT-carbonyl mixture.

$$\Delta DTT = \frac{A_0 - A}{A_0} DTT_0 \quad (3.4)$$

The mass normalized DTT consumption rate or DTT_r was defined as ΔDTT normalized by the mass of added carbonyl (m) and incubation time (t, 30 min), as shown in equation (3.5):

$$DTT_r = \frac{\Delta DTT}{m \times t} \quad (3.5)$$

3.2.4 GC/EI-MS analysis

Reaction mixtures (before the addition of DTNB) from the DTT assays were analyzed by gas chromatography/electron ionization-mass spectrometry (GC/EI-MS)[39] to identify DTT-carbonyl reaction adducts. To prevent clogging of the GC column by salts present in the potassium phosphate buffer, buffer solutions were substituted with Milli-Q water in the reactions. Reaction mixtures were dried under a gentle stream of N_2 gas, and then trimethylsilylated with 100 μL of N,O-bis(trimethylsilyl) trifluoroacetamide with trimethylchlorosilane (BSTFA+TMCS, 99:1) (≥99%, SUPELCO) and 50 μL anhydrous pyridine (≥99%, EMD Millipore Corporation) at 70 ºC for 1 hour. This derivatization procedure allowed the conversion of the hydroxyl functional groups into volatile trimethylsilyl (TMS) derivatives that could be subsequently analyzed with a GC/EI-MS system (Agilent 6890N GC coupled with 5975 MSD). An Agilent 7683B series autosampler was used to inject 5 μL of each derivatized sample in splitless mode. A J&W Scientific DB-5 column (30 m × 0.25 mm i.d., 0.25 μm film) was used to separate the TMS derivatives. Helium was used as the carrier gas at a flow rate of 1 mL min^{-1}. The temperature program of GC ran for 65.17 min with the following gradient: initial

temperature held at 60 ºC for 1 min, temperature ramp of 3 ºC min^{-1} up to 200 ºC, temperature held at 200 ºC for 2 min, temperature ramp of 20 ºC min^{-1} up to 310 ºC, and finally temperature held at 310 ºC for 10 min. A solvent delay time of 10.5 min was programed. The MS scan was performed in the *m/z* range of 50-650. The temperatures of the GC inlet and detector were set at 250 ºC and 280 ºC, respectively. No DTT-carbonyl adducts were detected in solvent blank samples.

3.3 Results and discussion

3.3.1 The chemical reactivity descriptors of carbonyl compounds

To study the chemical reactivity of carbonyls with varying chemical structures, the molecular descriptors (i.e., μ, η and ω) of selected carbonyl compounds were calculated using computational chemistry approaches, and the results are shown in Table 3.1. For simple carbonyls, nitrobenzaldehydes have the largest μ, followed by 4-formylbenzoic acid, benzaldehyde, 2-furaldehyde, and formaldehyde. For α,β-unsaturated carbonyls, *trans*-cinnamaldehyde has higher μ than citral and mesityl oxide. Chemical potential is a global thermodynamic property that describes the change in electronic energy during the electron transfer of a chemical process.[40] Thus, the electronegativity (χ) that describes the tendency of an atom or a molecule to attract a shared pair of electrons is also noted as the negative of chemical potential ($-\mu$).[41] Generally, an increase in electronegativity means an increase in reactivity. Among all tested compounds, nitrobenzaldeydes have the highest tendency to attract electrons while formaldehyde has the lowest. Furthermore, as shown in Eq. (2), μ can be estimated by averaging E_{LUMO} and E_{HOMO} values. Compared to E_{HOMO},

E_{LUMO} has larger variation (Table 3.1). Nitrobenzaldehydes have the largest E_{LUMO} values of -3.276 – -3.507 eV, while formaldehyde the lowest E_{LUMO} of -1.669 eV. The negative value of E_{LUMO} is an analogue to electron affinity, or the promptness of electrophiles to accept electrons.[34, 35] Thus, compounds with more negative E_{LUMO} values are commonly more electrophilic. E_{LUMO} has been correlated to the cytotoxicity of α,β-unsaturated aldehydes in the study of Chan et al. (2008).[13]

Table 3.1. The chemical reactivity descriptors (E_{HOMO}, E_{LUMO}, μ, η and ω) of carbonyl compounds calculated in water solvent.

Compound	Structure	E_{HOMO} eV	E_{LUMO} eV	μ eV	η eV	ω eV
Simple carbonyl						
Formaldehyde (FM)		-7.686	-1.669	-4.678	6.017	1.82
2-Furaldehyde (2-FA)	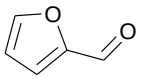	-7.142	-2.250	-4.696	4.892	2.25
Benzaldehyde (BA)	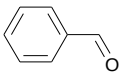	-7.504	-2.259	-4.882	5.245	2.27
4-Formylbenzoic acid (4-FBA)	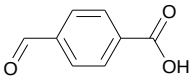	-7.712	-2.831	-5.272	4.881	2.85
2-Nitrobenzaldehyde (2-NBA)	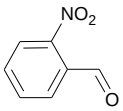	-7.823	-3.302	-5.563	4.521	3.42
3-Nitrobenzaldehyde (3-NBA)	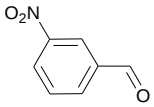	-7.807	-3.276	-5.542	4.531	3.39
4-Nitrobenzaldehyde (4-NBA)	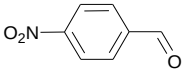	-7.834	-3.507	-5.671	4.327	3.72
α,β-unsaturated carbonyl						
Mesityl oxide (MPO)	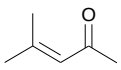	-7.019	-1.709	-4.364	5.31	1.79

Citral (CTR)	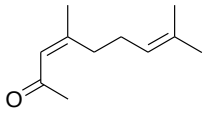	-6.567	-1.971	-4.269	4.596	1.98
trans-Cinnamaldehyde (*t*-CA)	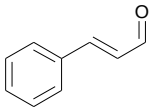	-6.880	-2.555	-4.718	4.325	2.57

Another important factor that determines the chemical reactivity of a compound is chemical hardness (η), which is associated with polarizability or the resistance to charge transfer.[42] In general, the lower η values means higher polarizability of the electrophile. For example, as shown in Table 3.1, 4-nitrobenzaldehyde is the most polarizable electrophiles among the three nitrobenzaldehydes, and it has the lowest η of 4.327 eV. Compared to other aromatic carbonyls, benzaldehyde has only one functional group (-CHO) that contributes to the polarizability. Thus, benzaldehyde has a relatively high η value (5.245 eV). Formaldehyde is least polarizable and has the highest η value of 6.017 eV. Based on the HSAB theory, electrophiles and nucleophiles can be categorized into hard or soft compounds depending on the distribution of their electrons. Soft electrophiles such as α,β-unsaturated carbonyls have delocalized electrons and preferentially react with soft nucleophiles such as thiols in cysteine residues.[18] This will be discussed further in the next section.

Though μ and η shed some light on the chemical reactivity of electrophiles, none of them can solely predict the toxic potency. Conversely, the global electrophilicity index, ω, a measure that combines μ and η (Eq. 1), can provide more comprehensive information of the reactivity for a given electrophile. As shown in Table 3.1, the calculated ω values in aqueous phase show an order of nitrobenzaldehydes > 4-formylbenzoic acid >

benzaldehyde > 2-furaldehyde > formaldehyde among simple carbonyls. The relatively higher absolute chemical potential values and lower hardness values lead to the higher electrophilicity indexes of nitrobenzaldehydes. Among α,β-unsaturated carbonyls, the order of calculated ω values appear to be *trans*-cinnamaldehyde > citral > mesityl oxide. The relatively lower absolute chemical potential and higher hardness of mesityl oxide results in its lower ω value.

The electrophilicity indexes calculated in this study were also compared with those reported in previous studies. Our global ω values for formaldehyde and *trans*-cinnamaldehyde in aqueous phase (Table 3.1) are slightly higher than those reported by LoPachin and Gavin,[18] mainly due to the different methods used to calculate hardness. The hardness in their study was calculated as $\eta = (E_{LUMO} - E_{HOMO})/2$. However, the factor of ½ was neglected in this study as suggested by Pearson.[37] Another possible reason is the different basis set utilized in their calculation. LoPhachin and Gavin used the double-zeta basis set of 6-31G* that includes a polarizability function (represented by "*") for non-H atoms, while the triple-zeta basis set of 6-311+G** was applied in this study that adds one Gaussian-type orbital to 6-31G and contains a diffusion function (represented by "+") for non-H atoms and a polarizability function (represented by "**") for both H and non-H atoms.[43] In order to compare the global ω values in gas phase reported in Pratihar's study, we also performed our calculations in gas phase. As shown in Table S3.1, overall, our computational results agree well with those reported in Pratihar's study that utilized the same B3LYP/ 6-311+G** level of theory.[19] Note that the ω value (3.78 eV, Table S3.1) of 4-nitrobenzaldehyde in this study is much higher than the ω reported in Pratihar's (2.73

eV),[19] which could be attributed to the difference in molecular geometries applied in calculations. The Gaussian optimized geometry of 4-nitrobenzaldehyde (Table S3.2) in this study has a planar configuration, but in Pratihar's study the configuration of 4-nitrobenzaldehyde is nonplanar.[19]

3.3.2 The toxic potency of carbonyls

The toxic potency of carbonyl compounds was studied by measuring the reactivities of carbonyls towards thiol groups in DTT, expressed as the mass-normalized DTT consumption rate (DTT_r, Eq. 5). As shown in Figure 3.1, among simple carbonyls, nitrobenzaldehydes (2.06×10^{-4}–6.43×10^{-4} nmol/min/μg) showed much higher DTT_r than other compounds (8.50×10^{-6}–1.67×10^{-4} nmol/min/μg) due to their more negative chemical potential and lower hardness values (Table 3.1). DTT is considered as a soft nucleophile due to its delocalized electron density; thus, it preferentially reacts with soft electrophiles. In contrast, benzaldehyde and formaldehyde, harder and less polar electrophiles, had much lower activities towards DTT. Among *α*,*β*-unsaturated carbonyls, *trans*-cinnamaldehyde has much higher DTT_r (1.51×10^{-3} nmol/min/μg) than citral (1.53×10^{-4} nmol/min/μg) and mesityl oxide (1.02×10^{-4} nmol/min/μg). *α*,*β*-Unsaturated carbonyl compounds are known as Michael acceptors and typically highly reactive with nucleophiles.[20] Schultz tested the reactivities of 51 polarized *α*,*β*-Michael acceptors to glutathione (a monothiol compound) and reported the rate constants (M^{-1} s^{-1}) ranged from <0.0003 to >4000.[20] Generally, the thiol reactivity decreases for longer chain carbonyls or those with a methyl group on C=C,[13, 44] which can explain the relatively low DTT_r of citral and mesityl oxide. It should

also be noted that GSH is a monothiol compound with a lower *p*Ka compared to DTT.[45] Thus, it may have different reactivities towards carbonyl compounds.

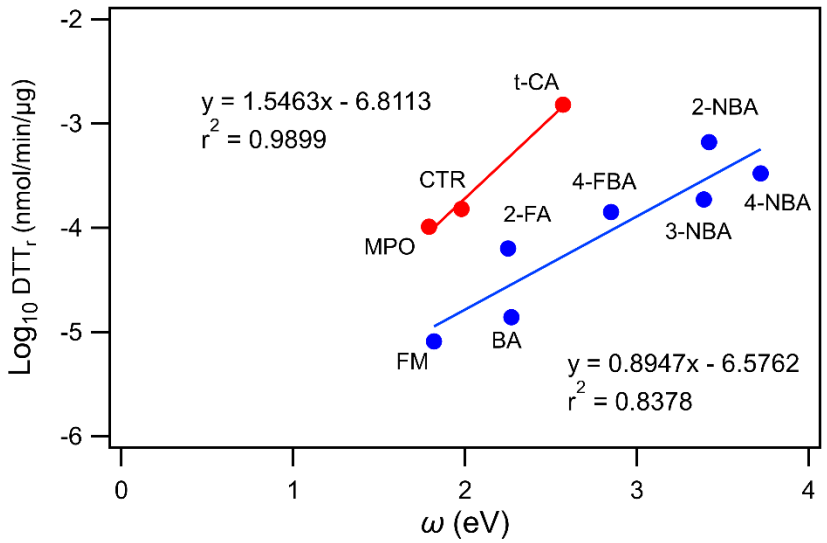

Figure 3.1. Comparison between the calculated electrophilicity index ω (eV) in water solvent and measured $Log_{10}(DTT_r)$ (nmol DTT consumed per reaction incubation minute per µg of sample). The r^2 values for simple (blue) and α,β-unsaturated (red) carbonyls are 0.8378 and 0.9899, respectively.

The DTT_r values of carbonyls in this study were also compared with those of other compounds and aerosol systems (Table S3.4). Overall, the DTT_r of soft aromatic carbonyls (i.e., nitrobenzaldehydes and 2-furaldehyde) are comparable or higher than those of alcohols or acids (4.44×10^{-5}–2.51×10^{-4}), but much lower than α,β-unsaturated carbonyls (1.02×10^{-4}–3.26×10^{-2}) and organic hydroperoxides (1.17×10^{-2}–4.90×10^{-1}). Compared to aerosol systems, soft aromatic carbonyls in this study have one or 2 order lower DTT_r.[24, 27, 44, 46-50] Despite the relatively lower DTT activities of simple carbonyls tested in this study, their importance in respect to nucleophile additions should also be highlighted due to their

high abundance in indoor and outdoor environments in both gas and aerosol phases.[6, 51, 52] Redox reactive species such as quinones and transition metals have been linked to the high DTT activities of ambient PM and quinone-enriched aerosol systems (e.g., naphthalene-derived secondary organic aerosols, or naphthalene SOA).[48, 53] Notably, recent studies by Jiang et al. have revealed the importance of non-redox compounds, mostly unsaturated carbonyls, in DTT consumption by aerosols.[44, 54] Unsaturated carbonyls are commonly found in the ring-opening products of aromatic SOA systems.[55, 56] According to the simulation by Jiang et al., unsaturated carbonyls could account for 32-75% of the total DTT consumption by toluene SOA.[54]

3.3.3 The comparison between ω and DTT activities

To examine the correlation between electrophilicity and toxic potency, the global electrophilicity indexes of carbonyl compounds (Table 3.1) were compared with corresponding DTT activities. As shown in Figure 3.1 and Figure S3.1, $Log_{10}(DTT_r)$ values of simple carbonyls showed a strong linear correlation with theoretical ω values in either water solvent (r^2=0.8378) or gas phase (r^2=0.8239). Similarly, the α,β-unsaturated carbonyls' $Log_{10}(DTT_r)$ values also linearly related to their ω values with a r^2=0.9899 in water solvent and r^2=0.9977 in gas phase. In respect to the ω values, α,β-unsaturated carbonyls have a greater slope in response to DTT_r compared to simple carbonyls, indicating that they are more reactive towards DTT at the given ω value. It should be noted that the ω value is a generalized global descriptor of chemical reactivity, but it lacks the information of site selectivity. Thus, it may not necessarily correlate to the chemical reactivity of an extended system with more than one highly reactive site.[57-59] Given that

α,*β*-unsaturated carbonyls possess two potential electrophilic sites (i.e., at the carbonyl and alkene groups), to have a better prediction of the intermolecular reactivity of all carbonyls towards DTT, the site selectivity for chemical reactions should also be considered.

The strong correlation between DTT_r and global electrophilicity indexes highlights the nucleophilic addition of DTT to carbonyls as an important toxicity pathway in the presence of atmospheric carbonyls. Note that beside the nucleophilic addition, other reaction pathways might also contribute to the DTT consumption by carbonyls. For example, Marteau et al. has reported that organic hydroperpoxides (a group of ROS) could be formed as intermediate oxidation product during the autooxidation of carbonyls by molecular oxygen.[60] Organic hydroperoxides are able to oxidize thiols to disulfides, sulfenic acids, sulfinic acid or sulfonic acids.[61] Therefore, both nucleophilic addition and redox reactions may co-exist and compete with each other during the DTT assay.

3.3.4 The identification of DTT-carbonyl adducts

The possible pathways of nucleophilic attack of DTT on carbonyls are shown in Scheme 3.1. Generally, one of the thiols in DTT can add to the C=O through 1,2-carbonyl additions (Scheme 3.1A).[62] For *α*,*β*-unsaturated carbonyls, however, the C=O bond can withdraw electrons from the C=C bond, which makes the β carbon (δ^+) to be more electrophilic. Thus, *α*,*β*-unsaturated carbonyls such as *trans*-cinnamaldehyde can also undergo the 1,4-conjugate addition, commonly known as Michael addition.[63]

Scheme 3.1. Nucleophilic addition reactions of DTT (nucleophile) onto (A) simple carbonyls and (B) *α, β*-unsaturated carbonyls.

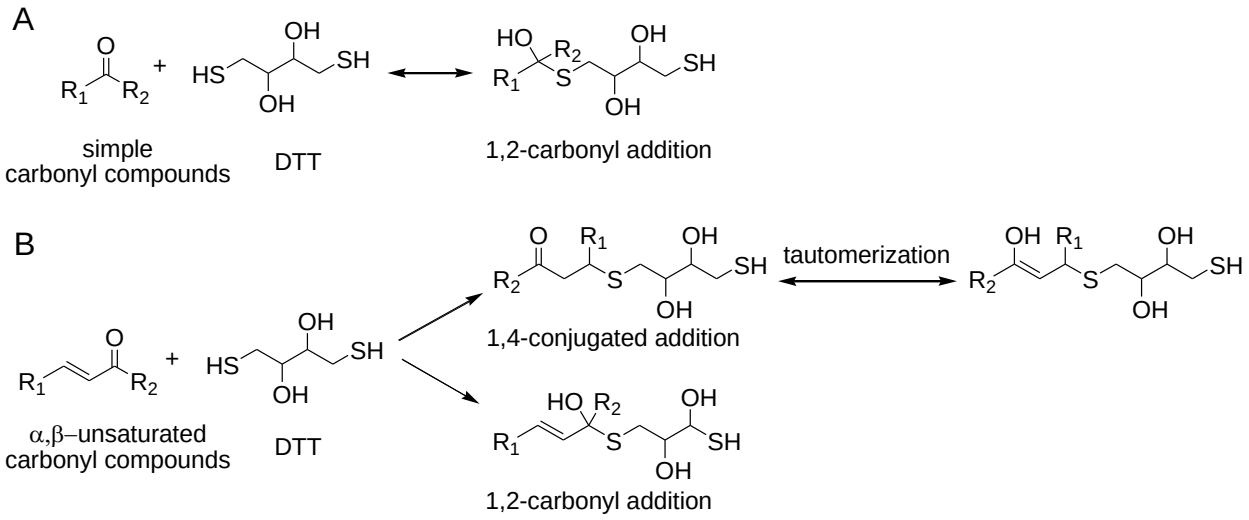

To confirm the reaction pathway through nucleophilic addition of thiols to carbonyls, the reaction products were characterized using the GC/EI-MS technique. As shown in Figure 3.2, all of the trimethylsilylated 1,2-addition adducts formed from the reaction between simple carbonyls and DTT were observed in the extracted ion chromatograms (EIC) for simple aldehydes. As shown in Figure 3.2B and 2C, only one peak appeared in the EICs of 2-furaldehyde-DTT mixture (*m*/*z* 466.15) and benzaldehyde-DTT mixture (*m*/*z* 476.17), validating the 1,2-addition of DTT to carbonyls. In Figure 3.2A, the 1,2-addition adducts (*m*/*z* 400.14) of formaldehyde and DTT was detected but displayed three distinct peaks (RT=34.762, 40.862, and 46.571 min) in the EIC, which can be attributed to the interaction between DTT and formaldehyde oligomers in aqueous solutions.[64-66] The adduct of formaldehyde oligomers and the DTT molecule can be fragmented in the ion source and lose one or two units of formaldehyde monomer, thus showing the same *m*/*z* value but with different retention times. The peaks of 1,2-carbonyl

addition adducts were also distinguishable in the EICs of nitrobenzaldehydes (*m*/*z* 521.16 in Figure 3.2D, 3.2E and 3.2F) and 4-formylbenzoic acid (*m*/*z* 592.2 in Figure 3.2G). Apart from the major peaks of reaction products, some minor peaks appeared in EICs even after background subtraction, which could be caused by the impurities (2-5%) of stereoisomers in our chemicals (e.g., the presence of *cis* or *trans* isomers of cinnamaldehyde and citral).

As shown in Table S3.5 and Figure S3.2, the local selectivity indexes computed using the condensed Fukui function (e.g., f+ for nucleophilic attack) for tested *α*,*β*-unsaturated carbonyls reveal that C_{β} and $C_{C=O}$ are the most reactive carbons within the molecules which can be related to the 1,4- and 1,2-additon reactions with DTT, respectively. Calculations were carried out with the UCA-FUKUI software.[67] However, as shown in Figure 3.3, for *α*,*β*-unsaturated carbonyls, all of the 1,4-conjugate addition adducts tested in this study were detected (*m*/*z* 454.19 for mesityl oxide, *m*/*z* 522.25 for citral, and *m*/*z* 502.19 for *trans*-cinnamaldehyde), whereas the signals of 1,2-carbonyl addition adducts were negligible. These observations can be explained by the kinetic versus thermodynamic control of the reaction. It has been established that for *α*,*β*-unsaturated carbonyls, the 1,2-carbonyl addition adducts are kinetic products that can form more rapidly but the reactions may be reversible.[63] On the contrary, the 1,4-conjugate addition adducts are thermodynamic products (i.e., more stable products of the reaction). Thus, the reaction between *α*,*β*-unsaturated carbonyls and DTT is dominated by the 1,4-conjugate additions. These results highlight the importance of taking site selectivity and transition states into account when considering the chemical reactivity of an extended chemical system containing more than one reactive site for the reaction.

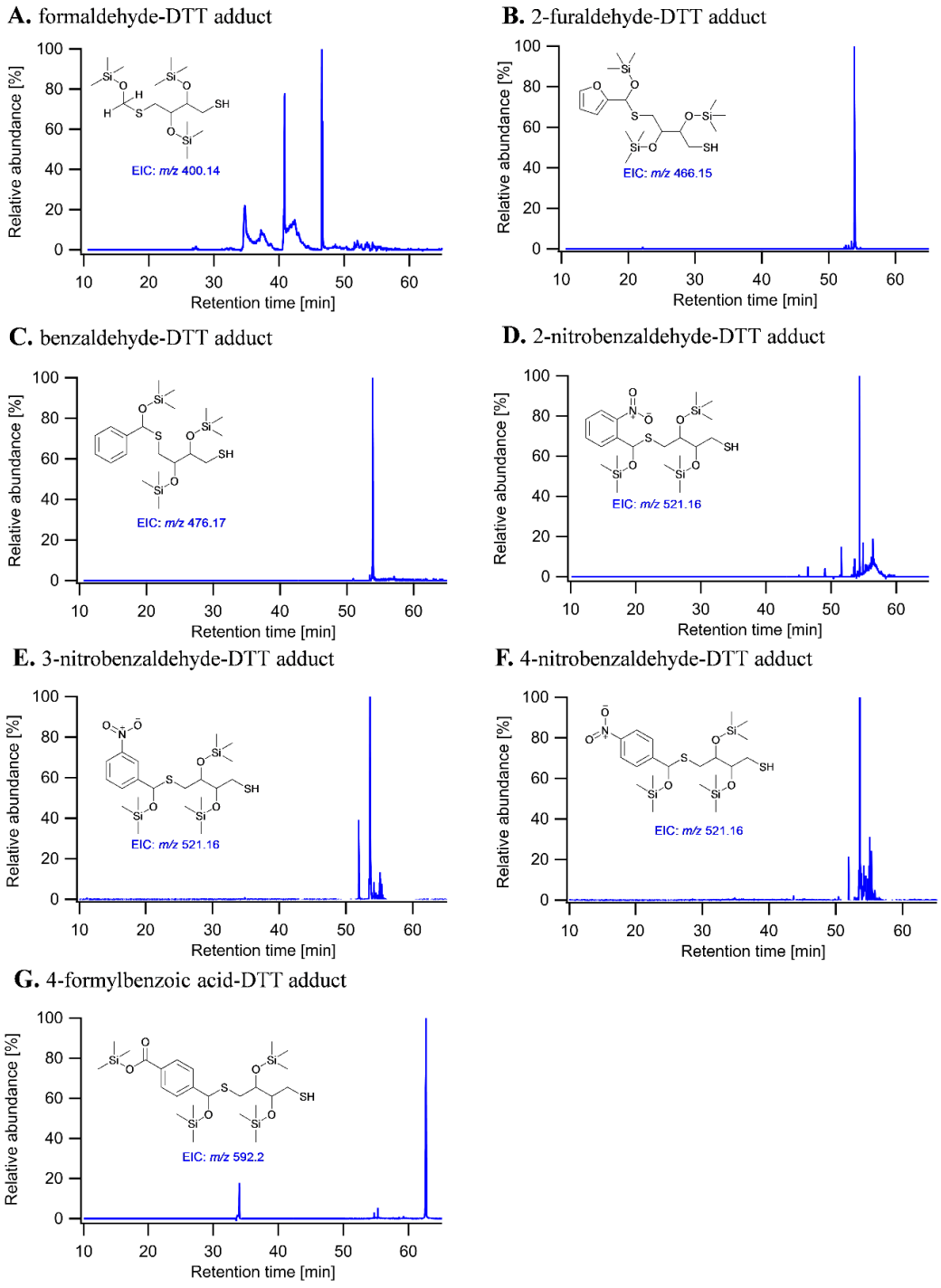

Figure 3.2. The GC/MS extracted ion chromatograms (EICs) of trimethylsilylated simple carbonyl- DTT adducts formed through 1,2-carbonyl additions. (A) Formaldehyde; (B) 2-Furaldehyde; (C) Benzaldehyde; (D) 2-Nitrobenzaldehyde; (E) 3-Nitrobenzaldehyde; (F) 4-Nitrobenzaldehyde; (G) 4-Formylbenzoic acid.

Although information regarding the toxicological consequences of reversible 1,2-addition of carbonyls with biological thiol moieties is limited, it has been reported that carbonyl compounds can react with thiol residues in biomolecules through 1,2-addition spontaneously, and lead to a rapid generation of an intermediate hemithioacetal compound followed by an isomerization to form a more stable product. This process has been correlated with the pathogenesis of diabetes and cancer.[68] The observation of 1,2-addition adducts formation in this study implicates the potential importance of carbonyl-thiol interactions in biological systems through the formation of hemithioacetal reaction intermediates.

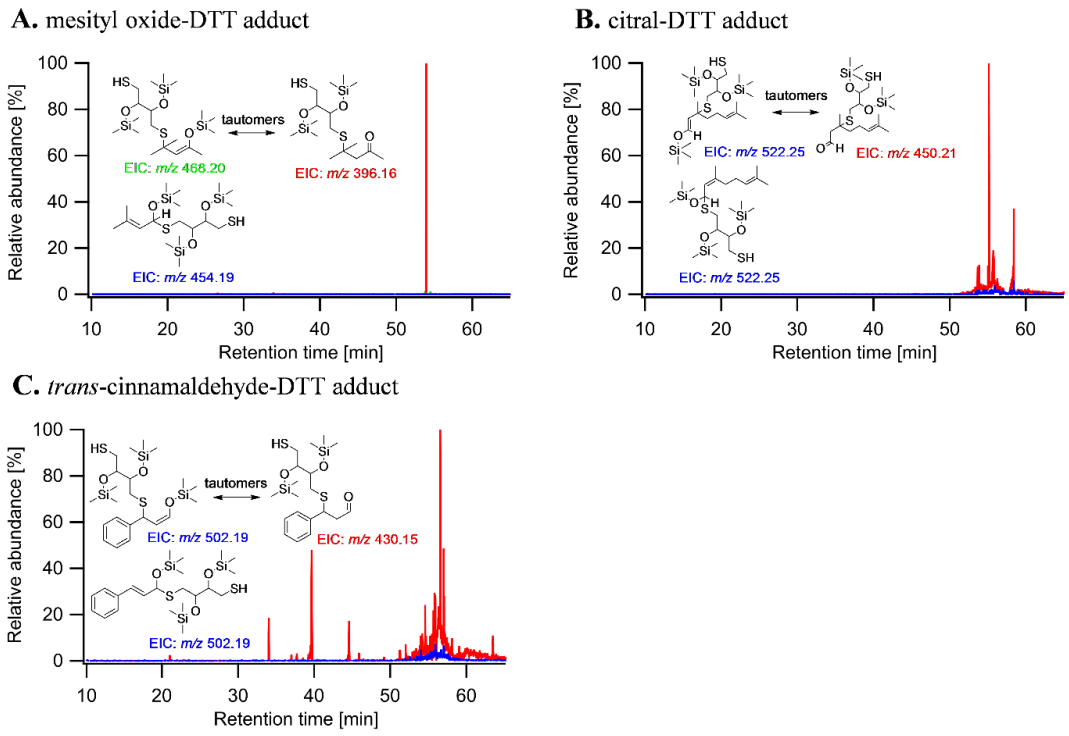

Figure 3.3. The GC/MS extracted ion chromatograms (EICs) of trimethylsilylated *α,β*-unsaturated carbonyl-DTT adducts formed through 1,2-carbonyl additions and 1,4-conjugate additions. All of the signals are normalized to the abundance of 1,4-addition products. (A) Mesityl oxide-DTT adducts with *m/z* of 454.19 (1,2-adduct, blue), 468.20 (enol tautomer of 1,4-adduct, green) and 396.16 (keto tautomer of 1,4-adduct, red); (B)

Citral-DTT adducts with *m/z* of 522.25 (1,2-adduct and ento tautomer of 1,4-adduct, blue) and 450.21(keto tautomer, red); (C) *trans*-Cinnamaldehyde-DTT adducts with *m/z* of 502.19 (1,2-adduct and enol tautomer of 1,4-adduct, blue), and 430.15 (keto tautomer of 1,4-adduct, red).

3.4 Sources of uncertainty

Some cautions are necessary in the interpretation of our results. First, in the present study only electrophilicity, mainly driven by electronic effects, is considered to predict the chemical reactivity of carbonyl compounds with DTT. The overall reactivity, however, consists of multiple factors including the steric effects.[18, 69] Steric hindrance can reduce the accessibility of the reaction target and decrease the rate of adduct formation.[17] In addition, current model predictions incorporate the effects of solute–solvent interactions using a pure solvent model. However, the molecular interactions among different compounds within complex aerosol systems (e.g., SOA) or in biological fluids, have not been considered during the calculation. Furthermore, the global electrophilicity index calculated in this study represents chemical reactivity of a molecule containing one strong electrophilic site. For compounds with multiple strong electrophilic sites, such as α,β-unsaturated carbonyls, descriptors that encompass information about selectivity of active sites such as Fukui function, local softness, or local electrophilicity index may better represent their overall intramolecular reactivity trend.[58, 59, 70] The DFT-based descriptors defined from a perturbative approach may not necessarily explain the observations in late transition states. Further transition state calculations of structures, activation energy and the kinetic reaction barrier are required to gain a better understanding of overall chemical reactivity and potential toxicity. Lastly, given that only ten carbonyl compounds were tested in this study,

more atmospheric carbonyls need to be further studied to examine the predictive power of electrophilicity index on their toxicity.

3.5 Conclusions

Taken together, we performed both theoretical calculations and experimental measurements to assess the chemical reactivities of targeted carbonyl compounds. The global electrophilicity indexes showed strong relationships with the measured DTT activities of carbonyl compounds (r^2=0.8378 and 0.9899 for calculations of simple and α,β-unsaturated carbonyls in water, respectively), indicating the feasibility of applying electrophilicity index to predict the thiol reactivity with atmospheric carbonyls. To account for the solute-solvent interactions, the inclusion of solvent models in the theoretical calculations is necessary.

Currently, the interpretation of DTT activities have been mostly associated with the production of ROS by quinones and transition metals in aerosols, and the term of "oxidative potential" has been used to denote the DTT consumption (rate). However, recent studies proposed that non-redox active species such as electron-deficient compounds (e.g., carbonyl compounds) also contributed to DTT removal through nucleophilic addition pathways.[44, 54] Such pathways have not been well-characterized when assessing DTT-based aerosol oxidative potential. In our work, the formation of nucleophilic addition products (i.e., carbonyl-DTT adducts) was confirmed by GC/EI-MS detection, which elicit the importance of taking the role of various functional groups and reaction pathways into consideration when interpreting DTT activity of aerosol oxidative potential. Thus,

"oxidative potential" should be used in caution when study the toxic potency of non-redox active species in air pollutants using DTT assay. Future work is needed to calculate the local philicity descriptors of α,β-unsaturated carbonyls and assess a wider array of carbonyl compounds present in the complex atmospheric mixture, such as carbonyls produced from the atmospheric oxidation of volatile organic carbons. Studies on relevant biological endpoints in response to carbonyl exposures are also required to further understand the health effects of atmospheric carbonyls.

3.6 Supporting Information

Table S3.1. The chemical reactivity descriptors EHOMO, ELUMO, μ, η and ω) of carbonyl compounds calculated in gas phase.

Compound	Structure	E_{HOMO} eV	E_{LUMO} eV	μ eV	η eV	ω eV
Simple carbonyl						
Formaldehyde (FM)		-7.667	-1.746	-4.707	5.921	1.87
2-Furaldehyde (2-FA)	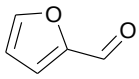	-7.207	-2.155	-4.681	5.052	2.17
Benzaldehyde (BA)	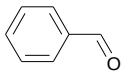	-7.340	-2.176	-4.758	5.164	2.19
4-Formylbenzoic acid (4-FBA)	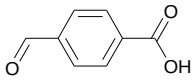	-7.632	-2.870	-5.251	4.762	2.90
2-Nitrobenzaldehyde (2-NBA)	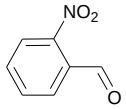	-7.768	-3.303	-5.536	4.465	3.43
3-Nitrobenzaldehyde (3-NBA)	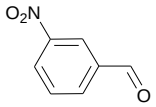	-7.908	-3.323	-5.616	4.585	3.44

4-Nitrobenzaldehyde (4-NBA)	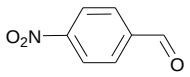	-7.963	-3.565	-5.764	4.398	3.78
α,β-unsaturated carbonyl						
Mesityl oxide (MPO)	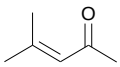	-6.763	-1.610	-4.187	5.153	1.70
Citral (CTR)	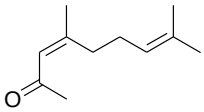	-6.706	-1.824	-4.265	4.882	1.86
trans-Cinnamaldehyde (*t*-CA)	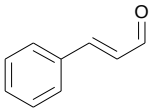	-6.959	-2.517	-4.738	4.442	2.53

Table S3. 2. Optimized geometry of carbonyls in gas phase and in water solvent from the Gaussian 09 program.

Gaussian Optimized Geometry, Gas Phase:

Formaldehyde

E(RB3LYP) = -114.541577701 Hartree (Eh)
Electronic state: 1-A
Cartesian Coordinates (Angstroms):

C	0.00000	0.52742	0.00000
O	0.00000	-0.67430	0.00000
H	-0.00001	1.11493	0.93973
H	-0.00001	1.11493	-0.93973

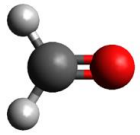

Benzaldehyde

E(RB3LYP) =-345.666239183 Hartree(Eh)
Electronic state: 1-A
Cartesian Coordinates (Angstroms):

C	-1.99189	0.46358	0.00005
C	-0.53400	0.20655	0.00008
C	0.35492	1.28690	0.00001
C	1.72933	1.06367	-0.00009
C	2.21651	-0.24269	-0.00007
C	1.33257	-1.32598	0.00006
C	-0.03833	-1.10446	0.00012
O	-2.84864	-0.39249	-0.00024
H	-2.27063	1.53915	0.00097
H	-0.03461	2.30040	0.00004
H	2.41747	1.90105	-0.00022
H	3.28638	-0.41923	-0.00014
H	1.71866	-2.33893	0.00012
H	-0.74281	-1.92794	0.00016

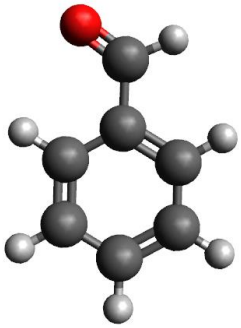

4-Formylbenzoic acid

E (RB3LYP) = -534.295211516 Hartree (Eh)
Electronic state: 1-A
Cartesian Coordinates (Angstroms):

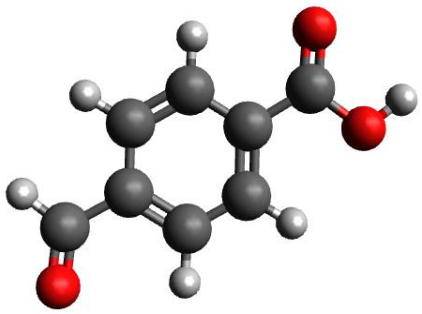

C	-3.23113	0.30439	-	0.00003
O	-3.98513	-0.64116		0.00033
C	-1.74968	0.20387	-	0.00008
C	-0.98081	1.37289	-	0.00006
C	0.40626	1.29788	-	0.00014
C	1.03309	0.04777	-	0.00024
C	2.52354	0.01713	-	0.00034
O	3.23205	0.99515		0.00035
O	3.02541	-1.24221		0.00021
C	0.26520	-1.12622	-0.00024	
C	-1.11952	-1.04708	-0.00012	
H	-3.62426	1.34258	0.00036	
H	-1.47336	2.33993	0.00003	
H	1.01854	2.19080	-0.00013	
H	3.99070	-1.16232	0.00065	
H	0.76000	-2.08826	-0.00032	
H	-1.73201	-1.94077	-0.00014	

2-Nitrobenzaldehyde

E (RB3LYP) = -550.212689420 Hartree (Eh)
Electronic state: 1-A
Cartesian Coordinates (Angstroms):

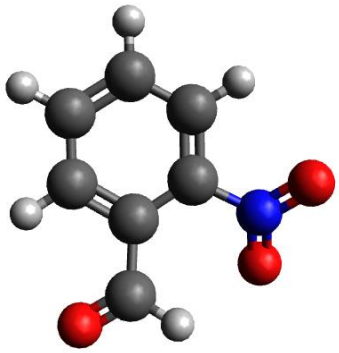

N	1.83296	-0.08103	0.03635
O	2.63301	-0.86133	-0.45962
O	2.12797	0.97566	0.58284
C	0.40030	-0.45191	-0.00568
C	-0.60112	0.52981	-0.05137
C	-0.36342	2.00300	-0.22224
O	-1.23679	2.81585	-0.02765
C	-1.93005	0.09177	-0.02279
C	-2.24238	-1.26077	0.05397
C	-1.22405	-2.21312	0.08571
C	0.10657	-1.80927	0.04920
H	0.63290	2.31205	-0.56903
H	-2.70753	0.84452	-0.07073
H	-3.27943	-1.57385	0.08181
H	-1.46182	-3.26855	0.14274
H	0.91658	-2.52549	0.07540

3-Nitrobenzaldehyde

E (RB3LYP) = -550.224223249 Hartree (Eh)
Electronic state: 1-A
Cartesian Coordinates (Angstroms):

N	2.30133	-0.48159	0.00001
O	2.38668	-1.70232	0.00058
O	3.25248	0.28780	-0.00071
C	0.94209	0.10894	0.00005
C	-0.15853	-0.73867	-0.00003
C	-1.43571	-0.17735	-0.00003
C	-2.62350	-1.07085	-0.00018
O	-3.76774	-0.68204	-0.00015
C	-1.59012	1.21616	0.00012
C	-0.47364	2.04368	0.00022
C	0.80806	1.49313	0.00016
H	-0.01170	-1.81166	-0.00009
H	-2.38897	-2.15505	-0.00023
H	-2.59319	1.62612	0.00014
H	-0.59255	3.12038	0.00035
H	1.69383	2.11363	0.00018

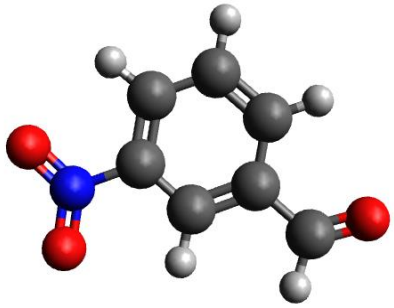

4-Nitrobenzaldehyde

E (RB3LYP) = -550.223245374 Hartree (Eh)
Electronic state: 1-A
Cartesian Coordinates (Angstroms):

N	-2.52393	-0.09984	0.00002
O	-3.16777	0.94050	0.00140
O	-3.00698	-1.22348	-0.00129
C	-1.04335	0.01008	-0.00001
C	-0.46916	1.27606	-0.00048
C	0.91822	1.36848	-0.00056
C	1.70472	0.21213	-0.00009
C	3.18690	0.33573	-0.00012
O	3.94913	-0.60174	0.00029
C	1.09852	-1.05105	0.00042
C	-0.28415	-1.15900	0.00041
H	-1.10187	2.15255	-0.00074
H	1.39329	2.34382	-0.00099
H	3.56628	1.37836	-0.00055
H	1.72631	-1.93378	0.00081
H	-0.78168	-2.11887	0.00070

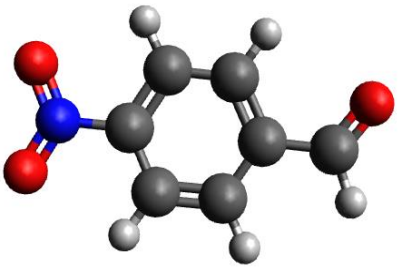

Mesityl oxide

E (RB3LYP) = -309.962942241 Hartree (Eh)
Electronic state: 1-A
Cartesian Coordinates (Angstroms):

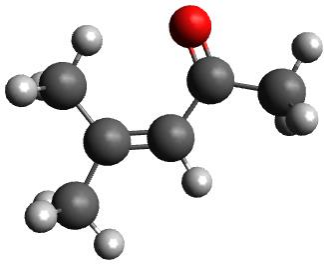

C	-1.53337	1.34384	0.04939
C	-1.20502	-0.12162	0.00165
C	0.04081	-0.63904	-0.02994
C	1.33307	0.08906	-0.01653
C	2.56623	-0.79824	0.04634
O	1.44556	1.30389	-0.05586
C	-2.40005	-1.03805	-0.01364
H	-2.01063	1.64096	-0.89279
H	-2.26714	1.53506	0.84028
H	-0.65381	1.96230	0.19919
H	0.13259	-1.72198	-0.05680
H	2.53706	-1.43105	0.93935
H	2.59604	-1.46729	-0.82005
H	3.46322	-0.18110	0.06241
H	-3.05672	-0.79399	-0.85637
H	-2.11766	-2.08934	-0.08670
H	-2.99737	-0.90034	0.89480

Citral

E (RB3LYP) = -466.002393482 Hartree (Eh)
Electronic state: 1-A
Cartesian Coordinates (Angstroms):

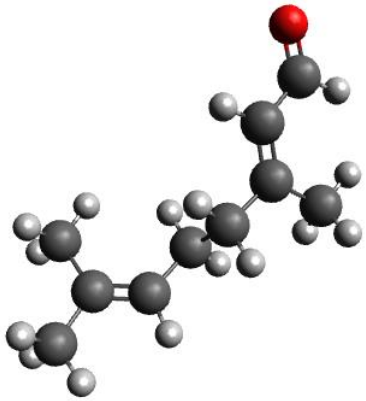

C	-2.98931	-1.66773	0.55963
C	-3.16763	-0.26054	0.04795
C	-4.54945	0.03863	-0.48046
C	-2.21477	0.68125	0.04499
C	-0.79279	0.57140	0.52159
C	0.22287	0.70312	-0.64573
C	1.66308	0.67274	-0.19056
C	2.17030	1.94664	0.43249
C	2.39320	-0.45065	-0.35563
C	3.78410	-0.65597	0.04947
O	4.38298	-1.70091	-0.12376
H	-3.68720	-1.86781	1.38103
H	-3.22240	-2.39239	-0.22894
H	-1.98173	-1.87596	0.91805
H	-5.30712	-0.11405	0.29716
H	-4.63401	1.06562	-0.84102

H	-4.80790	-0.63626	-1.30490
H	-2.48069	1.65729	-0.36031
H	-0.60316	1.36590	1.25321
H	-0.61272	-0.37339	1.03811
H	0.04071	-0.10638	-1.35677
H	0.02882	1.64477	-1.17385
H	1.52256	2.25386	1.25948
H	3.18816	1.87850	0.81090
H	2.13523	2.75502	-0.30652
H	1.93998	-1.31506	-0.83405
H	4.30003	0.19426	0.53603

***trans*-Cinnamaldehyde**

E (RB3LYP) = -423.083192755 Hartree (Eh)
Electronic state: 1-A
Cartesian Coordinates (Angstroms):

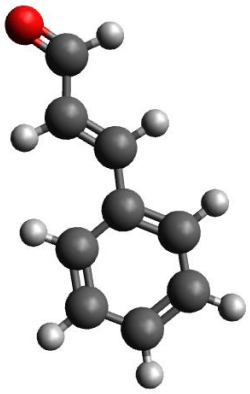

C	3.35775	-0.28859	0.00013
C	1.99490	0.24280	-0.00007
C	0.93371	-0.58683	0.00054
C	-0.48549	-0.23876	0.00028
C	-1.43620	-1.27341	-0.00008
C	-2.79963	-0.99575	-0.00042
C	-3.23974	0.32608	-0.00031
C	-2.30780	1.36679	0.00014
C	-0.94735	1.08978	0.00039
O	4.36337	0.39221	-0.00064
H	3.42717	-1.39833	0.00139
H	1.90193	1.32380	-0.00087
H	1.14233	-1.65628	0.00132
H	-1.09637	-2.30393	-0.00015
H	-3.51648	-1.80878	-0.00073
H	-4.30096	0.54709	-0.00054
H	-2.64645	2.39658	0.00029
H	-0.23901	1.90956	0.00082

Gaussian Optimized Geometry, Water Solvent:

Formaldehyde

E(RB3LYP) = -114.546525343 Hartree (Eh)
Hartree Electronic state: 1-A
Cartesian Coordinates (Angstroms):

C	0.00000	-0.53129	0.00000
O	0.00000	0.67678	0.00000
H	-0.00001	-1.11325	0.93844
H	-0.00001	-1.11325	-0.93844

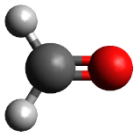

Benzaldehyde

E (RB3LYP) = -345.189785981 Hartree (Eh)
Electronic state: 1-A
Cartesian Coordinates (Angstroms):

C	-1.98644	0.46404	0.00016
C	-0.53560	0.20142	0.00015
C	0.35009	1.28710	0.00004
C	1.72528	1.06767	-0.00015
C	2.21713	-0.23785	-0.00013
C	1.33739	-1.32599	0.00008
C	-0.03440	-1.10945	0.00019
O	-2.85400	-0.39182	-0.00039
H	-2.26320	1.53582	0.00108
H	-0.04206	2.29889	0.00010
H	2.41016	1.90728	-0.00031
H	3.28733	-0.41060	-0.00025
H	1.72762	-2.33701	0.00016
H	-0.72850	-1.94144	0.00031

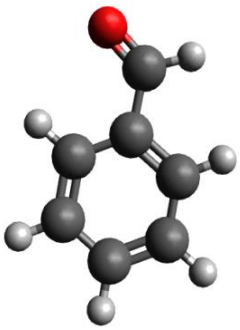

4-Formylbenzoic acid

E (RB3LYP) = -534.307733963 Hartree (Eh)
Electronic state: 1-A
Cartesian Coordinates (Angstroms):

C	3.22644	0.30767	0.00013
O	3.98916	-0.63914	-0.00034
C	1.74987	0.19977	0.00011
C	0.98361	1.37163	0.00014
C	-0.40376	1.29749	0.00016
C	-1.03379	0.04870	0.00015
C	-2.52478	0.01394	0.00016
O	-3.23261	0.99868	-0.00044
O	-3.02308	-1.23741	0.00006
C	-0.26793	-1.12739	0.00011
C	1.11668	-1.05074	0.00003
H	3.61699	1.34239	-0.00027
H	1.47577	2.33797	0.00014
H	-1.00658	2.19628	0.00019
H	-3.99143	-1.17845	-0.00028
H	-0.75966	-2.09065	0.00010
H	1.71904	-1.95085	0.00001

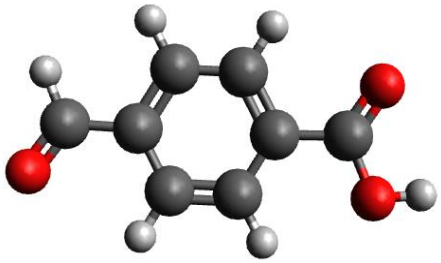

2-Nitrobenzaldehyde

E (RB3LYP) = -550.224630179 Hartree (Eh)
Electronic state: 1-A
Cartesian Coordinates (Angstroms):

N	1.79783	-0.25294	0.03803
O	2.54425	-1.11526	-0.40839
O	2.18437	0.79812	0.54450
C	0.34673	-0.49561	-0.01497
C	-0.55506	0.58045	-0.07126
C	-0.15941	2.00775	-0.26947
O	-0.87982	2.93103	0.04892
C	-1.91948	0.27681	-0.03930
C	-2.36143	-1.04068	0.04602
C	-1.44164	-2.08718	0.08983
C	-0.07637	-1.81676	0.05642
H	0.80341	2.19318	-0.76569
H	-2.62785	1.09318	-0.10283
H	-3.42363	-1.25074	0.07128
H	-1.78139	-3.11301	0.15776
H	0.65437	-2.61186	0.10938

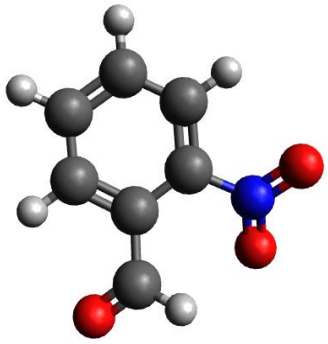

3-Nitrobenzaldehyde

E (RB3LYP) = -550.236789568 Hartree (Eh)
Electronic state: 1-A
Cartesian Coordinates (Angstroms):

N	-2.29157	-0.48030	0.00004
O	-2.38731	-1.70321	-0.00139
O	-3.25280	0.28131	0.00155
C	-0.94042	0.10871	-0.00004
C	0.16082	-0.73908	0.00015
C	1.43662	-0.17400	0.00008
C	2.61559	-1.07146	0.00038
O	3.76822	-0.68852	0.00030
C	1.58768	1.22078	-0.00028
C	0.47055	2.04766	-0.00050
C	-0.80914	1.49480	-0.00033
H	0.02359	-1.81255	0.00039
H	2.37943	-2.15149	0.00067
H	2.58610	1.64067	-0.00038
H	0.58733	3.12384	-0.00081
H	-1.69050	2.12057	-0.00047

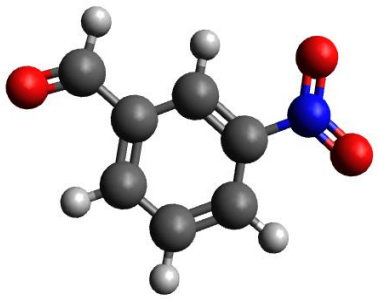

4-Nitrobenzaldehyde

E (RB3LYP) = -550.235866482 Hartree (Eh)
Electronic state: 1-A
Cartesian Coordinates (Angstroms):

N	-2.51565	-0.09780	-0.00004
O	-3.16971	0.93918	0.00222
O	-3.01121	-1.21924	-0.00190
C	-1.04215	0.01018	-0.00006
C	-0.46684	1.27655	-0.00075
C	0.92006	1.36790	-0.00085
C	1.70378	0.20868	-0.00018
C	3.18201	0.33918	-0.00026
O	3.95081	-0.60057	0.00056
C	1.09647	-1.05458	0.00056
C	-0.28542	-1.16161	0.00060
H	-1.09021	2.15894	-0.00125
H	1.39396	2.34272	-0.00148
H	3.55993	1.37763	-0.00050
H	1.71515	-1.94299	0.00113
H	-0.77578	-2.12443	0.00112

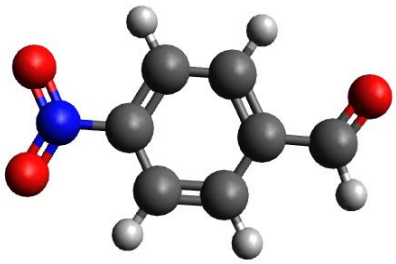

Mesityl oxide

E (RB3LYP) = -309.970343628 Hartree (Eh)
Electronic state: 1-A
Cartesian Coordinates (Angstroms):

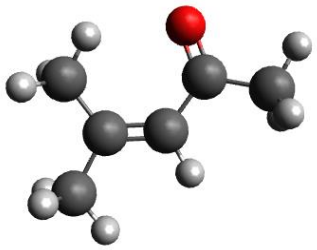

C	-1.52906	1.34092	0.11698
C	-1.20267	-0.12107	0.00213
C	0.04399	-0.64002	-0.06456
C	1.32954	0.08268	-0.03782
C	2.55762	-0.79446	0.10874
O	1.44287	1.30250	-0.13657
C	-2.39672	-1.03492	-0.03577
H	-1.83686	1.72329	-0.86432
H	-2.38091	1.48289	0.78831
H	-0.68259	1.93353	0.45264
H	0.13500	-1.72114	-0.11976
H	2.48450	-1.40602	1.01317
H	2.62450	-1.48578	-0.73754
H	3.45719	-0.18165	0.14969
H	-3.07531	-0.73526	-0.84218
H	-2.11743	-2.07905	-0.18136
H	-2.96716	-0.94960	0.89579

Citral

E (RB3LYP) = -466.012217419 Hartree (Eh)
Electronic state: 1-A
Cartesian Coordinates (Angstroms):

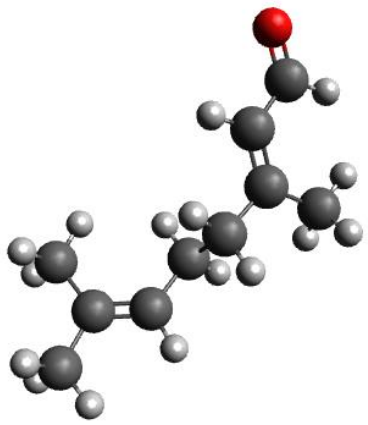

C	-2.98626	-1.68734	0.49855
C	-3.16476	-0.25827	0.05068
C	-4.55161	0.06803	-0.44956
C	-2.20758	0.68042	0.07707
C	-0.78133	0.54561	0.53598
C	0.22043	0.70054	-0.64239
C	1.66137	0.67578	-0.19565
C	2.17609	1.95779	0.39628
C	2.38551	-0.45899	-0.34565
C	3.76854	-0.64851	0.05468
O	4.38147	-1.70005	-0.10344
H	-3.68106	-1.92210	1.31330
H	-3.22703	-2.37406	-0.32106
H	-1.97661	-1.91283	0.84048
H	-5.30038	-0.11565	0.32998
H	-4.63555	1.10951	-0.76660

H	-4.82180	-0.57297	-1.29697
H	-2.47181	1.67353	-0.28573
H	-0.57542	1.32150	1.28204
H	-0.60375	-0.41396	1.02505
H	0.03883	-0.10249	-1.36071
H	0.01776	1.64979	-1.15095
H	1.50865	2.30293	1.19138
H	3.18256	1.89008	0.80301
H	2.16791	2.73710	-0.37366
H	1.91981	-1.32709	-0.80531
H	4.28373	0.20673	0.52329

***trans*-Cinnamaldehyde**

E (RB3LYP) = -423.093761553 Hartree (Eh)
Electronic state: 1-A
Cartesian Coordinates (Angstroms):

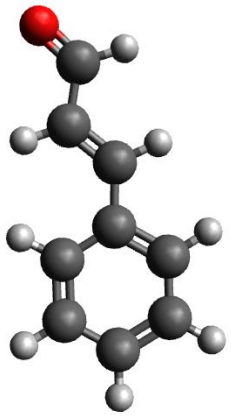

C	3.34476	-0.28972	0.00011
C	1.99525	0.24948	0.00001
C	0.93263	-0.58488	0.00042
C	-0.48392	-0.23640	0.00023
C	-1.43196	-1.27567	-0.00006
C	-2.79616	-0.99931	-0.00033
C	-3.23759	0.32335	-0.00023
C	-2.30783	1.36767	0.00013
C	-0.94627	1.09355	0.00022
O	4.36576	0.38663	-0.00052
H	3.41223	-1.39510	0.00097
H	1.89813	1.33014	-0.00054
H	1.14101	-1.65351	0.00100
H	-1.08954	-2.30493	-0.00010
H	-3.51216	-1.81284	-0.00059
H	-4.29910	0.54266	-0.00040
H	-2.64914	2.39638	0.00027
H	-0.24093	1.91572	0.00054

Table S3.3. The nanomoles of carbonyls added to the DTT assay.

Carbonyl	**nmol**
Formaldehyde	6.71×10^{4}—3.36×10^{5}
2-Furaldehyde	2.39×10^{2}—1.20×10^{3}
Benzaldehyde	9.70×10^{3}—4.85×10^{4}
4-Formylbenzoic acid	3.26×10^{1}—1.63×10^{2}
2-Nitrobenzaldehyde	6.85×10^{0}—1.37×10^{2}
3-Nitrobenzaldehyde	6.48×10^{0}—1.30×10^{2}
4-Nitrobenzaldehyde	6.79×10^{0}—1.36×10^{2}
Citral	1.11×10^{2}—5.57×10^{2}
trans-Cinnamaldehyde	3.78×10^{1}—1.89×10^{2}
Mesityl oxide	3.53×10^{3}

Table S3.4. The comparisons of DTTr of carbonyls in this study with other compounds and aerosol systems reported previously.

Compounds or aerosols system	DTT_r (nmol/min/μg)	Reference
Pure compound		
Formaldehyde	8.50×10^{-6}	This study
2-Furaldehyde	1.05×10^{-4}	This study
Benzaldehyde	1.53×10^{-5}	This study
4-Formylbenzoic acid	1.67×10^{-4}	This study
2-Nitrobenzaldehyde	6.43×10^{-4}	This study
3-Nitrobenzaldehyde	2.06×10^{-4}	This study
4-Nitrobenzaldehyde	3.52×10^{-4}	This study
Mesityl oxide	1.02×10^{-4}	This study
Citral	1.53×10^{-4}	This study
trans-Cinnamaldehyde	1.51×10^{-3}	This study
Isoprene epoxydiol (IEPOX)	$7.00\pm1.39\times10^{-5}$	Kramer et al.[27]
2-Methyltetrol	$4.44\pm0.92\times10^{-5}$	Kramer et al.[27]
Methacrylic acid epoxide (MAE)	$9.84\pm0.97\times10^{-5}$	Kramer et al.[27]
2-Methylglyceric acid	$2.51\pm0.37\times10^{-4}$	Kramer et al.[27]
2-Hydroperoxy-2-methyl-but-3-en-1-ol (ISOPOOH)	$4.90\pm2.20\times10^{-1}$	Kramer et al.[27]
Methacrolein	$3.26\pm0.10\times10^{-2}$	Jiang et al.[50]
9,10-Phenanthraquinone	25.46 ± 1.00	Jiang et al.[50]
1,2-Naphthoquinone	9.07 ± 0.29	Jiang et al.[50]
1,4-Naphthoquinone	2.92 ± 0.12	Jiang et al.[50]
tert-Butyl hydroperoxide	$1.17\pm0.19\times10^{-2}$	Jiang et al.[44]
Ambient PM		
Ambient PM	$\sim10^{-3}$–10^{-2}	Fang et al.[46]
Ambient PM	$\sim(2–6)\times10^{-2}$	Verma et al.[24]
Primary aerosol		
Accord diesel	$2.3\pm0.2\times10^{-2}$	Cheung et al.[47]
DPF-Accord diesel	$1.9\pm0.2\times10^{-2}$	Cheung et al.[47]
Corolla gasoline	$1.2\pm0.1\times10^{-2}$	Cheung et al.[47]
Golf diesel	$1.8\pm0.3\times10^{-2}$	Cheung et al.[47]
Golf biodiesel	$2.5\pm0.3\times10^{-2}$	Cheung et al.[47]
Wood smoke	$2.5\pm0.1\times10^{-2}$	Jiang et al.[50]
Secondary organic aerosol		
Naphthalene SOA	$11.8\pm1.4\times10^{-2}$	McWhinney et al.[48]
Toluene SOA	$(3.7–8.2)\times10^{-2}$	Jiang et al.[44, 50]
1,3,5-Trimethylbenzene SOA	$(1.4–2.5)\times10^{-2}$	Jiang et al. [44, 50]
Isoprene SOA	$(1.6–5.3)\times10^{-2}$	Jiang et al. [44, 50]
α-Pinene SOA	$(0.9–1.3)\times10^{-2}$	Jiang et al. [44, 50]
Isoprene SOA	$\sim10^{-2}$	Tuet et al.[49]
α-Pinene SOA	$\sim(2–3)\times10^{-2}$	Tuet et al.[49]
β-caryophyllene SOA	$\sim2\times10^{-2}$	Tuet et al. [49]
Pentadecane SOA	$\sim(1.5–2)\times10^{-2}$	Tuet et al. [49]
m-xylene SOA	$\sim(2–4)\times10^{-2}$	Tuet et al. [49]
Naphthalene SOA	~0.1-0.2	Tuet et al. [49]
Isoprene SOA	$2.10\pm0.22\times10^{-3}$	Kramer et al.[27]
Methacrolein SOA	$2.30\pm0.27\times10^{-3}$	Kramer et al. [27]
IEPOX-derived SOA	$1.79\pm0.16\times10^{-3}$	Kramer et al. [27]
MAE-derived SOA	$3.13\pm0.30\times10^{-3}$	Kramer et al. [27]

Table S3.5. Local selectivity indexes computed for the tested *α,β*-unsaturated carbonyls based on the condensed Fukui function using UCA-FUKUI software.[67]

***α,β*-Unsaturated carbonyl**	**Atom**	**f-**	**f+**	**f0**	**Dual-Descriptor**
Citral	C_{10}	-0.0001	0.2674	0.1336	0.2673
	C_7	0.0000	0.2384	0.1192	0.2383
trans-Cinnamaldehyde	C_3	0.0272	0.1893	0.1082	0.1621
	C_1	-0.018	0.1258	0.0539	0.1078
Mesityl oxide	C_4	0.0077	0.2319	0.1198	0.2242
	C_2	0.1363	0.2248	0.1805	0.0886

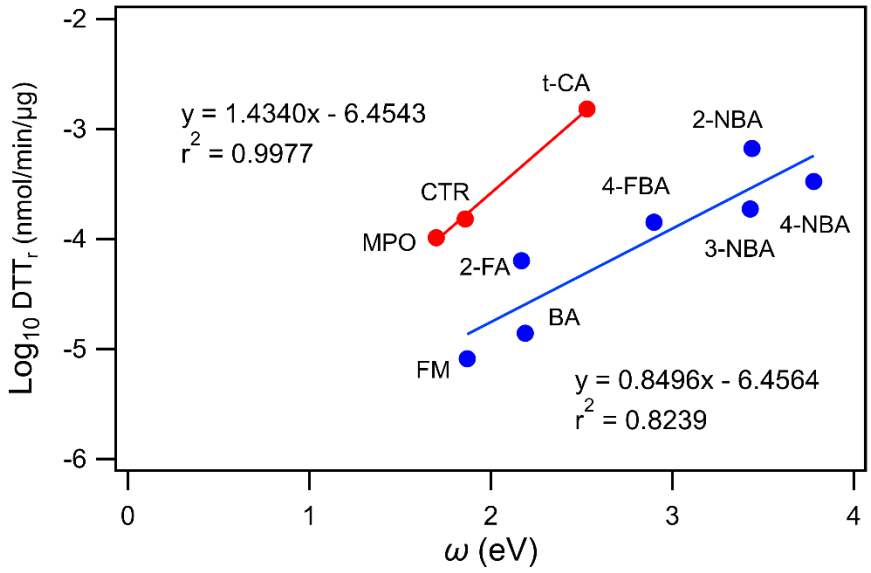

Figure S3.1. Comparison between the calculated electrophilicity index in gas phase and the measured Log_{10}(DTT activity) (nmol DTT consumed per reaction incubation minute per µg of sample). The r^2 values of simple (blue) and *α,β*-unsaturated (red) carbonyls are 0.8239 and 0.9977, respectively.

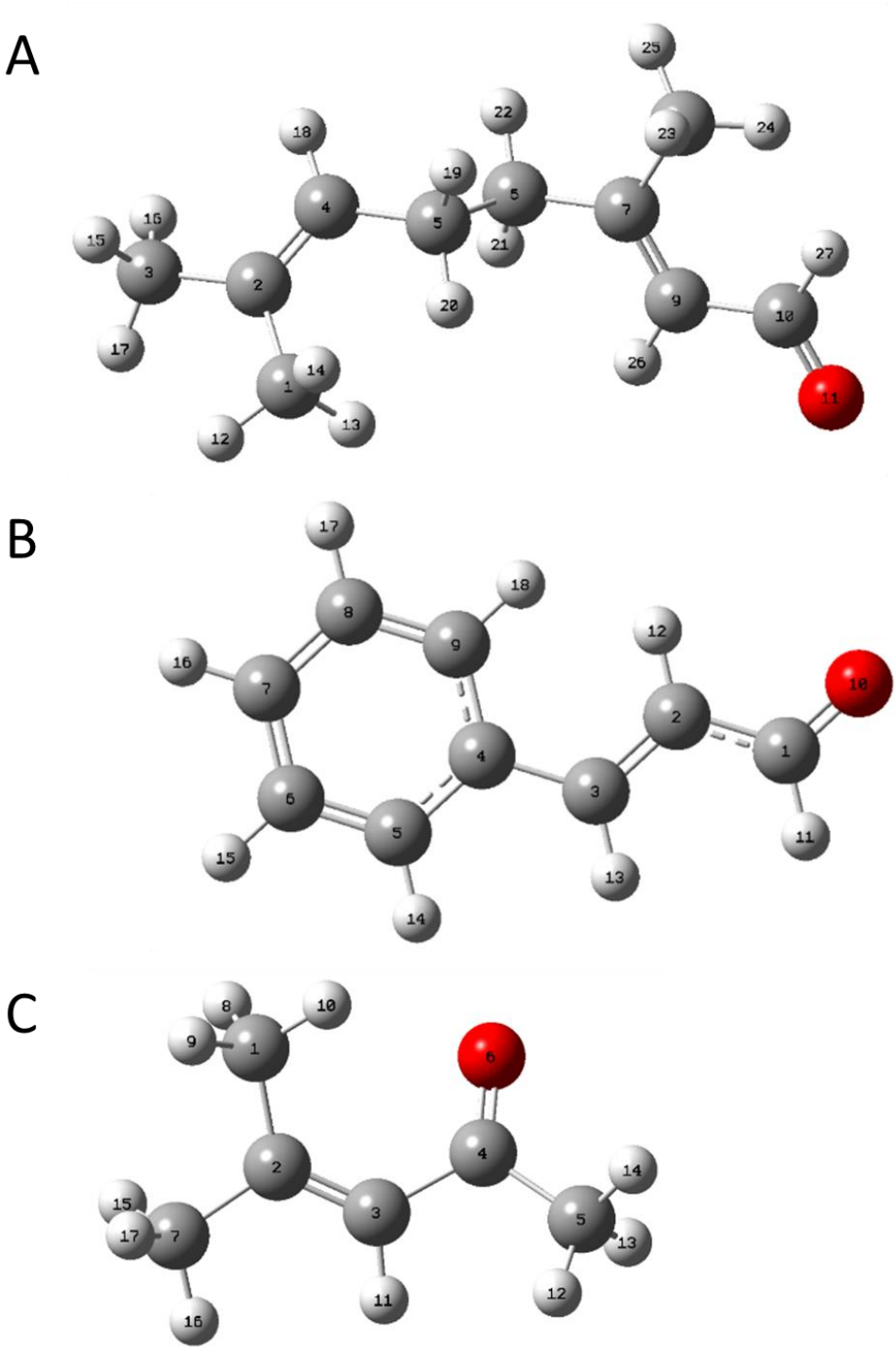

Figure S3.2. Molecular geometries showing atom labels for (A) citral, (B) *trans*-cinnamaldehyde and (C) mesityl oxide.

References

1. Pope, C.; Burnett, R.; Thun, M.; Calle, E.; Krewski, D.; Ito, K.; Thurston, G., Lung cancer, cardiopulmonary mortality, and long-term exposure to fine particulate air pollution. *JAMA* **2002,** *287* (9), 1132-1141.

2. Pope III, C. A.; Burnett, R. T.; Thurston, G. D.; Thun, M. J.; Calle, E. E.; Krewski, D.; Godleski, J. J., Cardiovascular mortality and long-term exposure to particulate air pollution: epidemiological evidence of general pathophysiological pathways of disease. *Circulation* **2004,** *109* (1), 71-77.

3. Nastos, P. T.; Paliatsos, A. G.; Anthracopoulos, M. B.; Roma, E. S.; Priftis, K. N., Outdoor particulate matter and childhood asthma admissions in Athens, Greece: a time-series study. *Environ. Health* **2010,** *9* (1), 45.

4. Schauer, J. J.; Kleeman, M. J.; Cass, G. R.; Simoneit, B. R., Measurement of emissions from air pollution sources. 4. C1− C27 organic compounds from cooking with seed oils. *Environ. Sci. Technol.* **2002,** *36* (4), 567-575.

5. Possanzini, M.; Di Palo, V.; Cecinato, A., Sources and photodecomposition of formaldehyde and acetaldehyde in Rome ambient air. *Atmos. Environ.* **2002,** *36* (19), 3195-3201.

6. Pang, X.; Lewis, A., Carbonyl compounds in gas and particle phases of mainstream cigarette smoke. *Sci. Total Environ.* **2011,** *409* (23), 5000-5009.

7. Ahmed, C. M. S.; Jiang, H.; Chen, J. Y.; Lin, Y.-H., Traffic-Related Particulate Matter and Cardiometabolic Syndrome: A Review. *Atmosphere* **2018,** *9* (9), 336.

8. Carter, W. P., A detailed mechanism for the gas-phase atmospheric reactions of organic compounds. *Atmos. Environ. Part A. General Topics* **1990,** *24* (3), 481-518.

9. Atkinson, R., Gas-phase tropospheric chemistry of volatile organic compounds .1. Alkanes and alkenes. *J. Phys. Chem. Ref. Data* **1997,** *26* (2), 215-290.

10. Kirkham, P. A.; Caramori, G.; Casolari, P.; Papi, A. A.; Edwards, M.; Shamji, B.; Triantaphyllopoulos, K.; Hussain, F.; Pinart, M.; Khan, Y., Oxidative stress–induced antibodies to carbonyl-modified protein correlate with severity of chronic obstructive pulmonary disease. *Am. J. Respir. Crit. Care Med.* **2011,** *184* (7), 796-802.

11. Kirkham, P. A.; Barnes, P. J., Oxidative stress in COPD. *Chest* **2013,** *144* (1), 266-273.

12. IARC *Chemical agents and related occupations*; International Agency for Research on Cancer: 2012.

13. Chan, K.; Poon, R.; O'Brien, P. J., Application of structure–activity relationships to investigate the molecular mechanisms of hepatocyte toxicity and electrophilic reactivity of α, β-unsaturated aldehydes. *J. Appl. Toxicol.* **2008,** *28* (8), 1027-1039.

14. Barrera, G.; Pizzimenti, S.; Daga, M.; Dianzani, C.; Arcaro, A.; Cetrangolo, G.; Giordano, G.; Cucci, M.; Graf, M.; Gentile, F., Lipid peroxidation-derived aldehydes, 4-hydroxynonenal and malondialdehyde in aging-related disorders. *Antioxidants* **2018,** *7* (8), 102.

15. Witz, G., Biological interactions of α, β-unsaturated aldehydes. *Free Radic. Biol. Med.* **1989,** *7* (3), 333-349.

16. Pearson, R. G., Hard and soft acids and bases. *J. Am. Chem. Soc.* **1963,** *85* (22), 3533-3539.

17. Parr, R.; Von Szentpaly, L.; Liu, S., Electrophilicity index. *J. Am. Chem. Soc.* **1999,** *121* (9), 1922-1924.

18. LoPachin, R.; Gavin, T., Molecular mechanisms of aldehyde toxicity: A chemical perspective. *Chem. Res. Toxicol.* **2014,** *27* (7), 1081-1091.

19. Pratihar, S., Electrophilicity and nucleophilicity of commonly used aldehydes. *Org. Biomol. Chem.* **2014,** *12* (30), 5781-5788.

20. Schultz, T. W.; Aptula, A. O., Kinetic-based reactivity for Michael acceptors: structural activity relationships and its relationship to excess acute fish toxicity. *Bull. Environ. Contam. Toxicol.* **2016,** *97* (6), 752-756.

21. Cho, A.; Sioutas, C.; Miguel, A.; Kumagai, Y.; Schmitz, D.; Singh, M.; Eiguren-Fernandez, A.; Froines, J., Redox activity of airborne particulate matter at different sites in the Los Angeles Basin. *Environ. Res.* **2005,** *99* (1), 40-47.

22. Verma, V.; Shafer, M. M.; Schauer, J. J.; Sioutas, C., Contribution of transition metals in the reactive oxygen species activity of PM emissions from retrofitted heavy-duty vehicles. *Atmos. Environ.* **2010,** *44* (39), 5165-5173.

23. Charrier, J. G.; Anastasio, C., On dithiothreitol (DTT) as a measure of oxidative potential for ambient particles: evidence for the importance of soluble transition metals. *Atmos. Chem. Phys.* **2012,** *12* (19), 9321-9333.

24. Verma, V.; Fang, T.; Guo, H.; King, L.; Bates, J. T.; Peltier, R. E.; Edgerton, E.; Russell, A. G.; Weber, R. J., Reactive oxygen species associated with water-soluble $PM_{2.5}$ in the southeastern United States: spatiotemporal trends and source apportionment. *Atmos. Chem. Phys.* **2014,** *14*, 12915-12930.

25. Fang, T.; Verma, V.; Bates, J.; Abrams, J.; Klein, M.; Strickland, M.; Sarnat, S.; Chang, H.; Mulholland, J.; Tolbert, P.; Russell, A.; Weber, R., Oxidative potential of ambient water-soluble $PM_{2.5}$ in the southeastern United States: contrasts in sources and health associations between ascorbic acid (AA) and dithiothreitol (DTT) assays. *Atmos. Chem. Phys.* **2016,** *16* (6), 3865-3879.

26. Verma, V.; Polidori, A.; Schauer, J. J.; Shafer, M. M.; Cassee, F. R.; Sioutas, C., Physicochemical and toxicological profiles of particulate matter in Los Angeles during the October 2007 southern California wildfires. *Environ. Sci. Technol.* **2009,** *43* (3), 954-960.

27. Kramer, A.; Rattanavaraha, W.; Zhang, Z.; Gold, A.; Surratt, J.; Lin, Y., Assessing the oxidative potential of isoprene-derived epoxides and secondary organic aerosol. *Atmos. Environ.* **2016,** *130*, 211-218.

28. Li, N.; Sioutas, C.; Cho, A.; Schmitz, D.; Misra, C.; Sempf, J.; Wang, M.; Oberley, T.; Froines, J.; Nel, A., Ultrafine particulate pollutants induce oxidative stress and mitochondrial damage. *Environ. Health Perspect.* **2003,** *111* (4), 455-460.

29. M. J. Frisch; G. W. Trucks; H. B. Schlegel; G. E. Scuseria; M. A. Robb; J. R. Cheeseman; G. Scalmani; V. Barone; G. A. Petersson; H. Nakatsuji; X. Li; M. Caricato; A. Marenich; J. Bloino; B. G. Janesko; R. Gomperts; B. Mennucci; H. P. Hratchian; J. V. Ortiz; A. F. Izmaylov; J. L. Sonnenberg; D. Williams-Young; F. Ding; F. Lipparini; F. Egidi; J. Goings; B. Peng; A. Petrone; T. Henderson; D. Ranasinghe; V. G. Zakrzewski; J. Gao; N. Rega; G. Zheng; W. Liang; M. Hada; M. Ehara; K. Toyota; R. Fukuda; J. Hasegawa; M. Ishida; T. Nakajima; Y. Honda; O. Kitao; H. Nakai; T. Vreven; K. Throssell; J. A. Montgomery; Jr., J. E. P.; F. Ogliaro; M. Bearpark; J. J. Heyd; E. Brothers; K. N. Kudin; V. N. Staroverov; T. Keith; R. Kobayashi; J. Normand; K. Raghavachari; A. Rendell; J. C. Burant; S. S. Iyengar; J. Tomasi; M. Cossi; J. M. Millam; M. Klene; C. Adamo; R. Cammi; J. W. Ochterski; R. L. Martin; K. Morokuma; O. Farkas; Foresman, J. B.; Fox, D. J., Gaussian 09, revision E.01. *Gaussian Inc. Wallingford CT* **2015**.

30. Becke, A. D., A new mixing of Hartree–Fock and local density-functional theories. *J. Chem. Phys.* **1993,** *98* (2), 1372-1377.

31. Becke, A. D., Density-functional thermochemistry. III. The role of exact exchange. *J. Chem. Phys.* **1993,** *98* (7), 5648-5652.

32. De Proft, F.; Martin, J. M.; Geerlings, P., Calculation of molecular electrostatic potentials and Fukui functions using density functional methods. *Chem. Phys. Lett.* **1996,** *256* (4-5), 400-408.

33. Hanwell, M. D.; Curtis, D. E.; Lonie, D. C.; Vandermeersch, T.; Zurek, E.; Hutchison, G. R., Avogadro: an advanced semantic chemical editor, visualization, and analysis platform. *J. Cheminformatics* **2012,** *4* (1), 17.

34. Koopmans, T., Über die Zuordnung von Wellenfunktionen und Eigenwerten zu den einzelnen Elektronen eines Atoms. *Physica* **1934,** *1* (1-6), 104-113.

35. Almbladh, C. O.; von Barth, U., Exact results for the charge and spin densities, exchange-correlation potentials, and density-functional eigenvalues. *Phys. Rev. B* **1985,** *31* (6), 3231-3244.

36. Zhan, C.-G.; Nichols, J. A.; Dixon, D. A., Ionization potential, electron affinity, electronegativity, hardness, and electron excitation energy: Molecular properties from density functional theory orbital energies. *J. Phys. Chem. A* **2003,** *107* (20), 4184-4195.

37. Pearson, R. G., Chemical hardness and density functional theory. *J. Chem. Sci.* **2005,** *117* (5), 369-377.

38. Namazian, M.; Coote, M., Accurate calculation of absolute one-electron redox potentials of some para-quinone derivatives in acetonitrile. *J. Phys. Chem. A* **2007,** *111* (30), 7227-7232.

39. Surratt, J. D.; Chan, A. W.; Eddingsaas, N. C.; Chan, M.; Loza, C. L.; Kwan, A. J.; Hersey, S. P.; Flagan, R. C.; Wennberg, P. O.; Seinfeld, J. H., Reactive intermediates revealed in secondary organic aerosol formation from isoprene. *Proc. Natl. Acad. Sci. U.S.A.* **2010,** *107* (15), 6640-6645.

40. Morell, C.; Grand, A.; Toro-Labbe, A., New dual descriptor for chemical reactivity. *J. Phys. Chem. A* **2005,** *109* (1), 205-212.

41. Parr, R. G.; Donnelly, R. A.; Levy, M.; Palke, W. E., Electronegativity: the density functional viewpoint. *J. Chem. Phys.* **1978,** *68* (8), 3801-3807.

42. Parr, R. G.; Pearson, R. G., Absolute hardness: companion parameter to absolute electronegativity. *J. Am. Chem. Soc.* **1983,** *105* (26), 7512-7516.

43. Foresman, J. B.; Frisch, Æ., *Exploring chemistry with electronic structure methods: a guide to using Gaussian*. 2nd ed.; Gaussian, Inc.: Wallingford, CT: 1996.

44. Jiang, H.; Jang, M.; Yu, Z., Dithiothreitol activity by particulate oxidizers of SOA produced from photooxidation of hydrocarbons under varied NO_x levels. *Atmos. Chem. Phys.* **2017,** *17* (16), 9965-9977.

45. Whitesides, G. M.; Lilburn, J. E.; Szajewski, R. P., Rates of thiol-disulfide interchange reactions between mono- and dithiols and Ellman's reagent. *J. Org. Chem.* **1977,** *42* (2), 332-338.

46. Fang, T.; Verma, V.; Guo, H.; King, L. E.; Edgerton, E. S.; Weber, R. J., A semi-automated system for quantifying the oxidative potential of ambient particles in aqueous extracts using the dithiothreitol (DTT) assay: results from the Southeastern Center for Air Pollution and Epidemiology (SCAPE). *Atmos. Meas. Tech.* **2015,** *8* (1), 471-482.

47. Cheung, K. L.; Polidori, A.; Ntziachristos, L.; Tzamkiozis, T.; Samaras, Z.; Cassee, F. R.; Gerlofs, M.; Sioutas, C., Chemical characteristics and oxidative potential of particulate matter emissions from gasoline, diesel, and biodiesel cars. *Environ. Sci. Technol.* **2009,** *43* (16), 6334-6340.

48. McWhinney, R. D.; Zhou, S.; Abbatt, J. P. D., Naphthalene SOA: redox activity and naphthoquinone gas–particle partitioning. *Atmos. Chem. Phys.* **2013,** *13* (19), 9731-9744.

49. Tuet, W. Y.; Chen, Y.; Xu, L.; Fok, S.; Gao, D.; Weber, R. J.; Ng, N. L., Chemical oxidative potential of secondary organic aerosol (SOA) generated from the photooxidation of biogenic and anthropogenic volatile organic compounds. *Atmos. Chem. Phys.* **2017,** *17* (2), 839-853.

50. Jiang, H.; Jang, M.; Sabo-Attwood, T.; Robinson, S. E., Oxidative potential of secondary organic aerosols produced from photooxidation of different hydrocarbons using outdoor chamber under ambient sunlight. *Atmos. Environ.* **2016,** *131*, 382-389.

51. Duan, H.; Liu, X.; Yan, M.; Wu, Y.; Liu, Z., Characteristics of carbonyls and volatile organic compounds (VOCs) in residences in Beijing, China. *Front. Environ. Sci. Eng.* **2016,** *10* (1), 73-84.

52. Shen, H.; Chen, Z.; Li, H.; Qian, X.; Qin, X.; Shi, W., Gas-Particle Partitioning of Carbonyl Compounds in the Ambient Atmosphere. *Environ. Sci. Technol.* **2018,** *52* (19), 10997-11006.

53. Verma, V.; Fang, T.; Xu, L.; Peltier, R. E.; Russell, A. G.; Ng, N. L.; Weber, R. J., Organic aerosols associated with the generation of reactive oxygen species (ROS) by water-soluble PM2.5. *Environ. Sci. Technol.* **2015,** *49* (7), 4646-4656.

54. Jiang, H.; Jang, M., Dynamic oxidative potential of atmospheric organic aerosol under ambient sunlight. *Environ. Sci. Technol.* **2018,** *52* (13), 7496-7504.

55. Jang, M.; Kamens, R. M., Characterization of secondary aerosol from the photooxidation of toluene in the presence of NO_x and 1-propene. *Environ. Sci. Technol.* **2001,** *35* (18), 3626-3639.

56. Forstner, H. J. L.; Flagan, R. C.; Seinfeld, J. H., Secondary organic aerosol from the photooxidation of aromatic hydrocarbons: Molecular composition. *Environ. Sci. Technol.* **1997,** *31* (5), 1345-1358.

57. Roy, R. K., On the reliability of global and local electrophilicity descriptors. *J. Phys. Chem. A* **2004,** *108* (22), 4934-4939.

58. Roy, R. K.; Usha, V.; Paulovič, J.; Hirao, K., Are the local electrophilicity descriptors reliable indicators of global electrophilicity trends? *J. Phys. Chem. A* **2005,** *109* (20), 4601-4606.

59. Chattaraj, P. K.; Maiti, B.; Sarkar, U., Philicity: A unified treatment of chemical reactivity and selectivity. *J. Phys. Chem. A* **2003,** *107* (25), 4973-4975.

60. Marteau, C.; Ruyffelaere, F.; Aubry, J.-M.; Penverne, C.; Favier, D.; Nardello-Rataj, V., Oxidative degradation of fragrant aldehydes. Autoxidation by molecular oxygen. *Tetrahedron* **2013,** *69* (10), 2268-2275.

61. Grek, C. L.; Zhang, J.; Manevich, Y.; Townsend, D. M.; Tew, K. D., Causes and consequences of cysteine S-glutathionylation. *J. Bio. Chem.* **2013,** *288* (37), 26497-26504.

62. Roberts, J. D.; Caserio, M. C., *Basic principles of organic chemistry*. WA Benjamin, Inc.: 1977; Vol. Ch 15&16.

63. Loudon, M.; Parise, J., *Organic Chemistry*. 6th ed.; Roberts and Company Publishers: 2009; Vol. Chapter 19.

64. Ryabova, R. S.; Voloshenko, G. I.; Maiorov, V. D.; Osipova, G. F., Equilibrium composition of formaldehyde oligomers in aqueous solutions from IR data. *Russ. J. Appl. Chem.* **2002,** *75* (1), 22-24.

65. Lebrun, N.; Dhamelincourt, P.; Focsa, C.; Chazallon, B.; Destombes, J. L.; Prevost, D., Raman analysis of formaldehyde aqueous solutions as a function of concentration. *J. Raman Spectrosc.* **2003,** *34* (6), 459-464.

66. Utterback, D. F.; Millington, D. S.; Gold, A., Characterization and determination of formaldehyde oligomers by capillary column gas chromatography. *Anal. Chem.* **1984,** *56* (3), 470-473.

67. Sánchez-Márquez, J.; Zorrilla, D.; Sánchez-Coronilla, A.; Desireé, M.; Navas, J.; Fernández-Lorenzo, C.; Alcántara, R.; Martín-Calleja, J., Introducing "UCA-FUKUI" software: reactivity-index calculations. *J. Mol. Model.* **2014,** *20* (11), 2492.

68. Huyen, N. T. T.; Eiamphungporn, W.; Mäder, U.; Liebeke, M.; Lalk, M.; Hecker, M.; Helmann, J. D.; Antelmann, H., Genome-wide responses to carbonyl electrophiles in Bacillus subtilis: control of the thiol-dependent formaldehyde dehydrogenase AdhA and cysteine proteinase YraA by the MerR-family regulator YraB (AdhR). *Mol. Microbiol.* **2009,** *71* (4), 876-894.

69. Schwöbel, J. A. H.; Wondrousch, D.; Koleva, Y. K.; Madden, J. C.; Cronin, M. T. D.; Schüürmann, G., Prediction of Michael-type acceptor reactivity toward glutathione. *Chem. Res. Toxicol.* **2010,** *23* (10), 1576-1585.

70. Wondrousch, D.; Böhme, A.; Thaens, D.; Ost, N.; Schüürmann, G., Local electrophilicity predicts the toxicity-relevant reactivity of Michael acceptors. *J. Phys. Chem. Lett.* **2010,** *1* (10), 1605-1610.

Chapter IV. Electrophilicity and Thiol Reactivity of Reactive Carbonyl Species in E-cigarette Vaping Emissions

4.1 Introduction

E-cigarettes are new and emerging tobacco products that use heat-not burn electronic devices to deliver aerosolized e-liquids containing nicotine, base solvents (e.g., propylene glycol (PG) and vegetable glycerin (VG), flavor chemicals and/or other ingredients into the users via inhalation. E-cigarettes have been used by many smokers to help with smoking cessation,[1] but the use of e-cigarettes among non-smoking teenagers and young adults are prevalent in the United States.[2] One factor that contributes to the widespread popularity of e-cigarettes among nonsmoking teenagers and adults alike is the use of flavored e-liquids, which come in a variety of flavors, including fruit, menthol, mint, and tobacco.[3, 4] While e-cigarette vaping is frequently marketed as a safer alternative to conventional tobacco products, the vaping-associated health outcomes have not been fully investigated. Recent studies have reported an association between e-cigarette vaping and illnesses such as lung injury[5] and oral health problems,[6] highlighting that vaping is not without harm.

Flavor chemicals used in e-liquids not only are appealing to users, but they may contribute to adverse health effects associated with e-cigarette vaping. For instance, cinnamaldehyde is a widely used food flavoring chemical which is regarded as safe for ingestion. However, cinnamaldehyde found in e-liquids and in vaped aerosols has been found to cause cytotoxicity,[7] to suppress immune functions of respiratory tract cells,[8] and to disrupt mitochondrial function of human bronchial epithelial cells.[9] In addition, many

studies have demonstrated that thermal decomposition of e-liquid diluents (e.g., PG and VG) and flavor chemicals can release reactive carbonyl species, such as formaldehyde, acetaldehyde, acrolein, and propionaldehyde.[10-13] Among commonly reported carbonyls in vaping emissions, formaldehyde is a known human carcinogen, which can cause a wide range of health implications such as irritations and pharyngeal cancer through inhalation exposure.[14]

Carbonyls are reactive electrophiles that can form adducts with biological nucleophiles such as glutathione (GSH),[15] protein residues,[16, 17] and DNA.[18, 19] For example, as an α,β-unsaturated carbonyl, acrolein can covalently modify proteins by forming adducts with the cysteine residue via Michael addition and Schiff base formation, as well as other nucleophilic side chains (e.g., the histidine and lysine residues) and free amino terminus of proteins.[20] Reactions of carbonyls toward cellular nucleophiles can result in a wide range of adverse health effects, including oxidative DNA breakage,[21] formation of protein adducts,[22] decrease or loss of protein functions,[23] and eventually pathogenesis. Exposure to exogenous carbonyls from cigarette smoke has been linked to DNA adduct formation and carcinogenesis.[24] Wang et al. detected an elevated level of formaldehyde-DNA adduct (N6-hydroxymethyldeoxyadenosine) in human leukocytes of smokers compared to nonsmokers, indicating that formaldehyde is a contributing factor of smoking-induced cancer.[25]

To assess reactivity and toxicity of various carbonyls associated with e-cigarette vaping, computational chemistry methods such as density functional theory and condensed Fukui functions have been used to study the global electrophilicity[26] and chemical

reactivity at specific sites within a molecule.[27, 28] Wondrousch et al. employed global electrophilicity index (ω) and local site-specific parameters (energy-weighted local electrophilicity (ω^E) and local charge-limited local electrophilicity (ω^q)) to predict reaction rates of 31 *α,β*-unsaturated carbonyls toward GSH.[29] Global and local electrophilicity parameters correlated well with experimental values with r^2 values around 0.88 and 0.89 respectively, which demonstrate the applicability of computational approaches to predict chemical reactivity.[29] Schwöbel et al. developed a model that uses local charge-limited electrophilicity index (ω^q)[29] at the *β*-carbon of Michael-type acceptors to predict the kinetic rate constants of 66 compounds (including aldehydes and ketones) toward GSH (k_{GSH}); predicted k_{GSH} values correlated well with experimental rate constants with r^2 of 0.91.[30] We have previously reported the global electrophilicity parameters for selected atmospheric carbonyls and compared the calculated reactivity descriptors with experimental consumption rates of dithiothreitol (k_{DTT}),[28] a commonly used assay to estimate the oxidative potential of atmospheric aerosols.[31] The results also indicated a strong correlation between the DTT consumption rates and the global electrophilicity descriptors (r^2= 0.84 and 0.99 for simple and *α,β*-unsaturated carbonyls, respectively).[28]

Given the potential for adverse health outcomes, many studies have been conducted to determine the effect of flavor chemicals on the production of small carbonyls through thermal degradation of e-liquid constituents.[11, 12, 32] Khlystov and Samburova compared aldehydes in vaping emissions of unflavored and flavored e-liquids, and reported that flavored e-liquids dominated the production of aldehydes (e.g., formaldehyde, acetaldehyde, acrolein, glyoxal, benzaldehyde, propionaldehyde, and m-tolualdehyde).[11]

Gillman et al. found that the emission of acetaldehyde increased 150-200% in flavored e-liquids compared to unflavored e-liquid during vaping.[12] However, the formation of carbonyls that are not typically monitored via other reaction routes, such as direct oxidation of alcohol-containing flavor compounds, has received less attention.

In this study, we characterized the reactive carbonyl species in vaping emissions, including thermal decomposition and direct oxidation products resulting from base solvents (PG and VG) and four alcohol-containing flavor chemicals (*trans*-2-hexenol, benzyl alcohol, l-(-)-menthol and linalool), using O-(2,3,4,5,6-pentafluorobenzyl)hydroxylamine derivatization coupled to solid-phase microextraction. The total carbonyl production was quantified using UV-Vis measurements of reaction products between carbonyls and 2,4-dinitrophenylhydrazine. The adduct formation between carbonyls in vaping emissions and GSH was identified using LC/ESI-QTOFMS. The global and local electrophilicity indices of target carbonyl compounds were calculated using computational chemistry methods to predict their chemical reactivity and potential toxicity.

4.2 Materials and Methods

4.2.1 Chemicals

Four alcohol-containing flavor chemicals selected and purchased for this study are: *trans*-2-hexenol (97%, Alfa Aesar), benzyl alcohol (Fisher Science Education), l-(-)-menthone (99.5%, Acros Organics), and linalool (>96%, TCI). PG (>99%, TCI) and VG (99.9%, Fisher Chemical) were used as the diluents for e-liquids. O-(2,3,4,5,6-

pentafluorobenzyl)hydroxylamine hydrochloride (PFBHA, Sigma-Aldrich), 2,4-dinitrophenylhydrazine (2,4-DNPH, 97%, Sigma-Aldrich), formaldehyde-DNPH (1000 μg/mL in acetonitrile, AccuStandard), HPLC grade acetonitrile (≥99.9%, Fisher Chemical), potassium hydroxide (KOH, Fisher Science Education), and 6N hydrochloric acid (HCl, Fisher Chemical) were purchased for identification and quantification of carbonyls in unvaped e-liquids and vaping emissions. In addition, L-glutathione (GSH, 97%, Alfa Aesar) and 5,5-dithio-bis-(2-nitrobenzoic acid) (DTNB, 99.2%, Chem-Impex Int'l Inc.) were purchased to analyze the formation of potential adducts between GSH and carbonyls in vaping emissions.

Most e-liquids contain flavor chemicals, and alcohol-containing chemicals is a class of compounds that occur frequently in e-liquids.[33-35] Omaiye et al. reported occurrence of menthol in 50% of 227 e-cigarette refill fluid samples, and addressed that linalool and benzyl alcohol ranked 4th and 11th as frequently occurred flavored chemicals in sampled refill fluids.[33] In addition, 2-hexenol has also been identified as an alcohol flavor chemical used in e-liquids.[35] The smell and taste of flavor chemicals are an important factor for why use of e-cigarettes is prevalent among teenagers and young adults. Menthol is known to attribute to a minty aroma,[36] while benzyl alcohol has a sweet or almond fruity taste,[34] linalool gives a sweet floral-woody with slight citrus flavor,[34] and 2-hexenol has an apple or fruity flavor.[37]

4.2.2 E-cigarette device, cartridges, and e-liquid preparation

A Vapros Spinner II (124.5 mm × 16.5 mm) vape pen was used for vaping experiments in this study. The pen consists of 1600 mAh battery capacity, a charging

voltage of 4.2V/420 mAh, and a variable voltage dial (3.3V-4.8V). The vape pen was operated at 3.8V for all vaping experiments. The cartridges (CCell TH2 510 thread) with a volume of 0.5 mL and resistance of 2.1 ohm were used. The average coil temperature was 125 °C (ranged 101 – 160 °C during vaping) as measured by a K-type thermocouple thermometer.

The e-liquid formulations were prepared by mixing PG-VG diluents and the flavor chemicals in-house. First, the diluent for the e-liquid samples was made of PG (70%) and VG (30%) in volume. Then, each flavored e-liquid consisted of 90% volume of PG-VG mixture and 10% volume of the alcohol-containing flavor compound. The unflavored e-liquid samples consisted of only the 70%PG-30%VG mixture.

4.2.3 Identification of carbonyls emitted from vaping

One objective of this study was to identify carbonyls in vaping emissions produced from thermal degradation and direct oxidation of alcohol-containing flavor chemicals during vaping. To collect the vaping emissions, the Vapros Spinner II pen was attached to a cold trap apparatus positioned inside a box filled with dry ice. The output of the cold trap was connected to a pump (Gast Manufacturing Inc.). A critical orifice was used to control the flow at around 0.46 liter per minute (LPM). Before the actual collection of vaping emissions, the e-cigarette pen was preconditioned with at least 25 puffs to avoid artifacts from dry puffs. Then, 100 puffs of vaping emissions were collected at 4 sec puff with 25 sec inter-puff rest using a programmable timer switch (Nearpow, model T319). This vaping topography is within the recommend range by Farsalinos et al.[38] For every 25 puffs, the vape pen was rested for 5 min.

Subsequently, a 1.5 mL of 1 mM PFBHA solution (dissolved in MiliQ water) was added to the cold trap sample. The sample was stored at room temperature for 24 hours to allow PFBHA to react with carbonyl compounds in the vaping emission samples. PFBHA can react with carbonyl compounds to form oxime derivatives, which can be analyzed using GC/MS methods. After 24 hours, a solid-phase microextration (SPME) fiber (65 μm PDMS/DVB fused silica, Supelco) was used to extract out the PFBHA-carbonyl oxime products from the sample solution. The fiber was submerged into the sample for 60 minutes, then used for GC/EI-MS analysis immediately.

The collected samples on SPME fibers were analyzed using a GC/EI-MS system (Agilent 6890N GC and 5975C MSD). The SPME fibers were manually injected into the GC inlet in splitless mode and desorbed for at least 2 min at 250 ^{o}C. Analytes desorbed from the SPME fibers were separated by an Agilent Technologies DB-5MS column (30 m × 0.25 mm i.d., 0.25 μm film). The flow rate of the carrier gas (i.e., helium) was 1 mL/min. The GC temperature gradient was initial temperature at 60 ^{o}C held for 4 min, temperature increased to 90 ^{o}C at 15 ^{o}C min^{-1} and held for 4 min, and temperature increased to 250 ^{o}C at 10 ^{o}C min^{-1} and held for 5 min. The total run time was 31 min. Data acquisition was performed in full-scan mode with *m/z* 30-500.

4.2.4 Quantification of carbonyls in vaping emissions and unvaped e-liquids

The 2,4-DNPH method used to compare the amount of carbonyls in vaping emissions and in unvaped e-liquids was modified from those published by Jiang et al.[39] The cold trap samples of vaping emissions (100 puffs total) were collected in the same manner as described in the Section 4.2.3. Then, 1.5 mL of 9.7 nM 2,4-DNPH solution was

added to react with the carbonyls in each emission sample for 90 min at 50 ^{o}C. Then, 5 μL of the sample was added to 200 μL of 5.6×10^{-1} nM KOH solution. The sample absorbance was measured at 300 nm to 700 nm using a UV-Vis spectrophotometer (Beckman DU-640). The intensity of the absorbance is proportional to the concentration of carbonyls based on the Beer-Lambert law.

4.2.5 Carbonyl-GSH adduct formation

Carbonyl compounds are reactive compounds that can form adducts with nucleophiles such as GSH. First, one sample of vaping emissions (100 puffs at 4 sec puff with 25 sec inter-puff rest) of each e-liquid was collected and 0.5 mL acetonitrile was added. Then, 20 μL of each vaping sample was added to a GSH reaction mixture which contained 100 μL acetonitrile, $1.39\text{x}10^{-3}$ M of GSH (in acetonitrile). The reaction mixture was incubated at 37 ^{o}C for 120 min, then 10 uL of $8.40\text{x}10^{-3}$ M of DTNB (in acetonitrile) was added to titrate the remaining GSH. The total reaction mixture volume was 135 μL. A GSH control sample was prepared with 120 μL acetonitrile, 5 μL GSH solution, and 10 μL DTNB solution. All samples were stored in a -20 ^{o}C freezer before liquid chromatography/quadrupole time-of-flight mass spectrometry (LC/Q-TOFMS) analysis.

The instrument used to analyze the carbonyl-GSH samples was an Agilent Technologies 6545 LC/Q-TOFMS system equipped with an electrospray ion source (ESI). The sample mixtures were separated by a Poroshell 120 EC-C18 column (3×100 mm, 2.7 μm). The mobile phase A was 0.1% formic acid in water, and mobile phase B was 0.1% formic acid in acetonitrile. The mobile phase gradient was 0% B-100% B from 2 min to 18 min. The column was washed with 100% B, and equilibrated with 100% A before running

the next gradient. The sample injection volume was 30 µL, and the instrument was operated in the negative ion mode.

4.2.6 Global electrophilicity and local site reactivity calculations

Global electrophilicity index (ω) introduced by Parr et al. in 1999 is a reactivity parameter that describes the stabilization energy of atoms or molecules when they accept additional electronic charge from the environment.[26] In this study, Gaussian 16W was used to optimize geometries and compute ω of target simple carbonyls (formaldehyde, acetaldehyde, benzaldehyde and l-menthone), and *α,β*-unsaturated carbonyls (*trans*-2-hexenal and linalool-8-aldehyde). Density functional theory was applied to optimize geometry at B3LYP/6-311+G(d,p) level of theory, and the conductor-like polarizable continuum model (CPCM) was implemented to include water as a solvent. The optimized geometries are shown in Figure S4.1. Afterwards, the highest occupied molecular orbital (HOMO) and lowest unoccupied molecular orbital (LUMO) energy values were obtained from the output file were used to calculate global electrophilicity descriptors such as chemical potential (µ), chemical hardness (η), and global electrophilicity index (ω) as shown in the following equations.[26, 40]

$$\mu = -\frac{I + A}{2} \approx \frac{E_{HOMO} + E_{LUMO}}{2} \quad (4.1)$$

$$\eta = \frac{I - A}{2} \approx E_{LUMO} - E_{HOMO} \quad (4.2)$$

$$\omega = \frac{\mu^2}{2\eta} \quad (4.3)$$

In addition to global electrophilicity calculations, the condensed Fukui functions which represent local reactivity at specific sites within a molecule were also calculated.[41]

First, Gaussian 16W was used to optimize geometries at B3LYP/6-311+G(d,p) level of theory in water using the CPCM solvation model. Then, the natural population analysis (NPA) in charges 0, -1 & +1 were calculated in Gaussian 16W. Afterwards, the output values (Figure S4.2) were uploaded into UCA-FUKUI 1.0 software (https://uca-fukui.software.informer.com/1.0/) to calculate the condensed Fukui functions (f_k^0, f_k^-, f_k^+, and dual-descriptor) using finite difference method.[41] The following equations show the condensed Fukui functions for the *k*th atom in the molecule.

$$f_k^- = q_k(N_0) - q_k(N_0 - 1), \text{ for electrophilic attack} \quad (4.4)$$

$$f_k^+ = q_k(N_0 + 1) - q_k(N_0), \text{ for nucleophilic attack} \quad (4.5)$$

$$f_k^0 = \frac{1}{2}(f_k^+ + f_k^-), \text{ for neutral (or radical) attack} \quad (4.6)$$

$$\text{Dual-descriptor} = f_k^+ + f_k^- \quad (4.7)$$

In the above equations, $q_k(N_0 - 1)$, $q_k(N_0 + 1)$, and $q_k(N_0)$ represent the number of electrons associated with the *k*th atom in the molecule, where the total number of the electrons in the molecule is N_0-1, N_0+1 and N_0.[41] The dual-descriptor is the sum of $f_k^+ + f_k^-$, and it is either > 0 or < 0.[41-43] If the dual-descriptor is > 0, it indicates that the reaction site favors for a nucleophilic attack, and if the dual-descriptor is < 0, an electrophilic attack may be favored.[41]

4.3 Results and Discussions

4.3.1 Identification of carbonyls in vaping emissions

Carbonyl compounds emitted from vaping of e-liquids were identified by reacting the vaping emission samples with PFBHA and followed by GC/EI-MS analysis. Figure 4.1

shows the extracted ion chromatograms (EICs) of *m/z* 181 for vaping emission samples of PG-VG and flavored e-liquids (i.e., *trans*-2-hexenol, benzyl alcohol, l-(-)-menthol, and linalool). Through NIST mass spectral library search, several carbonyl-PFBHA oxime derivatives were identified. The identified carbonyls shown in Figure 4.1A (vaping emissions of PG-VG e-liquid mixture) are formaldehyde (peaks 1 and 2), acetaldehyde (peaks 3 and 4), acetone (peak 5), propionaldehyde (peak 6), methyl glyoxal (peaks 7, 10 and 11), and glyoxal (peaks 8 and 9).

When comparing with PG-VG sample EICs, the flavored e-liquid vaping emissions samples also show peaks for carbonyls such as formaldehyde, methyl glyoxal, and glyoxal (Figure 4.1B-E). In contrast, the flavored e-liquid samples show unique EIC peaks that are not detected in the PG-VG sample. For example, t*rans*-2-hexenol sample (Figure 4.1B) shows oxime derivative peaks for n-butanal (peaks 1 and 2) and *trans*-2-hexenal (peak 3); these are not present in the PG-VG sample. In addition, *trans*-2-hexenal oximes are also detected in l-(-)-menthol sample (peak 1 in Figure 4. 1D) and in linalool sample (peak in in Figure 4.1E). On the other hand, benzaldehyde oxime derivatives (peaks 1 and 2) are detected in the benzyl alcohol sample (Figure 4.1C). In Figure 4.1D, peak 2 indicates l-menthone oxime derivative which was identified with EIC of *m/z* 349. But a proposed thermal oxidation product of linalool, linalool-8-aldehyde, was not detected.

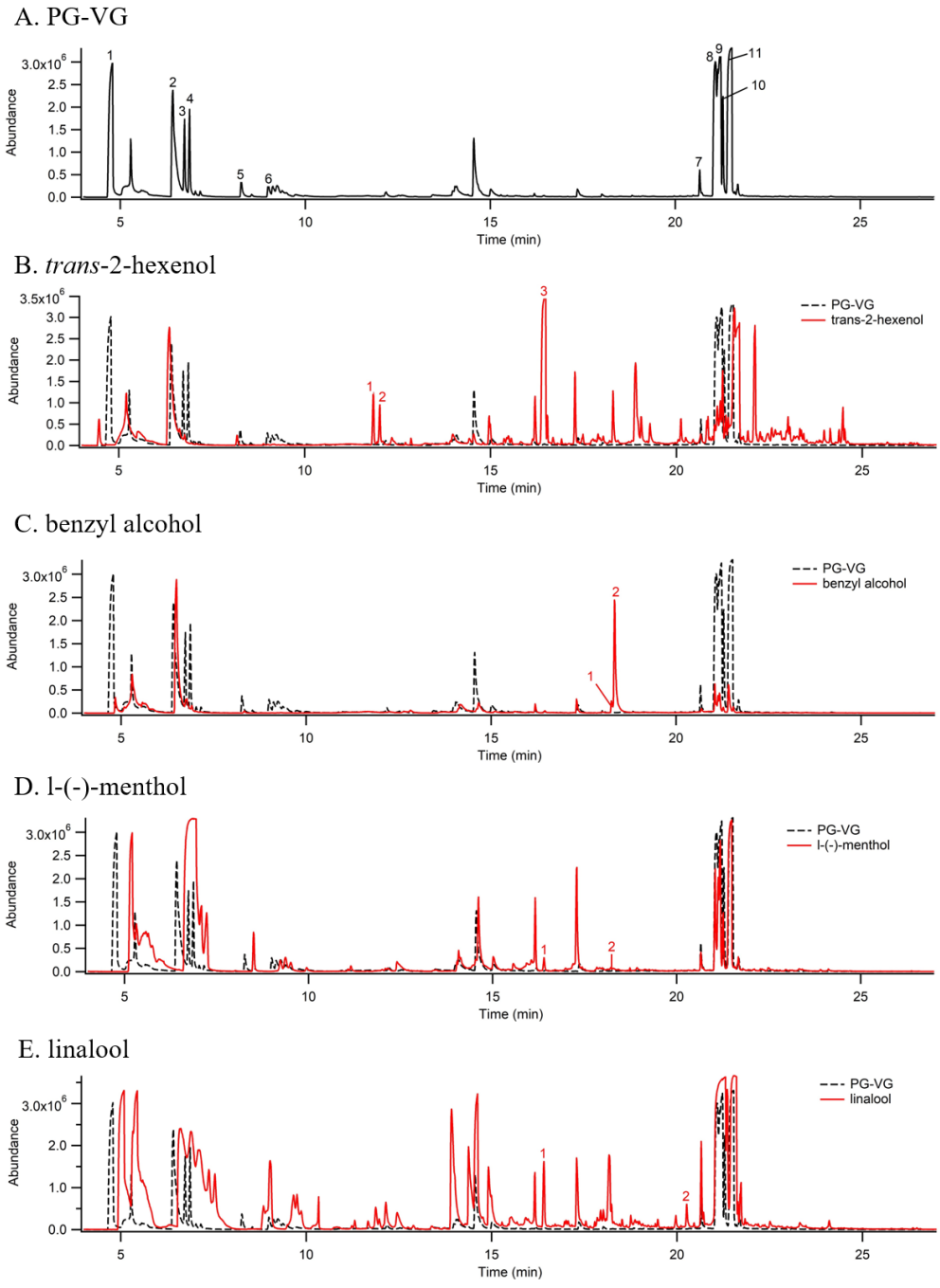

Figure 4.1. The extracted ion chromatograms of *m/z* 181 for oxime derivatives of carbonyls reacted with PFBHA. Samples analyzed are vaping emission from unflavored and flavored e-liquids. Unflavored e-liquid contained (A) only PG-VG, and (B-E) flavored e-liquids contained 90%/10% (v/v) of PG-VG and the alcohol-containing flavor chemical: (B) 2-hexenol, (C) benzyl alcohol, (D) l-(-)-menthol, and (E) linalool.

To compare total carbonyl-PFBHA derivative products in vaping emission samples, the total peak areas of EICs of m/z 181 were quantified as shown in Table S4.1. The EICs were integrated using these integration parameters: initial peak width = 0.120 and initial threshold = 17.0. The order of highest to lowest peak areas is linalool (4.66×10^9) > l-(-)-menthol (2.14×10^9) > *trans*-2-hexneol (1.98×10^9) > PG-VG (1.43×10^9) and benzyl alcohol (5.23×10^8).

Many studies have reported production of carbonyl compounds such as formaldehyde, acetaldehyde, acrolein, and propionaldehyde from thermal decomposition of e-liquid diluents such as PG and VG during vaping.[10, 44, 45] Our results in Figure 4.1 also shows that vaping PG and VG contributed to formation of multiple carbonyls such as formaldehyde, acetaldehyde, acetone, propionaldehyde, methyl glyoxal, and glyoxal. In contrast, the flavor chemicals in e-liquids yielded different carbonyls (e.g., *trans*-2-hexenal, n-butanal, and benzaldehyde) that are not present in the PG-VG vaping emissions. Adnan et al. has proposed that benzyl alcohol can oxidize to form benzaldehyde.[46] As *trans*-2-hexenol is a primary alcohol, it can be oxidized to produce aldehydes such as *trans*-2-hexenal.

4.3.2 Carbonyl-GSH adduct detection

Carbonyls are electrophiles that can form adducts with thiol-containing compounds via 1,2-carbonyl addition (Schiff base formation) or 1,4-conjugated addition (or Michael-addition).[28] A target search for potential formation of adducts between carbonyls (*trans*-2-hexenal and benzaldehyde) and GSH was conducted as shown in Figure 4.2. *Trans*-2-hexenal is an *α,β*-unsaturated carbonyl, which can form adducts with GSH via both 1,2-

carbonyl and 1,4-conjugated additions. In contrast, benzaldehyde classified as a simple carbonyl in this study can only undergo 1,2-addition to form adducts with GSH. The exact mass of deprotonated analytes (represented as $[M-H]^-$) was used to plot EIC and locate the retention times of target carbonyl-GSH adducts, with EIC *m/z* 404.14969 for the *trans*-2-hexenal-GSH adduct (~1.7 min) and the *m/z* 412.11839 for benzaldehyde-GSH (~10.3 min). The counts of *trans*-2-hexenal- and benzaldehyde-GSH adducts is expected to be correlated with both the abundance of carbonyls in vaping emission, the reactivity of the carbonyls toward GSH, and the stability of carbonyl-GSH adduct. For example, benzaldehyde form kinetic adducts with GSH via 1,2-carbonyl addition, but this reaction pathway maybe reversible.[47] In contrast, the *trans*-2-hexenal-GSH adducts formed via 1,4-conjugate addition are thermodynamic products which are more stable than kinetic products.[48]

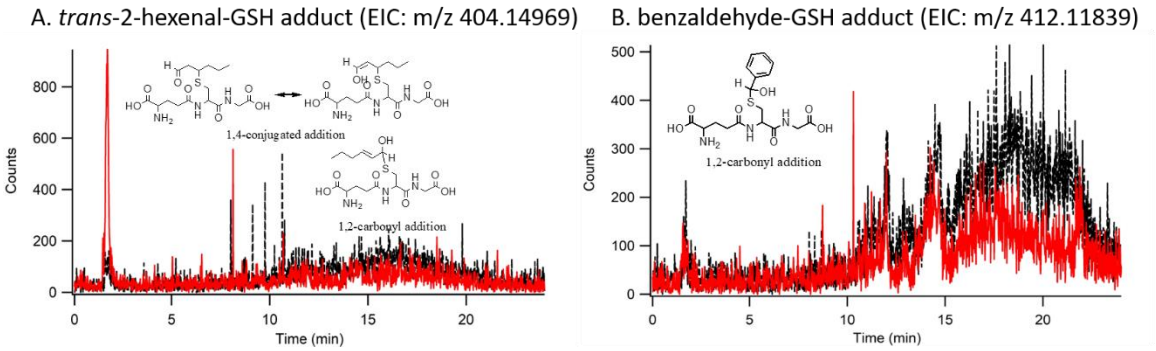

Figure 4.2. LC/Q-TOFMS data showing adduct formations between GSH (A) *trans*-2-hexenal and (B) benzaldehyde. The GSH blank sample is represented by the black color, and flavored samples are represented by the red color.

4.3.3 Quantification of carbonyls in vaping emissions and unvaped e-liquids

2,4-DNPH was used to estimate concentrations of carbonyls in vaping emissions and unvaped e-liquids. Carbonyls reacted with 2,4-DNPH form hydrazone derivatives, which absorbance can be measured to determine the concentration of carbonyls in a sample. Figure S4.1 shows the absorbance of vaping emission samples and 2,4-DNPH measured from 300 nm to 700 nm. The absorbance spectra show two peaks which represent the two isomer forms of carbonyl-2,4-DNPH products. The absorbance values at 550 nm are selected for subsequence quantification of carbonyl concentrations, because the 2,4-DNPH sample barely have any absorbance at 550 nm (Figure S4.1). In this study, we compared the carbonyl concentrations (nmol carbonyls per mL of sample) in vaping emissions and unvaped e-liquids. Figure 4.3 shows carbonyl concentrations in unvaped e-liquids and vaping emission samples of PG-VG and each of the flavored e-liquid. The concentrations of total carbonyls were quantified using a calibration curve of formaldehyde-DNPH standard compound (Figure S4.2), whose trendline has a r^2=0.9467, and y=0.0182x (with y-intercept set as 0).

For unvaped e-liquid samples, the order of highest to lowest carbonyl concentrations (nmol carbonyls per mL sample with ±standard deviation) is *trans*-2-hexenol (11.3±1.4) > benzyl alcohol (7.3±1.3) > linalool (0.1±0.2), l-(-)-menthol (-1.1±0.3), PG-VG (-1.5±0.4). Both *trans*-2-hexenol and benzyl alcohol unvaped e-liquids contained an abundance of carbonyls than PG-VG, l-(-)-menthol and linalool (which barely had any carbonyl detections). For vaping emission samples, the order of highest to lowest carbonyl concentrations (nmol carbonyls per mL sample with ±standard deviation) is

benzyl alcohol (25.3±0.8) > *trans*-2-hexenol (19.6±3.1) > PG-VG (10.2±1.7) > l-(-)-menthol (9.9±2.5) > linalool (2.9±1.4). Among vaping emission samples, *trans*-2-hexenol and benzyl alcohol e-liquids had higher carbonyl concentrations (9.4 and 15.1 nmol carbonyls per mL sample more) than PG-VG. Comparing to respective unvaped e-liquids, vaping emission samples from PG-VG and 4 flavored e-liquids had higher carbonyl concentrations.

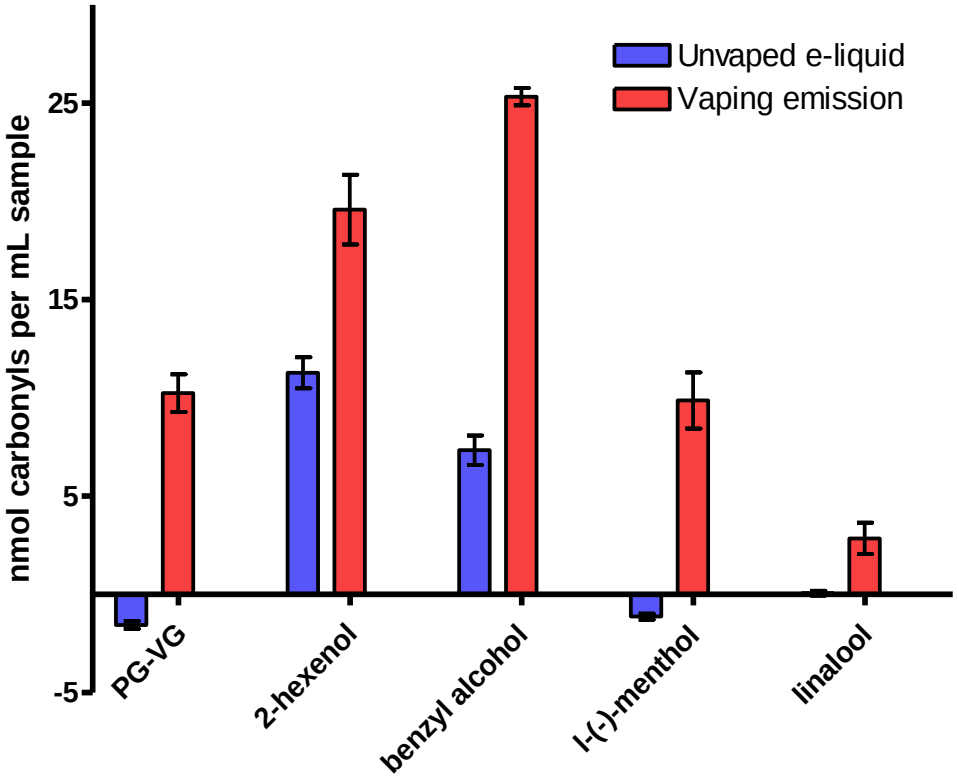

Figure 4.3. nmol of carbonyls per mL pf sample for unvaped e-liquids (blue) and vaping emissions (red).

4.3.4 Global electrophilicity and local site reactivities of carbonyls

Global electrophilicity and local site reactivities of selected carbonyls, including formaldehyde, acetaldehyde, benzaldehyde, l-(-)-menthone, *trans*-2-hexenal, and linalool-8-aldehyde were calculated using computational chemistry approaches. The optimized geometries for the selected carbonyls are shown in Table S4.2. In Table 4.1, the global electrophilicity parameters (E_{HOMO}, E_{LUMO}, μ, η, and ω) were calculated using the density functional theory. E_{HOMO} and E_{LUMO} represent the energy values for the highest occupied and lowest unoccupied molecular orbitals, respectively. E_{HOMO} and E_{LUMO} are used to calculate μ (chemical potential), η (chemical hardness), and ω (global electrophilicity), which are important for assessing global reactivity of carbonyls. Typically, the higher the ω value, the more electrophilic the compound. When comparing the ω values for simple carbonyls, benzaldehyde has the highest ω value (2.27 eV), followed by formaldehyde (1.82 eV), acetaldehyde (1.57), and menthone (1.26). For *α,β*-unsaturated carbonyls, *trans*-2-hexenal and linalool-8-aldehyde have the same ω value of 2.03 eV, which could be due to their structural similarities. As ω works well to predict the overall reactivity of carbonyl compounds, condensed Fukui parameters are favorable for compounds with multiple reactive sites (e.g., *α,β*-unsaturated carbonyls).

Table 4.1. Global electrophilicity parameters (E_{HOMO}, E_{LUMO}, μ, η, and ω) calculated using density functional theory.

Compound	Structure	E_{HOMO} (eV)	E_{LUMO} (eV)	μ (eV)	η (eV)	ω (eV)
simple carbonyl						
formaldehyde	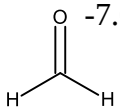	-7.686	-1.669	-4.677	6.016	1.82
acetaldehyde	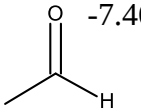	-7.467	-1.319	-4.393	6.148	1.57
benzaldehyde	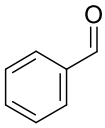	-7.504	-2.257	-4.881	5.247	2.27
l-menthone	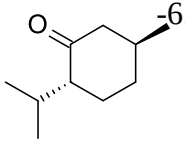	-6.902	-0.879	-3.891	6.024	1.26
α,β-unsaturated carbonyl						
trans-2-hexenal	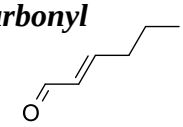	-7.414	-1.975	-4.695	5.438	2.03
linalool-8-aldehyde	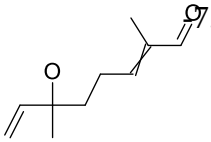	-7.224	-1.990	-4.607	5.234	2.03

Condensed Fukui parameters (f_k^0, f_k^-, f_k^+, and dual-descriptor) are useful for predicting local site reactivities of *α,β*-unsaturated carbonyls. f_k^0 is used to represent a neutral or radical attack, f_k^- represents an electrophilic attack, f_k^+ represents a nucleophilic attack, and the dual-descriptor -/+ represents an electrophilic/a nucleophilic attack. Table 4.2 shows the calculated f_k^+ values for α-carbon (C_α), β-carbon (C_β), carbonyl-carbon ($C_{carbonyl}$), and carbonyl-oxygen ($O_{carbonyl}$) for different carbonyls listed. The output data from the NPA analysis used to calculate the condensed Fukui functions are shown in Table

S4.2. The calculated values for f_k^0, f_k^-, and the dual-descriptor are shown in Tables S4.4 – S4.6. The condensed Fukui functions for C_α and C_β are only applicable to *α,β*-unsaturated carbonyls.

For simple carbonyls, f_k^+ values for $C_{carbonyl}$ are greater than the values for $O_{carbonyl}$. This is reasonable as simple carbonyls can form adducts with nucleophiles (e.g., GSH) via 1,2-carbonyl addition (Table 4.2). For *α,β*-unsaturated carbonyls, C_β has highest f^+ values, followed by $C_{carbonyl}$, $O_{carbonyl,}$ and C_α (Table 4.2). These results support that *α,β*-unsaturated carbonyls can form adducts with GSH through both 1,4-conjugated and 1,2-carbony additions. When examining the dual-descriptor parameters, the values for $C_{carbonyl}$ for all simple carbonyls are all negatives, which indicate that these simple carbonyls may favor an electrophilic attack. The dual-descriptor values for $C_{carbonyl}$ for *trans*-2-hexenal and linalool-8-aldehyde are positives and indicate that their $C_{carbonyl}$ may favor a nucleophilic attack. The dual-descriptor for *trans*-2-hexenal's C_β is positive (0.1287), but linalool-8-aldehyde's C_β is negative (-0.1627).

Table 4.2. Condensed Fukui function, f_k^+, of carbonyl compounds calculated using UCA-FUKUI software.

		f_k^+ (nucleophilic attack)			
simple carbonyl	**structure**	**$O_{carbonyl}^1$**	**$C_{carbonyl}^2$**	**C_α^3**	**C_β^4**
formaldehyde		0.3465	0.5923	n/a	n/a
acetaldehyde		0.3365	0.4817	n/a	n/a
benzaldehyde	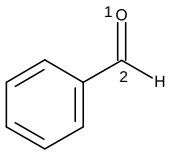	0.2260	0.2426	n/a	n/a
l-menthone	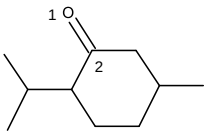	0.284	0.3864	n/a	n/a
α,β-unsaturated carbonyl					
trans-2-hexenal	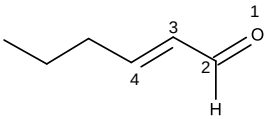	0.2146	0.2426	0.0563	0.2619
linalool-8-aldehyde	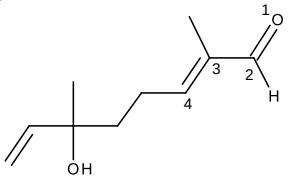	0.2506	0.2636	0.0395	0.2370

4.4 Sources of Uncertainty

One source of uncertainty in this study is the identification of carbonyl-GSH adducts. The adduct formation of proposed *trans*-2-hexenal-GSH and benzaldehyde-GSH are identified by their exact mass values of deprotonated products ($[M-H]^-$). To confirm

the identity of these adducts, analytical standards of *trans*-2-hexenal-GSH and benzaldehyde-GSH adducts are required. In addition, the quantification of carbonyls in unvaped e-liquids and vaping emissions using 2,4-DNPH assays is estimated using a calibration curve of formaldehyde-DNPH. Given that the response factor for different carbonyl-DNPH adducts may be different at 550 nm, the quantification of total carbonyls can only be interpreted as formaldehyde-equivalent concentrations, but not the absolute concentrations of total carbonyls. Nevertheless, the relative abundance of carbonyls between vaping emissions versus unvaped e-liquids determined by this approach still provides valuable information to estimate the production of carbonyls from different e-liquid formulations.

4.4 Conclusion and Implications

This study characterized carbonyl composition and abundance in unvaped e-liquids and vaping emissions, and carbonyl reactivities were predicted by density functional theory and condensed Fukui functions. Adduct formations between carbonyls and GSH were characterized using the LC/ESI-QTOFMS method. Common carbonyls emitted from vaping of unflavored (PG-VG) and flavored (10% volume of *trans*-2-hexenol, benzyl alcohol, l-(-)-menthone, or linalool) e-liquids include formaldehyde, acetaldehyde, glyoxal and methyl glyoxal. The results are consistent with previous reports,[10, 44, 45] showing a wide array of small carbonyl compounds can be produced through thermal decomposition of e-liquid diluents. Carbonyls that were only produced from vaping of flavored e-liquids include *trans*-2-hexenol, b-butanal, and benzaldehyde. Some of unique carbonyls were

generated from the direct oxidation of alcohol-containing flavor chemicals, showing the potential importance of this reaction route to produce reactive carbonyls. Moreover, using 2,4-DNPH assays, carbonyls were found in vaping emission samples of all e-liquid samples, and found abundant in two unvaped e-liquids (*trans*-2-hexenol and benzyl alcohol). But carbonyls were more abundant in the vaping emission samples comparing with unvaped e-liquids. In addition, global electrophilicity and local reactivity at specific sites within selected simple carbonyls (formaldehyde, acetaldehyde, benzaldehyde, and l-menthone) and α,β-unsaturated carbonyls (*trans*-2-hexenol and linalool) were computed. The calculated electrophilicity parameters indicated that simple carbonyls could attack or covalently modify nucleophiles such as GSH via 1,2-carbonyl addition, while α,β-unsaturated carbonyls can covalently modify GSH via 1,2-carbonyl addition and 1,4-conjugated addition. Overall, results from this study implicates that flavor chemicals used in e-liquids can also contribute to the emission of toxic carbonyls during vaping.

This study used model alcohol-containing flavor chemicals to demonstrate the formation of reactive carbonyls through direct oxidation of the alcohol functional group. The resulting carbonyls are not commonly measured, but these emission products may pose potential health risks upon inhalation, depending on their abundance in the emissions as well as the chemical reactivity. Further studies are required to comprehensively profile the emission products from flavor chemicals to gain a better understanding of potential health effects associated with vaping.

4.5 Supporting Information

Table S4.1. Total peak area from extracted ion chromatograms (EIC) of *m/z* 181 to quantify carbonyls (derivatized with PFBHA) in vaping emissions from unflavored and flavored e-liquids. The EICs were integrated using these settings: initial peak width = 0.120 and initial threshold = 17.0.

E-liquid sample	Total peak area
PG-VG	1.43×10^9
trans-2-hexenol	1.98×10^9
benzyl alcohol	5.23×10^8
l-(-)-menthol	2.14×10^9
linalool	4.66×10^9

Table S4.2. Optimized geometries of target carbonyls calculated by DFT/B3LYP/6-311+G(d, p) level of theory and in water solvation using Gaussian 16W program.

Formaldehyde

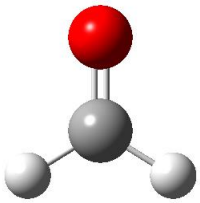

Charge = 0
E(UB3LYP) = -114.432708094 Hartree (Eh)
Electronic state: 1-A
Cartesian Coordinates (Angstroms):

O	-0.000041	0.676752	0.000000
C	-0.000041	-0.531376	0.000000
H	-0.938433	-1.112848	0.000000
H	0.939008	-1.112912	0.000000

Charge = -1
E(UB3LYP) = -114.624580950 Hartree (Eh)
Electronic state: 1-A
Cartesian Coordinates (Angstroms):

O	-0.000009	0.727861	0.000000
C	-0.000009	-0.584091	0.000000
H	-0.936931	-1.159157	0.000000
H	0.937051	-1.159186	0.000000

Charge = +1
E(UB3LYP) = -114.160019523 Hartree (Eh)
Electronic state: 1-A
Cartesian Coordinates (Angstroms):

O	-0.000105	0.663897	0.000000
C	-0.000105	-0.522196	0.000000
H	-0.962402	-1.089947	0.000000
H	0.963872	-1.088057	0.000000

Acetaldehyde

Charge = 0
E(UB3LYP) = -153.354522985 Hartree (Eh)
Electronic state: 1-A
Cartesian Coordinates (Angstroms):

C	0.000000	0.471652	0.000000
O	-1.207923	0.355997	0.000000
C	0.949642	-0.693883	0.000000
H	0.452229	1.482132	0.000000
H	1.989744	-0.367922	0.000000
H	0.761779	-1.314399	0.881325
H	0.761779	-1.314399	-0.881325

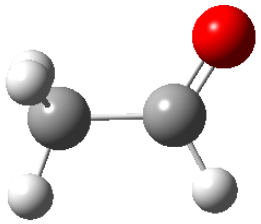

Charge = -1
E(UB3LYP) = -153.370677836 Hartree (Eh)
Electronic state: 1-A
Cartesian Coordinates (Angstroms):

C	0.000000	0.497419	0.000000
O	-1.293321	0.239851	0.000000
C	1.016429	-0.611764	0.000000
H	0.360356	1.536615	0.000000
H	2.038719	-0.214048	0.000000
H	0.924458	-1.277656	0.878966
H	0.924458	-1.277656	-0.878966

Charge = +1
E(UB3LYP) = -153.102042126 Hartree (Eh)
Electronic state: 1-A
Cartesian Coordinates (Angstroms):

C	0.000000	0.451208	0.000000
O	-1.192126	0.398092	0.000000
C	0.949359	-0.730416	0.000000
H	0.434009	1.484123	0.000000
H	1.968672	-0.358366	0.000000
H	0.719088	-1.317621	0.893620
H	0.719088	-1.317621	-0.893620

Benzaldehyde

Charge = 0
E(UB3LYP) = -345.676360401 Hartree (Eh)
Electronic state: 1-A
Cartesian Coordinates (Angstroms):

O	2.854181	-0.391611	-0.000078
C	1.986641	0.463916	0.000076

C	0.535584	0.200982	0.000040
C	0.034053	-1.109905	0.000036
C	-0.349770	1.286844	0.000010
C	-1.337636	-1.325852	0.000002
C	-1.725199	1.067938	-0.000021
C	-2.217196	-0.237321	-0.000027
H	2.262757	1.535775	-0.000056
H	0.728135	-1.941920	0.000060
H	0.042746	2.298463	0.000017
H	-1.728700	-2.336551	0.000000
H	-2.409849	1.907725	-0.000044
H	-3.287394	-0.410225	-0.000052

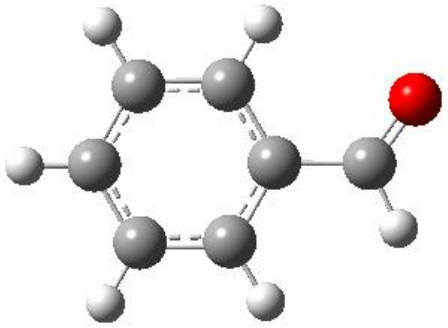

Charge = -1
E(UB3LYP) = -345.763742749 Hartree (Eh)
Electronic state: 1-A
Cartesian Coordinates (Angstroms):

O	2.905663	-0.399770	-0.000288
C	1.972124	0.479781	0.000285
C	0.571895	0.221027	0.000170
C	0.032434	-1.108894	0.000139
C	-0.377215	1.294520	0.000046
C	-1.336634	-1.327406	0.000006
C	-1.739152	1.059533	-0.000084
C	-2.249060	-0.257790	-0.000107
H	2.251592	1.550684	-0.000317
H	0.718860	-1.948297	0.000218
H	-0.007260	2.317049	0.000055
H	-1.710758	-2.347931	-0.000009
H	-2.426349	1.900977	-0.000163
H	-3.317749	-0.438952	-0.000207

Charge = +1
E(UB3LYP) = -345.403731647 Hartree (Eh)
Electronic state: 1-A
Cartesian Coordinates (Angstroms):

O	2.820665	-0.456620	-0.000006
C	2.032758	0.460995	0.000007
C	0.555395	0.250624	0.000003
C	0.029491	-1.077953	0.000004
C	-0.313875	1.310038	0.000002
C	-1.375061	-1.320978	-0.000001

C	-1.725245	1.063451	-0.000007
C	-2.243289	-0.258955	0.000003
H	2.360204	1.513283	-0.000007
H	0.725059	-1.909611	-0.000001
H	0.044530	2.332454	0.000002
H	-1.735073	-2.341198	-0.000013
H	-2.406862	1.905372	-0.000010
H	-3.314216	-0.410675	0.000011

L-menthone

Charge = 0
E(UB3LYP) = -467.277887079 Hartree (Eh)
Electronic state: 1-A
Cartesian Coordinates (Angstroms):

C	0.705453	-0.166167	0.214637
C	-2.299470	-0.105428	-0.228956
C	2.936602	0.941211	0.688351
C	2.910825	-1.444362	-0.096967
C	-3.738444	-0.130546	0.293387
O	0.365020	1.987997	-0.839537
C	-0.081506	-1.365419	-0.386251
C	-1.519956	1.106745	0.337916
C	-1.540854	-1.401905	0.084807
C	-0.085160	1.090657	-0.146177
C	2.195724	-0.087039	-0.183220
H	0.642087	-0.270089	1.307989
H	-0.043135	-1.308385	-1.481338
H	0.412450	-2.296017	-0.101920
H	-1.985481	2.049334	0.042108
H	-1.523660	1.047423	1.433576
H	2.240503	0.254691	-1.223549
H	-1.566773	-1.578026	1.168360
H	-2.054254	-2.248937	-0.382035
H	-2.334471	0.009553	-1.320655
H	2.952446	0.616500	1.734919
H	3.974495	1.048867	0.359828
H	2.467377	1.925392	0.644717
H	2.518529	-2.170000	-0.812385
H	3.976438	-1.318231	-0.309217
H	2.822927	-1.876362	0.906298
H	-4.268022	0.792810	0.041765

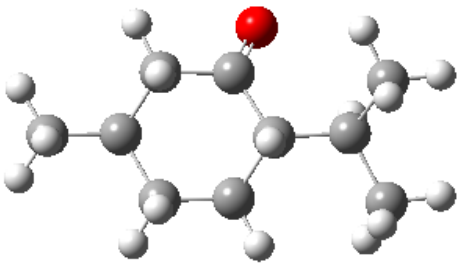

H -4.295398 -0.966427 -0.139953
H -3.755511 -0.242552 1.382630

Charge = -1
E(UB3LYP) = -467.315041323 Hartree (Eh)
Electronic state: 1-A
Cartesian Coordinates (Angstroms):

C 0.680762 -0.119390 0.187859
C -2.319222 -0.171453 -0.286619
C 3.018634 0.807702 0.635788
C 2.829633 -1.525006 -0.250080
C -3.770576 -0.144477 0.207614
O 0.512615 2.284409 -0.377696
C -0.087531 -1.406559 -0.190541
C -1.556384 1.116985 0.060887
C -1.551292 -1.378437 0.264971
C -0.082038 1.115727 -0.308058
C 2.176991 -0.131736 -0.243869
H 0.684325 -0.094667 1.305566
H -0.050100 -1.543492 -1.279701
H 0.399182 -2.281658 0.252104
H -2.036876 1.980739 -0.414325
H -1.659126 1.284966 1.159974
H 2.212643 0.251962 -1.271966
H -1.583857 -1.342397 1.363901
H -2.051764 -2.309908 -0.028159
H -2.337409 -0.260433 -1.382116
H 3.071472 0.424141 1.662335
H 4.045517 0.884441 0.259544
H 2.573448 1.802299 0.659159
H 2.363445 -2.206585 -0.965619
H 3.888103 -1.440151 -0.518601
H 2.780750 -1.993600 0.739812
H -4.313975 0.713501 -0.202053
H -4.308852 -1.052105 -0.086343
H -3.811702 -0.072454 1.300345

Charge = +1
E(UB3LYP) = -467.022135178 Hartree (Eh)
Electronic state: 1-A
Cartesian Coordinates (Angstroms):

C 0.729604 -0.248757 0.196491

C	-2.299519	-0.079706	-0.250720
C	2.946081	1.017628	0.447199
C	2.906472	-1.478737	0.153504
C	-3.733306	-0.114645	0.320040
O	0.376291	2.017864	-0.696341
C	-0.105887	-1.341143	-0.490114
C	-1.548849	1.083967	0.407158
C	-1.562477	-1.403783	-0.023133
C	-0.075200	1.102399	-0.100502
C	2.206880	-0.147681	-0.216896
H	0.632229	-0.336538	1.285674
H	-0.037142	-1.235294	-1.577159
H	0.379837	-2.289007	-0.233950
H	-1.969082	2.059299	0.169598
H	-1.471410	0.957453	1.491227
H	2.250269	-0.028158	-1.304083
H	-1.597732	-1.663884	1.040373
H	-2.076669	-2.200476	-0.564976
H	-2.365616	0.119201	-1.325349
H	2.889320	0.955075	1.537889
H	3.999948	0.997258	0.161688
H	2.550899	1.988396	0.135566
H	2.505755	-2.322209	-0.409857
H	3.969527	-1.389669	-0.078945
H	2.811970	-1.694753	1.221695
H	-4.257077	0.823626	0.128332
H	-4.285752	-0.924239	-0.162763
H	-3.722397	-0.296243	1.397602

Trans-2-hexenal

Charge = 0
E(UB3LYP) = -309.958896545 Hartree (Eh)
Electronic state: 1-A
Cartesian Coordinates (Angstroms):

C	-2.638669	0.319521	-0.003206
C	-1.357376	-0.374257	0.034723
C	-0.244343	0.262892	0.436141
C	1.123625	-0.329315	0.513109
C	2.148214	0.426447	-0.358354
C	3.559730	-0.152190	-0.233532
O	-3.695828	-0.186820	-0.351412

H	-2.609234	1.380353	0.313763
H	-1.342381	-1.416907	-0.270720
H	-0.330353	1.310276	0.726660
H	1.459484	-0.282706	1.557916
H	1.095248	-1.385688	0.229712
H	1.823340	0.389462	-1.403455
H	2.154769	1.483431	-0.070627
H	4.264537	0.396518	-0.863782
H	3.919126	-0.096430	0.798560
H	3.584988	-1.202335	-0.540017

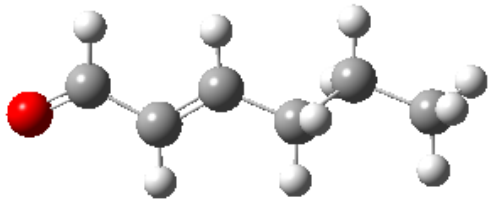

Charge = -1
E(UB3LYP) = -310.031522249 Hartree (Eh)
Electronic state: 1-A
Cartesian Coordinates (Angstroms):

C	-2.672951	0.253138	-0.140291
C	-1.376611	-0.190528	0.179681
C	-0.218484	0.587608	0.257114
C	1.141394	0.052921	0.604013
C	2.185152	0.156002	-0.529532
C	3.574874	-0.343986	-0.121547
O	-3.744389	-0.471509	-0.209510
H	-2.768165	1.337295	-0.353498
H	-1.280673	-1.259051	0.391294
H	-0.288957	1.655873	0.049252
H	1.558396	0.580524	1.478330
H	1.054235	-0.999730	0.904042
H	1.825427	-0.412510	-1.395260
H	2.252955	1.201015	-0.855850
H	4.290784	-0.258109	-0.944386
H	3.968415	0.231434	0.723064
H	3.542453	-1.395604	0.182461

Charge = +1
E(UB3LYP) = -309.687393075 Hartree (Eh)
Electronic state: 1-A
Cartesian Coordinates (Angstroms):

C	-2.585359	0.294347	0.004884
C	-1.349933	-0.406959	0.009250
C	-0.239085	0.250077	0.441860
C	1.106798	-0.350496	0.499560
C	2.133001	0.453198	-0.344018

C	3.536416	-0.145962	-0.233474
O	-3.682338	-0.140600	-0.344444
H	-2.622612	1.354055	0.336706
H	-1.347230	-1.434081	-0.332454
H	-0.330998	1.285572	0.762097
H	1.426822	-0.312376	1.550862
H	1.086097	-1.397333	0.190107
H	1.808354	0.456420	-1.388058
H	2.139440	1.493539	-0.006288
H	4.241349	0.428485	-0.839553
H	3.891547	-0.134177	0.800658
H	3.554909	-1.180531	-0.586898

Linalool-8-aldehyde

Charge = 0
E(UB3LYP) = -541.264732853 Hartree (Eh)
Electronic state: 1-A
Cartesian Coordinates (Angstroms):

O	-2.607483	-0.212004	1.373312
C	-2.206337	0.249043	0.072412
C	-0.821773	-0.343885	-0.297530
C	0.318985	0.013068	0.676366
C	1.534532	-0.824197	0.412356
C	2.782959	-0.454612	0.050337
C	3.129150	0.957011	-0.158536
O	4.245357	1.342382	-0.480178
C	3.885717	-1.460728	-0.162939
C	-3.199300	-0.165451	-0.997760
C	-4.344946	-0.812322	-0.796515
C	-2.176961	1.780150	0.171220
H	-2.653723	-1.176185	1.358297
H	-0.928666	-1.434156	-0.345583
H	-0.554768	-0.016120	-1.307126
H	0.533521	1.079722	0.633925
H	-0.019416	-0.204409	1.696279
H	1.361755	-1.893605	0.531956
H	2.323311	1.695027	-0.017779
H	4.281634	-1.398533	-1.180699
H	4.724201	-1.271430	0.513647
H	3.525306	-2.476020	0.008080
H	-2.912036	0.111662	-2.010049

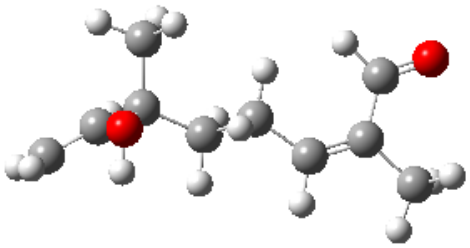

H	-4.678367	-1.098582	0.195119
H	-4.993708	-1.070152	-1.626008
H	-1.492920	2.105480	0.957135
H	-1.855950	2.221136	-0.775057
H	-3.175317	2.154676	0.406326

Charge = -1
E(UB3LYP) = -541.341547185 Hartree (Eh)
Electronic state: 1-A
Cartesian Coordinates (Angstroms):

O	-2.386825	0.676122	1.304449
C	-2.280132	0.265290	-0.072246
C	-0.993204	-0.569587	-0.285936
C	0.338635	0.134475	0.010909
C	1.506949	-0.815056	-0.058596
C	2.853312	-0.441266	-0.012549
C	3.299662	0.897218	0.109377
O	4.535828	1.284390	0.150840
C	3.913106	-1.523297	-0.090237
C	-3.471926	-0.578956	-0.486314
C	-4.513729	-0.899710	0.277890
C	-2.277861	1.565904	-0.886478
H	-2.315589	-0.108541	1.861591
H	-1.074471	-1.462762	0.348037
H	-0.988317	-0.934358	-1.319426
H	0.477392	0.961652	-0.699689
H	0.273136	0.616719	0.999011
H	1.272344	-1.874816	-0.129171
H	2.517293	1.673136	0.172488
H	4.597534	-1.361028	-0.930570
H	4.536745	-1.548924	0.811180
H	3.457892	-2.510083	-0.211219
H	-3.431940	-0.939715	-1.512465
H	-4.600366	-0.556014	1.302971
H	-5.319906	-1.515619	-0.104982
H	-1.441621	2.202606	-0.593026
H	-2.192750	1.350574	-1.954102
H	-3.208283	2.112980	-0.717861

Charge = +1
E(UB3LYP) = -541.005230385 Hartree (Eh)
Electronic state: 1-A
Cartesian Coordinates (Angstroms):

O	-2.631467	-0.563036	1.227356
C	-2.138021	0.239023	0.184510
C	-0.699840	-0.308008	-0.274640
C	0.292161	-0.318123	0.944447
C	1.486991	-1.008167	0.442628
C	2.683801	-0.450561	0.018620
C	2.836850	1.027906	-0.123578
O	3.831819	1.523881	-0.607351
C	3.866982	-1.287653	-0.293769
C	-2.938095	0.157677	-1.089217
C	-4.034742	-0.592344	-1.277752
C	-2.061551	1.673079	0.708531
H	-2.764475	-1.471330	0.923512
H	-0.827907	-1.321024	-0.658910
H	-0.322985	0.318367	-1.083287
H	0.479480	0.690685	1.300362
H	-0.181063	-0.901865	1.737610
H	1.399661	-2.087881	0.348801
H	2.010333	1.659176	0.232434
H	4.330641	-0.946099	-1.225570
H	4.633690	-1.153093	0.480559
H	3.615005	-2.344925	-0.351765
H	-2.562203	0.774278	-1.899570
H	-4.451060	-1.229147	-0.505882
H	-4.569542	-0.551644	-2.219066
H	-1.489773	1.715173	1.635834
H	-1.598532	2.332407	-0.026791
H	-3.071305	2.033183	0.913009

Table S4. 3. Condensed Fukui parameters (f^0, f^-, f^+, and dual descriptor) calculated using NPA data by UCA-Fukui software.

Formaldehyde

Atom	NPA neutral	NPA anion	NPA cation	f^-	f^+	f^0	Dual descriptor
O	-0.5521	-0.8986	0.0149	0.5670	0.3465	0.4568	-0.2205
C	0.3153	-0.2770	0.3305	0.0152	0.5923	0.3037	0.5771
H	0.1184	0.0878	0.3272	0.2088	0.0306	0.1197	-0.1782
H	0.1184	0.0878	0.3274	0.2090	0.0306	0.1198	-0.1785

Acetaldehyde

Atom	NPA neutral	NPA anion	NPA cation	f^-	f^+	f^0	Dual descriptor
C	0.4636	-0.0180	0.4809	0.0172	0.4817	0.2494	0.4644
O	-0.5898	-0.9263	-0.0454	0.5445	0.3365	0.4405	-0.2080
C	-0.6949	-0.6606	-0.6248	0.0702	-0.0343	0.0179	-0.0358
H	0.1196	0.0842	0.3307	0.2110	0.0354	0.1232	-0.1756
H	0.2206	0.1893	0.2707	0.0501	0.0313	0.0407	-0.0188
H	0.2405	0.1657	0.2940	0.0535	0.0747	0.0641	0.0212
H	0.2405	0.1657	0.2940	0.0535	0.0747	0.0641	0.0212

Benzaldehyde

Atom	NPA neutral	NPA anion	NPA cation	f^-	f^+	f^0	Dual descriptor
O	-0.5885	-0.8144	-0.5189	0.0696	0.2260	0.1564	-0.3404
C	0.4320	0.1894	0.4330	0.0010	0.2426	0.2416	0.1945
C	-0.1804	-0.1998	-0.1452	0.0352	0.0194	-0.0157	0.0129
C	-0.1554	-0.2622	0.1126	0.2681	0.1067	-0.1614	0.0780
C	-0.1572	-0.2296	-0.0936	0.0636	0.0724	0.0088	0.0173
C	-0.2082	-0.2243	-0.1296	0.0786	0.0161	-0.0625	-0.0080
C	-0.2122	-0.2422	0.0807	0.2928	0.0300	-0.2628	0.0203
C	-0.1686	-0.3120	-0.1507	0.0179	0.1435	0.1256	0.0809
H	0.1267	0.0942	0.1546	0.0279	0.0325	0.0046	-0.1421
H	0.2266	0.2038	0.2483	0.0217	0.0229	0.0012	0.0085
H	0.2217	0.1970	0.2554	0.0337	0.0247	-0.0090	0.0042

H	0.2212	0.1993	0.2543	0.0331	0.0219	-0.0112	0.0016
H	0.2219	0.2005	0.2437	0.0218	0.0215	-0.0003	0.0024
H	0.2203	0.2004	0.2554	0.0352	0.0199	-0.0153	0.0082

L-menthone

Atom	NPA neutral	NPA anion	NPA cation	f^-	f^+	f^0	Dual descriptor
C	-0.3055	-0.3125	-0.2108	0.0947	0.0070	0.0508	-0.0877
C	-0.2159	-0.2259	-0.2225	-0.0066	0.0101	0.0017	0.0035
C	-0.5738	-0.5788	-0.5791	-0.0053	0.0050	0.0001	-0.0003
C	-0.5763	-0.5763	-0.5626	0.0137	-0.0001	0.0068	-0.0137
C	-0.5714	-0.5712	-0.5581	0.0132	-0.0001	0.0065	-0.0131
O	-0.6201	-0.9042	-0.2456	0.3745	0.2840	0.3293	-0.0905
C	-0.3741	-0.3769	-0.3912	-0.0171	0.0028	0.0072	-0.0143
C	-0.4728	-0.4582	-0.4030	0.0697	-0.0146	0.0276	-0.0552
C	-0.3826	-0.3748	-0.3870	-0.0044	-0.0078	0.0061	0.0035
C	0.6284	0.2420	0.6823	0.0539	0.3864	0.2201	0.3326
C	-0.2288	-0.2240	-0.2324	-0.0036	-0.0048	0.0042	0.0012
H	0.2232	0.1529	0.2620	0.0388	0.0702	0.0545	0.0314
H	0.1994	0.1816	0.2280	0.0286	0.0179	0.0232	-0.0107
H	0.2153	0.1896	0.2636	0.0483	0.0257	0.0370	-0.0225
H	0.2182	0.1914	0.2614	0.0433	0.0268	0.0350	-0.0165
H	0.2236	0.1496	0.2644	0.0408	0.0740	0.0574	0.0332
H	0.1992	0.1838	0.2183	0.0191	0.0154	0.0173	-0.0037
H	0.1964	0.1817	0.2141	0.0176	0.0147	0.0162	-0.0029
H	0.2110	0.1941	0.2336	0.0225	0.0170	0.0198	-0.0056
H	0.1941	0.1800	0.2249	0.0308	0.0141	0.0224	-0.0168
H	0.1935	0.1821	0.2094	0.0159	0.0114	0.0136	-0.0045
H	0.2009	0.1859	0.2216	0.0206	0.0151	0.0178	-0.0056
H	0.2072	0.2224	0.2161	0.0089	-0.0153	0.0032	0.0063
H	0.2028	0.1975	0.2115	0.0087	0.0053	0.0070	-0.0034
H	0.2038	0.1954	0.2216	0.0179	0.0084	0.0131	-0.0095
H	0.1962	0.1895	0.2102	0.0140	0.0067	0.0104	-0.0073
H	0.2046	0.1965	0.2164	0.0117	0.0081	0.0099	-0.0036
H	0.2054	0.1956	0.2231	0.0178	0.0097	0.0138	-0.0080
H	0.1982	0.1913	0.2100	0.0118	0.0069	0.0093	-0.0049

Trans-2-hexenal

Atom	NPA neutral	NPA anion	NPA cation	f^-	f^+	f^0	Dual descriptor
C	0.4029	0.1602	0.3721	-0.0307	0.2426	0.1059	0.2119
C	-0.3295	-0.3857	-0.3162	0.0133	0.0563	0.0348	0.0430
C	-0.0420	-0.3039	0.0912	0.1332	0.2619	0.1976	0.1287
C	-0.4341	-0.4094	-0.4456	-0.0116	-0.0247	0.0181	0.0131
C	-0.3755	-0.3794	-0.3722	0.0034	0.0039	0.0036	0.0005
C	-0.5761	-0.5803	-0.5745	0.0016	0.0042	0.0029	0.0026
O	-0.6050	-0.8196	-0.0606	0.5443	0.2146	0.3795	-0.3298
H	0.1202	0.0676	0.3094	0.1892	0.0526	0.1209	-0.1366
H	0.2142	0.1757	0.2647	0.0505	0.0385	0.0445	-0.0120
H	0.2012	0.1615	0.2244	0.0233	0.0397	0.0315	0.0164
H	0.2236	0.1781	0.2559	0.0323	0.0455	0.0389	0.0132
H	0.2087	0.1871	0.2253	0.0166	0.0216	0.0191	0.0050
H	0.1961	0.1842	0.2054	0.0093	0.0120	0.0106	0.0027
H	0.1961	0.1847	0.2049	0.0088	0.0114	0.0101	0.0026
H	0.2048	0.1964	0.2127	0.0078	0.0084	0.0081	0.0006
H	0.1971	0.1914	0.2013	0.0042	0.0057	0.0050	0.0015
H	0.1973	0.1915	0.2018	0.0044	0.0058	0.0051	0.0014

Linalool-8-aldehyde

Atom	NPA neutral	NPA anion	NPA cation	f^-	f^+	f^0	Dual descriptor
O	-0.7721	-0.7762	-0.7073	0.0648	0.0041	0.0344	-0.0607
C	0.2310	0.2288	0.2541	0.0232	0.0022	0.0127	-0.0210
C	-0.3876	-0.3876	-0.3476	0.0400	0.0000	0.0200	-0.0400
C	-0.4362	-0.4305	-0.4446	-0.0085	-0.0056	0.0070	-0.0029
C	-0.0552	-0.2923	0.0521	0.1074	0.2370	0.1722	0.1297
C	-0.1539	-0.1934	0.0483	0.2022	0.0395	0.1208	-0.1627
C	0.4087	0.1451	0.3915	-0.0172	0.2636	0.1232	0.2464
O	-0.6026	-0.8532	-0.4930	0.1096	0.2506	0.1801	0.1411
C	-0.5955	-0.5886	-0.6283	-0.0328	-0.0069	0.0198	-0.0259
C	-0.1983	-0.1942	-0.1637	0.0346	-0.0041	0.0153	-0.0305
C	-0.3940	-0.4015	-0.2790	0.1150	0.0074	0.0612	-0.1075
C	-0.5848	-0.5845	-0.5896	-0.0048	-0.0004	0.0026	-0.0044
H	0.4732	0.4713	0.4861	0.0129	0.0019	0.0074	-0.0109

H	0.2061	0.1959	0.2311	0.0250	0.0102	0.0176	-0.0147
H	0.2126	0.2034	0.2331	0.0206	0.0092	0.0149	-0.0114
H	0.2099	0.1891	0.2358	0.0259	0.0208	0.0234	-0.0051
H	0.2313	0.1912	0.2643	0.0331	0.0401	0.0366	0.0070
H	0.2003	0.1738	0.2325	0.0322	0.0265	0.0293	-0.0057
H	0.1277	0.0984	0.1565	0.0288	0.0293	0.0291	0.0005
H	0.2168	0.1957	0.2576	0.0408	0.0211	0.0310	-0.0197
H	0.2170	0.1946	0.2631	0.0461	0.0224	0.0343	-0.0238
H	0.2106	0.1918	0.2344	0.0238	0.0189	0.0213	-0.0049
H	0.2056	0.2025	0.2260	0.0204	0.0031	0.0117	-0.0173
H	0.1945	0.1941	0.2003	0.0058	0.0003	0.0031	-0.0055
H	0.1999	0.1976	0.2142	0.0143	0.0024	0.0083	-0.0119
H	0.2103	0.2105	0.2204	0.0101	-0.0002	0.0049	-0.0099
H	0.2123	0.2098	0.2238	0.0115	0.0026	0.0070	-0.0090
H	0.2125	0.2085	0.2279	0.0154	0.0040	0.0097	-0.0114

Table S4.4. Condensed Fukui function, f_k^-, of carbonyl compounds calculated using UCA-FUKUI software.

		f_k^- (electrophilic attack)			
simple carbonyl	**structure**	**$O_{carbonyl}$[1]**	**$C_{carbonyl}$[2]**	**C_α[3]**	**C_β[4]**
formaldehyde		0.567	0.0152	n/a	n/a
acetaldehyde		0.5445	0.0172	n/a	n/a
benzaldehyde	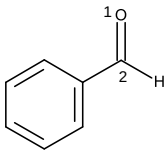	0.0696	0.0010	n/a	n/a
l-menthone	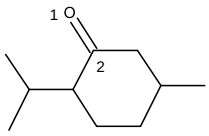	0.3745	0.0539	n/a	n/a
α,β-unsaturated carbonyl					
trans-2-hexenal	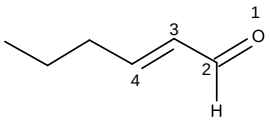	0.5443	-0.0307	0.0133	0.1332
linalool-8-aldehyde	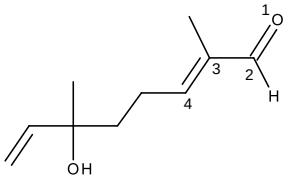	0.1096	-0.0172	0.2022	0.1074

Table S4.5. Condensed Fukui function, f_k^0, of carbonyl compounds calculated using UCA-FUKUI software.

		f_k^0 (local neutral/radical attack)			
simple carbonyl	**structure**	**$O_{carbonyl}^1$**	**$C_{carbonyl}^2$**	**C_α^3**	**C_β^4**
formaldehyde		0.4568	0.3037	n/a	n/a
acetaldehyde		0.4405	0.2494	n/a	n/a
benzaldehyde	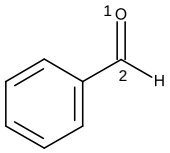	0.1564	0.2416	n/a	n/a
l-menthone	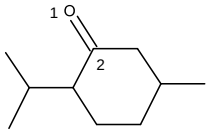	0.3293	0.2201	n/a	n/a
α,β-unsaturated carbonyl					
trans-2-hexenal	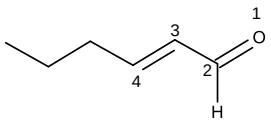	0.3795	0.1059	0.0348	0.1976
linalool-8-aldehyde	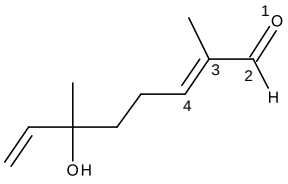	0.1801	0.1232	0.1208	0.1722

Table S4. 6. Condensed Fukui function, dual-descriptor, of carbonyl compounds calculated using UCA-FUKUI software.

		dual-descriptor			
simple carbonyl	**structure**	**$O_{carbonyl}^{1}$**	**$C_{carbonyl}^{2}$**	**C_{α}^{3}**	**C_{β}^{4}**
formaldehyde		-0.2205	0.5771	n/a	n/a
acetaldehyde		-0.2080	0.4644	n/a	n/a
benzaldehyde	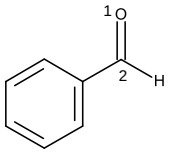	-0.3403	0.1945	n/a	n/a
l-menthone	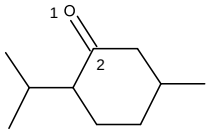	-0.0905	0.3326	n/a	n/a
α,β-unsaturated carbonyl					
trans-2-hexenal	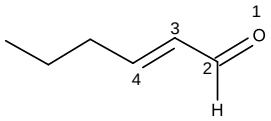	-0.3298	0.2119	0.0430	0.1287
linalool-8-aldehyde	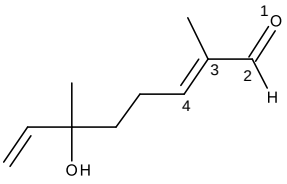	0.1411	0.2464	0.1297	-0.1627

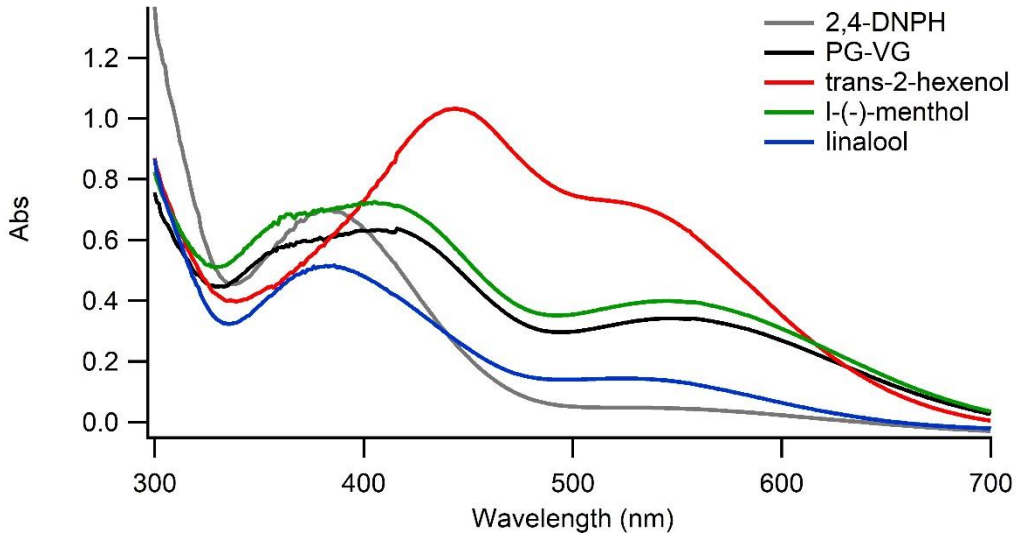

Figure S4.1. UV-Vis spectra of vaped e-liquid vaping emissions reacted with 2, 4-DNPH. Two maximum peaks shown are at around 450 nm and 550 nm. Spectra colors represent DNPH (gray), PG-VG (black), 2-hexenol (red), 1-(-)-menthol (green) and linalool (blue).

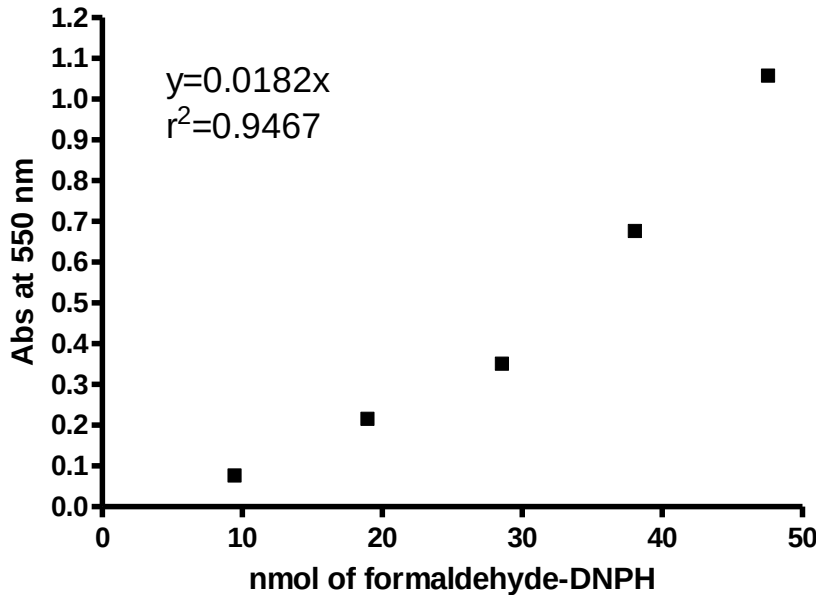

Figure S4.2. The calibration curve of nmol of formaldehyde-DDNPH vs absorbance at 550 nm. After setting the y-intercept as 0, the trendline of the data yields r^2=0.9467, and y=0.0182x.

References

1. Siegel, M. B.; Tanwar, K. L.; Wood, K. S., Electronic cigarettes as a smoking-cessation tool: results from an online survey. *American journal of preventive medicine* **2011,** *40* (4), 472-475.

2. Cullen, K. A.; Gentzke, A. S.; Sawdey, M. D.; Chang, J. T.; Anic, G. M.; Wang, T. W.; Creamer, M. R.; Jamal, A.; Ambrose, B. K.; King, B. A., E-cigarette use among youth in the United States, 2019. *Jama* **2019,** *322* (21), 2095-2103.

3. Morean, M. E.; Butler, E. R.; Bold, K. W.; Kong, G.; Camenga, D. R.; Cavallo, D. A.; Simon, P.; O'Malley, S. S.; Krishnan-Sarin, S., Preferring more e-cigarette flavors is associated with e-cigarette use frequency among adolescents but not adults. *PloS one* **2018,** *13* (1), e0189015.

4. Wasowicz, A.; Feleszko, W.; Goniewicz, M. L., E-Cigarette use among children and young people: the need for regulation. Taylor & Francis: 2015.

5. Krishnasamy, V. P.; Hallowell, B. D.; Ko, J. Y.; Board, A.; Hartnett, K. P.; Salvatore, P. P.; Danielson, M.; Kite-Powell, A.; Twentyman, E.; Kim, L., Update: characteristics of a nationwide outbreak of e-cigarette, or vaping, product use–associated lung injury—United States, August 2019–January 2020. *Morbidity and Mortality Weekly Report* **2020,** *69* (3), 90.

6. Almeida-da-Silva, C. L. C.; Dakafay, H. M.; O'Brien, K.; Montierth, D.; Xiao, N.; Ojcius, D. M., Effects of electronic cigarette smoke exposure on oral and systemic health. *Biomedical Journal* **2020**.

7. Behar, R. Z.; Luo, W.; Lin, S. C.; Wang, Y.; Valle, J.; Pankow, J. F.; Talbot, P., Distribution, quantification and toxicity of cinnamaldehyde in electronic cigarette refill fluids and aerosols. *Tobacco control* **2016,** *25* (Suppl 2), ii94-ii102.

8. Clapp, P. W.; Pawlak, E. A.; Lackey, J. T.; Keating, J. E.; Reeber, S. L.; Glish, G. L.; Jaspers, I., Flavored e-cigarette liquids and cinnamaldehyde impair respiratory innate immune cell function. *American Journal of Physiology-Lung Cellular and Molecular Physiology* **2017,** *313* (2), L278-L292.

9. Clapp, P. W.; Lavrich, K. S.; van Heusden, C. A.; Lazarowski, E. R.; Carson, J. L.; Jaspers, I., Cinnamaldehyde in flavored e-cigarette liquids temporarily suppresses bronchial epithelial cell ciliary motility by dysregulation of mitochondrial function. *American Journal of Physiology-Lung Cellular and Molecular Physiology237* **2019,** *316* (3), L470-L486.

10. Jiang, H.; Ahmed, C. S.; Martin, T. J.; Canchola, A.; Oswald, I. W.; Garcia, J. A.; Chen, J. Y.; Koby, K. A.; Buchanan, A. J.; Zhao, Z., Chemical and toxicological characterization of vaping emission products from commonly used vape juice diluents. *Chemical Research in Toxicology* **2020,** *33* (8), 2157-2163.

11. Khlystov, A.; Samburova, V., Flavoring compounds dominate toxic aldehyde production during e-cigarette vaping. *Environmental science & technology* **2016,** *50* (23), 13080-13085.

12. Gillman, I. G.; Pennington, A. S.; Humphries, K. E.; Oldham, M. J., Determining the impact of flavored e-liquids on aldehyde production during Vaping. *Regulatory Toxicology and Pharmacology* **2020,** *112*, 104588.

13. Ogunwale, M. A.; Li, M.; Ramakrishnam Raju, M. V.; Chen, Y.; Nantz, M. H.; Conklin, D. J.; Fu, X.-A., Aldehyde detection in electronic cigarette aerosols. *ACS omega* **2017,** *2* (3), 1207-1214.

14. Kim, K.-H.; Jahan, S. A.; Lee, J.-T., Exposure to formaldehyde and its potential human health hazards. *Journal of Environmental Science and Health, Part C* **2011,** *29* (4), 277-299.

15. Esterbauer, H.; Zöllner, H.; Scholz, N., Reaction of glutathione with conjugated carbonyls. *Zeitschrift für Naturforschung C* **1975,** *30* (7-8), 466-473.

16. LoPachin, R. M.; DeCaprio, A. P., Protein adduct formation as a molecular mechanism in neurotoxicity. *Toxicological Sciences* **2005,** *86* (2), 214-225.

17. Grimsrud, P. A.; Xie, H.; Griffin, T. J.; Bernlohr, D. A., Oxidative stress and covalent modification of protein with bioactive aldehydes. *Journal of Biological Chemistry* **2008,** *283* (32), 21837-21841.

18. Eder, E.; Hoffman, C.; Bastian, H.; Deininger, C.; Scheckenbach, S., Molecular mechanisms of DNA damage initiated by alpha, beta-unsaturated carbonyl compounds as criteria for genotoxicity and mutagenicity. *Environmental Health Perspectives* **1990,** *88*, 99-106.

19. Eder, E.; Scheckenbach, S.; Deininger, C.; Huffman, C., The possible role of α, β-unsaturated carbonyl compounds in mutagenesis and carcinogenesis. *Toxicology letters* **1993,** *67* (1-3), 87-103.

20. Cai, J.; Bhatnagar, A.; Pierce Jr, W. M., Protein modification by acrolein: formation and stability of cysteine adducts. *Chemical research in toxicology* **2009,** *22* (4), 708-716.

21. Janzowski, C.; Glaab, V.; Mueller, C.; Straesser, U.; Kamp, H.; Eisenbrand, G., α, β-Unsaturated carbonyl compounds: induction of oxidative DNA damage in mammalian cells. *Mutagenesis* **2003,** *18* (5), 465-470.

22. Colzani, M.; Aldini, G.; Carini, M., Mass spectrometric approaches for the identification and quantification of reactive carbonyl species protein adducts. *Journal of proteomics* **2013,** *92*, 28-50.

23. Suzuki, Y. J.; Carini, M.; Butterfield, D. A., Protein carbonylation. *Antioxidants & redox signaling* **2010,** *12* (3), 323-325.

24. Lu, K.; Collins, L. B.; Ru, H.; Bermudez, E.; Swenberg, J. A., Distribution of DNA adducts caused by inhaled formaldehyde is consistent with induction of nasal carcinoma but not leukemia. *Toxicological sciences* **2010,** *116* (2), 441-451.

25. Wang, M.; Cheng, G.; Balbo, S.; Carmella, S. G.; Villalta, P. W.; Hecht, S. S., Clear differences in levels of a formaldehyde-DNA adduct in leukocytes of smokers and nonsmokers. *Cancer research* **2009,** *69* (18), 7170-7174.

26. Parr, R.; Von Szentpaly, L.; Liu, S., Electrophilicity index. *J. Am. Chem. Soc.* **1999,** *121* (9), 1922-1924.

27. LoPachin, R.; Gavin, T., Molecular mechanisms of aldehyde toxicity: A chemical perspective. *Chem. Res. Toxicol.* **2014,** *27* (7), 1081-1091.

28. Chen, J. Y.; Jiang, H.; Chen, S. J.; Cullen, C.; Ahmed, C. S.; Lin, Y.-H., Characterization of electrophilicity and oxidative potential of atmospheric carbonyls. *Environmental Science: Processes & Impacts* **2019,** *21* (5), 856-866.

29. Wondrousch, D.; Böhme, A.; Thaens, D.; Ost, N.; Schüürmann, G., Local electrophilicity predicts the toxicity-relevant reactivity of Michael acceptors. *J. Phys. Chem. Lett.* **2010,** *1* (10), 1605-1610.

30. Schwöbel, J. A. H.; Wondrousch, D.; Koleva, Y. K.; Madden, J. C.; Cronin, M. T. D.; Schüürmann, G., Prediction of Michael-type acceptor reactivity toward glutathione. *Chem. Res. Toxicol.* **2010,** *23* (10), 1576-1585.

31. Jiang, H.; Ahmed, C.; Canchola, A.; Chen, J. Y.; Lin, Y.-H., Use of dithiothreitol assay to evaluate the oxidative potential of atmospheric aerosols. *Atmosphere* **2019,** *10* (10), 571.

32. Son, Y.; Bhattarai, C.; Samburova, V.; Khlystov, A., Carbonyls and carbon monoxide emissions from electronic cigarettes affected by device type and use patterns. *International journal of environmental research and public health* **2020,** *17* (8), 2767.

33. Omaiye, E. E.; McWhirter, K. J.; Luo, W.; Tierney, P. A.; Pankow, J. F.; Talbot, P., High concentrations of flavor chemicals are present in electronic cigarette refill fluids. *Scientific reports* **2019,** *9* (1), 2468.

34. Krüsemann, E. J.; Pennings, J. L.; Cremers, J. W.; Bakker, F.; Boesveldt, S.; Talhout, R., GC–MS analysis of e-cigarette refill solutions: A comparison of flavoring composition between flavor categories. *Journal of Pharmaceutical and Biomedical Analysis* **2020,** *188*, 113364.

35. Tierney, P. A.; Karpinski, C. D.; Brown, J. E.; Luo, W.; Pankow, J. F., Flavour chemicals in electronic cigarette fluids. *Tobacco control* **2016,** *25* (e1), e10-e15.

36. Patel, T.; Ishiuji, Y.; Yosipovitch, G., Menthol: a refreshing look at this ancient compound. *Journal of the American Academy of Dermatology* **2007,** *57* (5), 873-878.

37. Parker, J. K.; Elmore, S.; Methven, L., *Flavour development, analysis and perception in food and beverages*. Elsevier: 2014.

38. Farsalinos, K. E.; Romagna, G.; Tsiapras, D.; Kyrzopoulos, S.; Voudris, V., Evaluation of electronic cigarette use (vaping) topography and estimation of liquid consumption: implications for research protocol standards definition and for public health authorities' regulation. *International journal of environmental research and public health* **2013,** *10* (6), 2500-2514.

39. Jiang, H.; Ahmed, C. S.; Zhao, Z.; Chen, J. Y.; Zhang, H.; Canchola, A.; Lin, Y.-H., Role of functional groups in reaction kinetics of dithiothreitol with secondary organic aerosols. *Environmental Pollution* **2020,** *263*, 114402.

40. Jupp, A. R.; Johnstone, T. C.; Stephan, D. W., The global electrophilicity index as a metric for Lewis acidity. *Dalton Transactions* **2018,** *47* (20), 7029-7035.

41. Sánchez-Márquez, J.; Zorrilla, D.; Sánchez-Coronilla, A.; Desireé, M.; Navas, J.; Fernández-Lorenzo, C.; Alcántara, R.; Martín-Calleja, J., Introducing "UCA-FUKUI" software: reactivity-index calculations. *J. Mol. Model.* **2014,** *20* (11), 2492.

42. Morell, C.; Grand, A.; Toro-Labbe, A., New dual descriptor for chemical reactivity. *J. Phys. Chem. A* **2005,** *109* (1), 205-212.

43. Tognetti, V.; Morell, C.; Ayers, P. W.; Joubert, L.; Chermette, H., A proposal for an extended dual descriptor: a possible solution when frontier molecular orbital theory fails. *Physical Chemistry Chemical Physics* **2013,** *15* (34), 14465-14475.

44. Sleiman, M.; Logue, J. M.; Montesinos, V. N.; Russell, M. L.; Litter, M. I.; Gundel, L. A.; Destaillats, H., Emissions from electronic cigarettes: key parameters

affecting the release of harmful chemicals. *Environmental science & technology* **2016,** *50* (17), 9644-9651.

45. Son, Y.; Weisel, C.; Wackowski, O.; Schwander, S.; Delnevo, C.; Meng, Q., The Impact of Device Settings, Use Patterns, and Flavorings on Carbonyl Emissions from Electronic Cigarettes. *International journal of environmental research and public health* **2020,** *17* (16), 5650.

46. Adnan, R. H.; Andersson, G. G.; Polson, M. I.; Metha, G. F.; Golovko, V. B., Factors influencing the catalytic oxidation of benzyl alcohol using supported phosphine-capped gold nanoparticles. *Catalysis Science & Technology* **2015,** *5* (2), 1323-1333.

47. Loudon, M.; Parise, J., *Organic Chemistry*. 6th ed.; Roberts and Company Publishers: 2009; Vol. Chapter 19.

48. Stecko, S.; Paśniczek, K.; Jurczak, M.; Urbańczyk-Lipkowska, Z.; Chmielewski, M., Kinetic and thermodynamic aspects in the 1, 3-dipolar cycloaddition of five-membered cyclic nitrones to α, β-unsaturated γ-and δ-lactones. *Tetrahedron: Asymmetry* **2007,** *18* (9), 1085-1093.

Chapter V. Conclusion and Implications

This dissertation overall examines light-absorbing properties of brown carbon (BrC) chromophores, and reactive properties of carbonyl compounds in the atmosphere and in e-cigarette vaping emissions by using a combination of computational chemistry and experimental approaches. In Chapter II, time-dependent density functional theory (TD-DFT) and experimental UV-Vis measurements were conducted to evaluate light-absorbing properties of 16 selected organonitrogen species (nitroaromatics, nitro-heterocyclic compounds, organonitrates and Maillard-type reaction products) in BrC. Absorbance calculated using TD-DFT at PBE0 and B3LYP level of theory compared best with experimental absorbance data. Absorbance calculated in gas phase have blue-shifts comparing to absorbance calculated in water and methanol solvation. Furthermore, pH affected absorbance of weak acids (e.g., nitrophenols and nitrocatechols). In basic conditions, nitrophenols and nitrocatechols had stronger absorbance at longer wavelengths than in acidic conditions. Results in Chapter II show that TD-DFT is efficient at predicting light-absorbing properties of organonitrogen chromophores in BrC, and help to increase our understanding on the role of BrC in climate change. For future research, molecular dynamic studies can be incorporated to better predict light absorbance of solvated BrC chromophores.

In Chapter III, electrophilicity properties and oxidative potential of 10 atmospheric-relevant carbonyls (simple carbonyls: formaldehyde, 2-furaldehyde, benzaldehyde, 4-formylbenzoic acid, 2-, 3- and 4-nitrobenzalehyde, and α, β-unsaturated carbonyls: mesityl oxide, citral and *trans*-cinnamaldehyde) were computed and measured using density

functional theory (DFT) and dithiothreitol (DTT) chemical reactivity approaches. Computed global electrophilicity (ω) values correlated well with experimental DTT consumptions rates with r^2 values of 0.8378 & 0.9899 for simple and α, β-unsaturated carbonyls, respectively. In addition, adduct formations between selected carbonyls and DTT were identified using GC/EI-MS method, which indicated that carbonyls can deplete DTT via 1,2-carbonyl and 1,4-conjugated additions. Results from this chapter demonstrate that electrophilicity parameters can potentially be used to predict reactivity and toxicity of atmospheric carbonyls towards thiol-containing molecules, and highlights the significance of carbonyls in consumption of DTT. Future work is needed to calculate local site electrophilicity of α, β-unsaturated carbonyls to better assess reactivity of these compounds. Also, analysis of effects of carbonyl exposure in vivo is needed to further understand the potential health effects of carbonyl exposure.

In Chapter IV, vaping-associated carbonyl chemical composition, toxicity, and adduct formation with GSH were characterized using computational chemistry approaches, GSH reactivity assays, and analytic chemistry methods. First, formaldehyde, acetaldehyde, glyoxal and methyl glyoxal were detected in vaping emissions of both unflavored (PG-VG) and flavored (10% volume of *trans*-2-hexenol, benzyl alcohol, l-(-)-menthone, or linalool) e-liquids, whereas *trans*-2-hexenal, n-butanal and benzaldehyde were only found in vaping emissions of one or more flavored e-liquids, but not in vaping emissions of the unflavored e-liquid. This implies the importance of flavoring chemicals on production of carbonyls during vaping. Then after reacting vaping emissions of flavored e-liquids with GSH, adduct formations of trans-2-hexenal-GSH and benzaldehyde-GSH were identified

using LC/Q-TOFMS analysis. The ability of reactive carbonyls to form adducts with thiol-containing biomolecules (e.g., GSH) signifies potential health implications associated with e-cigarette vaping. In future, more work is needed to identify emission of carbonyls from vaping of different flavored e-liquids. Also, studies on adduct formation between carbonyls and biological proteins and DNA are needed to better understand the health implications associated with e-cigarette vaping.

In summary, Chapters II-IV assessed importance of organonitrogen species in BrC on climate change based on their light-absorbing properties, and characterized electrophilic properties and health implications of carbonyls in the atmosphere and e-cigarette vaping emissions. Computational chemistry methods (TD-DFT, DFT, and condensed Fukui function) have been found to predict optical properties, global and local site reactivities of organonitrogen species and carbonyls well in comparison with experimental data. Also, computational chemistry methods come in handy when standards of target compounds are not available on market. On the other hand, experiment approaches (UV-Vis measurements, thiol reactivity assays, GC/EI-MS, and LC/Q-TOFMS) are crucial off-line analyses for characterizing chemical composition, adduct-formation between carbonyls and nucleophiles (DTT and GSH), and for evaluating theoretical absorbance and electrophilicity values. Overall, combined computational and experimental approaches are beneficial to study effects of air pollution on climate change and human health.